

CHALMERS



Upgrading of an old steel bridge using FRP composite deck

A feasibility study

*Master of Science Thesis in the Master's Programme Structural Engineering and
Building Performance Design*

**KARL ENGDAHL
KRESNADYA DESHA ROUSSTIA**

Department of Civil and Environmental Engineering
Division of Structural Engineering
Steel and Timber Structures
CHALMERS UNIVERSITY OF TECHNOLOGY
Göteborg, Sweden 2012
Master's Thesis 2012:116

MASTER'S THESIS 2012:116

Upgrading of an old steel bridge using FRP composite deck

A feasibility study

*Master of Science Thesis in the Master's Programme Structural Engineering and
Building Performance Design*

KARL ENGDAHL

KRESNADYA DESHA ROUSSTIA

Department of Civil and Environmental Engineering
*Division of Structural Engineering
Steel and Timber Structures*

CHALMERS UNIVERSITY OF TECHNOLOGY

Göteborg, Sweden 2012

Upgrading of an old steel bridge using FRP composite deck
A feasibility study
*Master of Science Thesis in the Master's Programme Structural Engineering and
Building Performance Design*
KARL ENGDAHL
KRESNADYA DESHA ROUSSTIA

© KARL ENGDAHL, KRESNADYA DESHA ROUSSTIA, 2012

Examensarbete/Institutionen för bygg- och miljöteknik,
Chalmers tekniska högskola 2012:116

Department of Civil and Environmental Engineering
Division of Structural Engineering
Steel and Timber Structures
Chalmers University of Technology
SE-412 96 Göteborg
Sweden
Telephone: + 46 (0)31-772 1000

Cover:
Picture of Koninginne Bridge in Rotterdam, Netherlands.
http://nl.wikipedia.org/wiki/Bestand:Koninginnebrug_en_Hef_Rotterdam.jpg

Chalmers reproservice
Göteborg, Sweden 2012

Upgrading of an old steel bridge using FRP composite deck

A feasibility study

Master of Science Thesis in the Master's Programme Structural Engineering and Building Performance Design

KARL ENGDAHL

KRESNADYA DESHA ROUSSTIA

Department of Civil and Environmental Engineering

Division of Structural Engineering

Steel and Timber Structures

Chalmers University of Technology

ABSTRACT

Today a vast number of bridges is in need of rehabilitation, most of the existing bridges in Europe are 50 years or older. Increased traffic loads together with deterioration make a lot of bridges structurally deficient. Bridges often work as important joints in the infrastructure, making longer traffic disruption unacceptable. Substituting the existing deck with a prefabricated and light-weight Fibre Reinforced Polymer (FRP) bridge deck will both lower the self-weight and generate a shorter traffic disruption compared to rebuilding the bridge. The reduction in self-weight will enable higher traffic loads, due to lower stresses in the rest of the bridge.

A finite element (FE) model was developed according to old drawings of Koninginne Bridge in Rotterdam, Netherlands. Another FE model was created with the old deck substituted by an FRP deck. The FE model uses shell elements, which made it possible to measure stresses in positions of interest.

The objective was to compare the existing bridge with its plate deck compared to an FRP deck. The model was used to analyse fatigue stresses, which decreased dramatically in some key locations. One of the aims was to assess if the bridge could reach the capacity to carry standard Eurocode traffic loading. Composite action between the FRP deck and longitudinal beams together with higher lateral stiffness within the FRP deck lowers the general stresses in the critical members.

The analysis showed that with an FRP deck the bridge can carry standard Eurocode traffic load, the bridge also meets the requirements regarding stresses and deflection. Upgrading the existing bridge with a new FRP deck is to be considered to be a feasible option of rehabilitation.

Key words: Fibre reinforced polymer, FRP bridge deck, finite element model, fatigue, composite action

Svensk översättning av titeln

Examensarbete inom *Master's Programme Structural Engineering and Building Performance Design*

KARL ENGDAHL

KRESNADYA DESHA ROUSSTIA

Institutionen för bygg- och miljöteknik

Avdelningen för Konstruktionsteknik

Stål- och träbyggnad

Chalmers tekniska högskola

SAMMANFATTNING

Ett stort antal broar är i behov av förstärkningsarbete, majoriteten av Europas broar är 50 år eller äldre. Ökade trafiklaster i kombination med förfall gör många broar konstruktionsmässigt undermåliga. Broar agerar ofta som viktiga knutpunkter i infrastrukturen, vilket medför att längre trafikuppehåll ofta inte är acceptabelt. Genom att byta ut det befintliga brodäcket med ett prefabricerat lättviktsbrodäck tillverkat av fiberförstärkt polymer (Fibre reinforced polymer - FRP) kan en sänkning av egentyngheten uppnås samtidigt som trafikavbrottet inte behöver bli särskilt långvarigt. Den lägre egentyngheten möjliggör högre trafiklaster då spänningarna i övriga bron är lägre.

En finit element (FE) modell skapades enligt gamla ritningar av Koninginne-bron i Rotterdam, Nederländerna. Ytterligare en FE-modell skapades då det befintliga brodäcket bytts ut mot ett brodäck i FRP. FE-modellen bestod av skalelement, vilket möjliggjorde kontroll av spänningar för intressanta punkter.

Ett syfte var att jämföra den befintliga bron med dess brodäck bestående av en stålplatta kontra samma bro fast med ett FRP-brodäck. Modellerna användes för att analysera utmattningsspänningar, vilka minskade dramatiskt i vissa kritiska punkter. Ett annat mål var att undersöka om bron skulle kunna bära trafiklaster enligt Eurocode. Interaktion mellan FRP-brodäcket och de längsgående balkarna tillsammans med den högre laterala styvheten i FRP-brodäcket sänker spänningarna i de kritiska bärverken.

Analysen visade att det var möjligt att med FRP-brodäcket bära trafiklaster i enlighet med Eurocode, bron uppfyllde även kraven på spänningar och nedböjning. Att uppgradera Koninginne-bron med ett nytt brodäck i FRP bör konstateras som ett rimligt alternativ till förstärkning.

Nyckelord: Fibre reinforced polymer, FRP bridge deck, finite element model, fatigue, composite action

Contents

ABSTRACT	I
SAMMANFATTNING	II
CONTENTS	I
PREFACE	III
NOTATIONS	IV
1 INTRODUCTION	1
1.1 Background	1
1.2 Aim	1
1.3 Objectives	2
1.4 Method	3
1.5 Limitations and assumptions	3
1.6 Outline of the thesis	3
2 FIBRE REINFORCED POLYMER	5
2.1 Introduction of FRP	5
2.1.1 Reinforcing Fibres	5
2.1.2 Resin Polymers	6
2.2 Manufacturing Methods	7
2.2.1 Pultrusion Process	7
2.2.2 Hand Layup Process	8
2.3 FRP Bridge Decks	8
2.4 Field applications	11
2.4.1 Broadway Bridge	11
2.4.2 The Grasshopper Bridge	13
3 FATIGUE	14
3.1 Introduction of fatigue	14
3.2 Fatigue assessment	15
3.3 Fatigue load model 3 (FLM3)	15
3.4 Nominal stress method	16
4 CONCEPT OF FORCE TRANSFER BETWEEN DECK AND STEEL GIRDER	19
4.1 Composite Action - Theory	19
4.2 Lateral Distribution of Load – Theory	21
5 DESCRIPTION AND MODELLING OF THE BRIDGE	22

5.1	Background of the Bridge	22
5.2	Bridge Data	22
5.3	Bridge Modelling	27
5.4	Simplifications	29
5.5	FRP Deck Shape Suggestion	31
6	RESULTS	32
6.1	Concept of force transfer - results	32
6.1.1	Composite Action - Result	32
6.1.2	Lateral Distribution of Load – Result	33
6.2	Fatigue	40
6.2.1	Background information	40
6.2.2	Method of analysis	40
6.2.3	Results fatigue	41
6.3	Static	52
6.3.1	Vertical load	52
6.3.2	Horizontal load	57
6.3.3	Result summary of static load	57
6.4	Stresses in adhesives connection	58
7	CONCLUSION	60
8	DISCUSSION	61
9	REFERENCES	62

Preface

This project was carried out at the Department of Structural Engineering, Division of Steel and Timber Structures, Chalmers University of Technology, Sweden.

We would like to start to extend our deepest gratitude towards our supervisor assistant professor Reza Haghani and our examiner associate professor Mohammad Al-Emrani. Without their expertise and willingness to help and assist us in our work it would not have been possible to finish with this thesis.

We would like to show our gratitude to doctorate candidate Mustafa Aygül for valuable assistance and guidance how to create accurate finite element models in Abaqus.

We would like to thank doctorate student Valbona Mara for her work regarding FRP bridge decks and her will to assist when we had questions. We also would like to thank doctorate student Mohsen Heshmati for his compliance to discuss and help us with problems regarding fatigue.

Many thanks go to Ton Siemerink and Kambiz Elmi Anaraki from *Gemeente Rotterdam* for providing us with drawings and for a warm welcoming in Rotterdam. We also would like to thank Linda Abspoel-Bukman from *TNO-Delft* for her support and involvement in the PANTURA project.

Special thanks are also directed to our opponent group Joakim Carlberg and Binyam Toyib for their feedback and cooperation during master thesis work.

Last but not least we would like to thank our families and friends for the support throughout the work with the thesis.

Göteborg June 2012

Karl Engdahl and Kresnadya Desha Rousstia

Notations

Roman upper case letters

E_x	Elastic modulus in x-direction
E_y	Elastic modulus in y-direction
G_{xy}	Shear modulus in the xy-plane
G_{xz}	Shear modulus in the xz-plane
G_{yz}	Shear modulus in the yz-plane
L	Length of the bridge
Q_{ik}	Vertical axle load acting in lane i
Q_k	Horizontal brake load

Roman lower case letters

f_{xu}	Ultimate strength in x-direction
f_{yu}	Ultimate strength in y-direction
q_{ik}	Distributed traffic load lane i
w_i	Lane width for lane i

Greek letters

α_{Qi}	Adjustment factor for axle load acting in lane i
α_{qi}	Adjustment factor for distributed traffic load acting in lane i
$\Delta \sigma$	Stress variation
ν	Poisson's ratio

Abbreviations

DOF	Degree of freedom
FRP	Fibre reinforced polymer
LDF	Load distribution factor
LM	Load model
MPC	Multiple point constraint
LDF	Load distribution factor
FLM	Fatigue load model
SLS	Serviceability limit state
ULS	Ultimate limit state

1 Introduction

1.1 Background

Many existing bridges in Europe are relatively old and with an age of more than 50 years. Bridge decks often deteriorate from corrosion caused by de-icing agents in combination with the increase in traffic load the last decades. With regard to insufficient load carrying capacity of these old bridges, effective and efficient solutions need to be developed. Construction of a new bridge could be considered as an option, however it is very expensive and the construction time in most cases is not acceptable. One promising solution is to use fibre reinforced polymer (FRP) decks. With its special characteristics such as immunity to corrosion and a high strength to weight ratio, it has been shown that FRP materials can considerably reduce the total weight of the bridge. It means solving the problems about load capacities, deterioration of the deck, and also keeping the landmark value of the existing bridge itself. Moreover, the prefabricated FRP decks will make it possible to minimize traffic disruption during the assembly on site.

In this master thesis work a feasibility study, by substituting the old deteriorated deck of the Koninginne Bridge with the new FRP deck, will be studied. The Koninginne Bridge is located in the centre of Rotterdam, Netherlands. The city of Rotterdam has a city plan with different alternatives for how to solve problems with the urban traffic in the inner city, one of the possible solutions is to lighten and strengthen the Koninginne Bridge. This bridge is a case study bridge within an EU research project PANTURA at the department of civil and environmental engineering. The bridge is a bascule (vertically open-close) steel bridge and it is a crucial connector for the urban traffic. Today the bridge suffers from problems such as excessive self-weight which causes damage to mechanical parts and overstressing of the hinges, which the bridge rotates about when opened. Therefore, the bridge is currently limited to traffic axle loads up to 10 tons. One potential solution is to upgrade the Koninginne Bridge with an FRP deck, which would considerably lower the self-weight of the bridge. The capacity for higher traffic loads would also be achieved simultaneously as the counter weights could be reduced and thereby reducing the stresses in the overstressed parts of the bridge.

1.2 Aim

Since the Koninginne Bridge is very old it has a monumental value and therefore there are interests to preserve the bridge instead of replacing it. Another aspect is the importance of the traffic connection that the bridge offer, any traffic disruption would cause serious problems in the urban traffic, see Figure 1.1. The proposed solution is to replace the existing steel deck and replace it with an FRP deck. Upgrading with FRP deck is not only cheaper in total cost but also faster to install in situ in comparison to construction of a new bridge. With that in mind, more studies should be done to measure the possibility of rehabilitation of the existing Koninginne Bridge.

The overall aim of this thesis is to evaluate the existing condition of Koninginne Bridge with regard to data from original drawings provided by city of Rotterdam and to investigate the possibility of increasing the load carrying capacity, according to Eurocode, while reducing the self-weight of the bridge by replacing the old deck with a new FRP composite deck.

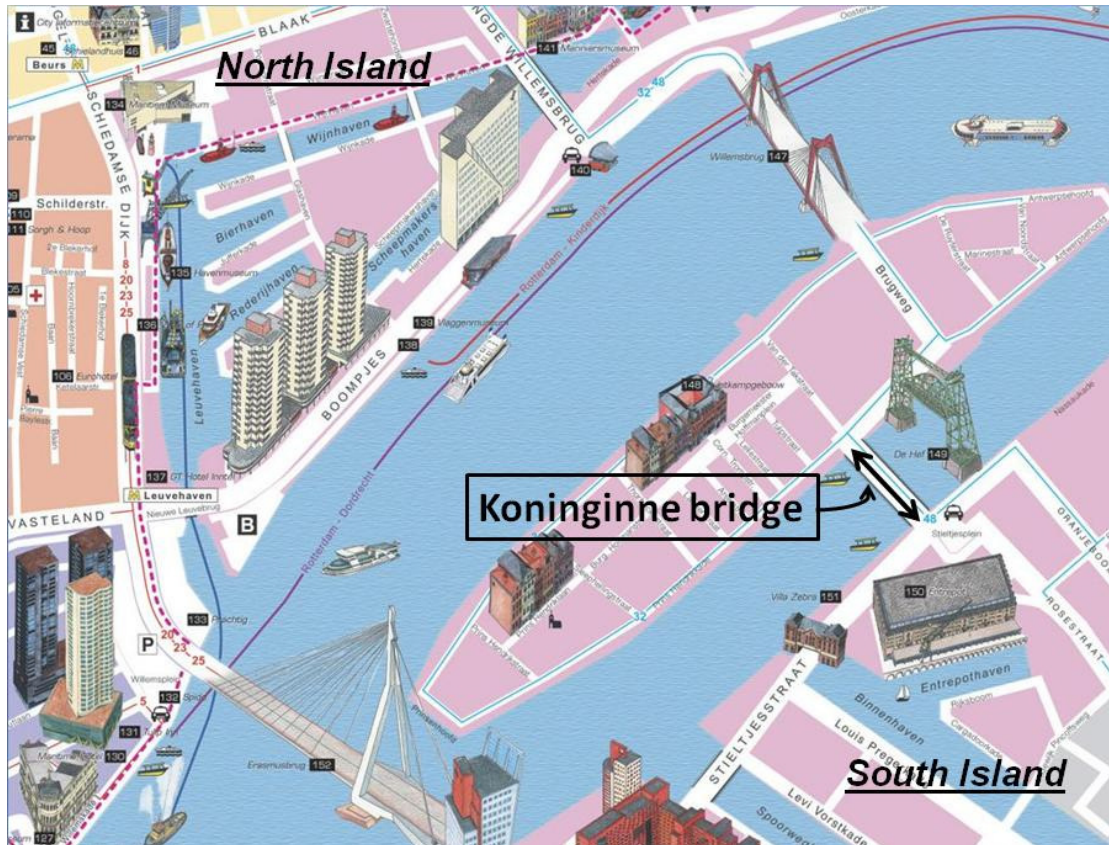


Figure 1.1 Aerial map location of Koninginne Bridge

Replacing the existing deck to an FRP deck will change how the existing members will behave in correlation with the new FRP deck. Other aspects, such as: Load distribution, composite action, and connection are investigated.

1.3 Objectives

In order to achieve a realistic assessment of the condition of the bridge, a good understanding of the bridge's behaviour is necessary. To achieve the main goal of the thesis work several steps should be taken, including:

- Modelling the existing bridge according to Eurocode traffic loads and interpretation of the behaviour and identify possible problems:
 - Verification of the model in correlation with deflections and stresses.
 - Check members with respect to fatigue in order to get a rough representation of the existing condition.
 - Calculate the self-weight of the existing deck.
 - Estimate load carrying capacity of the bridge with exiting condition

- Analysis of the upgraded bridge model with an FRP deck and investigation of advantages and disadvantages associated with the FRP decks:
 - Verification of the model in correlation of deflections and stresses.
 - Check members for fatigue assessment.
 - Contribution of the FRP deck in load carrying capacity
 - How much of the counter weight could be removed due to the lighter FRP deck?

- Check the stresses in the adhesive layer between stringers and the FRP deck.
- Load carrying capacity of the upgraded bridge.

1.4 Method

In this thesis work, the way to achieve the objectives is by analytical work. Basic principles of how the structures behave were studied. In the following chapter, these basic principles will be called concept of force transfer between deck and steel girder.

In the beginning, a literature study was performed in order to get familiar with the concept of FRP materials and FRP decks. Meanwhile, relevant drawings of Koninginne Bridge and its reports from previous assessment were collected and studied.

Numerical modelling of the finite element method was performed by using Abaqus software. Simply small Abaqus model of steel plate decks and stringers was modelled. The behaviour of that model was compared with another small model of FRP decks and stringers. Thereafter, whole Koninginne Bridge was created according to the drawings. From the results of finite element analyses, the behaviour of the bridge with the existing deck and the FRP deck could be studied and some of the bridge's potential issues could be identified.

1.5 Limitations and assumptions

In this thesis work, the finite element models are done with the assumption of linear-elastic material properties. Because of the interest is focused only in the global behaviour of the bridge, local behaviour of the structure such as plate buckling, dynamic behaviour are not included in the assessment.

For the Eurocode traffic loads applied in the bridge design, only load model 1 was used for the vertical traffic load and for checking the fatigue stresses fatigue load model 3 was utilized.

This master thesis work is based on old drawings of the Koninginne bridge and also a report of an investigation made in 2004. The FE model was based on the old drawings which later showed to have some small differences in the cross-sectional dimensions in some of the many longitudinal beams. This is discussed more in the final chapter called *discussion*.

1.6 Outline of the thesis

The first chapter presents the background and aim of the master thesis work. The sub-chapter about objectives is also provided to give a description of how to achieve the aims of this thesis work. In addition, some limitations giving boundaries to the analyses are presented.

The second and the third chapter present basic literature studies related to the topic of this master thesis work. In the second chapter, basics of fibre reinforcement polymer (FRP) material are presented. In this chapter, the properties of several polymers are provided. Moreover, manufacturing processes and FRP deck chosen are described.

The theory and methodology of fatigue analysis are also provided in the following chapter.

Chapter four presents a concept of force transference between the deck and the steel girders. The theory is explaining basic principles of this master thesis work. Basic principles of the master thesis work are to see how the behaviour changed when different structure applied to existing bridge. Small model of different structures will be studied in this chapter. The fifth chapter will provide general information about how the bridge has been modelled and also the assumptions that has been used.

The sixth chapter provides results of the concept of force transference, fatigue, and static analysis. The result from a small model of the deck, which related to concept of force transference, will be offered. Moreover, the results of the fatigue and the static analysis based on Eurocode are also presented. Estimative calculations were performed to check the stresses in the adhesive zone.

Conclusion of the master thesis work and discussion for further research are discussed in chapter seven and eight respectively.

2 Fibre Reinforced Polymer

2.1 Introduction of FRP

FRP stands for fibre reinforced polymer, which is a composite material consists of fibres embedded in matrix. Fibre works as reinforcement for the composite and provides the strength of the FRP material. Resin based polymers are widely used for FRP products. Matrix material bind the fibres together, protect them and also transfers stresses to the fibres.

2.1.1 Reinforcing fibres

The fibres in an FRP composite material consist of thousands individual filaments. The mechanical properties of fibres are higher than those of resin polymer; but the fibres cannot be used as a stand-alone construction material and should be used together with resins. There are three common types of fibres, namely glass, carbon, and aramid fibres.

Glass based fibres are used for some FRP products such as reinforcing concrete bars strengthening fabrics, and FRP structural profiles. Different grades of glass fibres are distinguished by their letter nomenclature see Table 2.1. E-glass fibres are electrically non-conductive. A-glass fibre usually is used as a basic material for glass windows. C-glass fibres have a good corrosion resistance and are produced for application in structural engineering. S-glass fibres, due to their high performance, are used in aerospace industry. Protection by resin is an important issue for glass based fibres due to sensitivity of these fibres to moisture. However, glass based fibres are inexpensive and a good insulator.

Table 2.1 Approximate properties of common grades of glass fibres.

Grade of Glass Fibre	Density	Tensile Modulus	Tensile Strength	Max. Elongation
	[g/cm ³]	[Gpa]	[Mpa]	[%]
E	2.57	72.5	3400	2.5
A	2.46	73	2760	2.5
C	2.46	74	2350	2.5
S	2.47	88	4600	3

* Source: Bank, Lawrence Colin. (2006)

Carbon based fibres are used in many structural engineering application such as FRP strengthening sheet and fabrics, FRP strengthening strips, and FRP pre-stressing tendons. Carbon fibres are produced in different grades, namely standard, high strength, high modulus, and ultrahigh modulus, see Table 2.2. Carbon fibres can be said to be a durable material due to their ability to perform very well in hot and moist condition, and resistance to fatigue loads.

Table 2.2 Approximate properties of common grades of carbon fibres.

Grade of Carbon Fibre	Density	Tensile Modulus	Tensile Strength	Max. Elongation
	[g/cm ³]	[Gpa]	[Mpa]	[%]
Standard	1.7	250	3700	1.2
High Strength	1.8	250	4800	1.4
High Modulus	1.9	500	3000	0.5
Ultra High Modulus	2.1	800	2400	0.2

* Source: Bank, Lawrence Colin. (2006)

Aramid fibres are mostly used for FRP wrap in column strengthening. A combination of their expensive price, low melting point, difficulty in processing, and poor compressive properties have made aramid based fibres infamous for FRP structural engineering applications. In fact, their advantages to absorb energy have made them applicable for bullet proof vests, helmets, and automotive safety technology.

2.1.2 Resin polymers

There are two main groups of resin polymer nowadays, thermosetting polymers and thermoplastic polymers. In FRP for structural engineering, thermoset type of polymers is used. The strong covalent bonded atoms in this type of polymers makes the material resistive for softening when reheated after the solidification, which would explain the brittle characteristic of this material. On the other hand, thermoplastic type of polymers has the ability to be softened and re-shaped when heated. Polymer resins have the ability to prevent conductivity of heat and electricity due to its low void ratios. Because of small possibility of the water can fill voids, this makes polymer resin an insulator type material. Thermosetting polymer resins are generally not suitable for use at temperatures greater than 180 degree Celsius (Bank, 2006). Fire ratings of thermosetting polymer can be upgraded by design it with special protection system and additives.

There are three main types of thermosetting resin polymer. They are polyester, epoxy, and vinyl ester resin. Polyester resin is used commonly to make pultruded FRP profiles. Pultrusion is one of manufacturing process which will be explained in following section. The polyester resin itself can be divided by three types, which are orthophthalic, isophthalic, and teraphthalic polyesters. The different properties are achieved because of these different monomers. Low cost and adequate structural properties have made polyester resin the most preferred material for bridge deck.

Different with polyester, epoxy resin is not extensively used to produce FRP profiles. Mostly, this resin is used as an adhesive to bond pre-cured FRP strip to other materials (concrete, steel, etc). Epoxy resin has also been used to make FRP tendons for pre-stressing concrete and cable stay bridges. Known superior quality, such as excellent corrosion resistance and less shrinkage, makes higher cost of this type resin compared to other type resins.

Vinyl ester resin is also called a hybrid resin because of its properties in combination between polyester and epoxy resins. This type of resin has an attractive FRP product for structural engineering option after polyester resin due to their properties. Superior

environment durability in alkaline condition has made vinyl ester resin replacing polyester resins.

Other thermosetting type resins are also available such as phenolic and polyurethane resins. But, almost the same cost and inferior quality compare to newly types of resin has made phenolic and polyurethane resins infamous in structural engineering application nowadays. In Table 2.3 different approximate properties of thermosetting polymer resins can be seen.

Table 2.3 Approximate properties of thermosetting polymer resins.

	Density	Tensile Modulus	Tensile Strength	Max. Elongation
	[g/cm ³]	[Gpa]	[Mpa]	[%]
Polyester	1.2	4	65	2.5
Epoxy	1.2	3	90	8
Vinylester	1.12	3.5	82	6
Phenolic	1.24	2.5	40	1.8
Polyurethane	varies	2.9	71	5.9

* Source: Bank, Lawrence Colin. (2006)

The fibres can be oriented in a variety of different directions, thus making FRP an orthotropic material. By reinforcing the plastic matrix, a wide variety of physical strengths and properties can be designed into the FRP composite. Additionally, the type and configuration of the reinforcement can be selected, along with the type of plastic and additives within the matrix. These variations allow an incredible range of strength and physical properties to be obtained. FRP composites can be developed specifically for the performance required versus traditional materials: wood, metal, ceramics, etc.

2.2 Manufacturing methods

There exist several manufacturing methods for FRP decks and the common ones are pultrusion process, hand layup process, vacuum assisted resin transfer moulding (VARTM), and filament winding process. In structural engineering, pultrusion and hand layup are two most common principal methods used to manufacture FRP composite products.

2.2.1 Pultrusion process

Pultrusion process is a process to arrange the fibres by pulling it through a resin bath and heated as it passes through to produce a section. A section then can be combined together with an adhesive to form deck panels, see Figure 2.1. In this process the FRP product is produced and assembled as small parts (bridge deck) in fabrication, then shipped to construction site to be assembled as a bigger deck. Pultrusion process is usually used to manufacture constant cross section such as; FRP profiles, FRP strengthening strips, and FRP reinforcing bars.

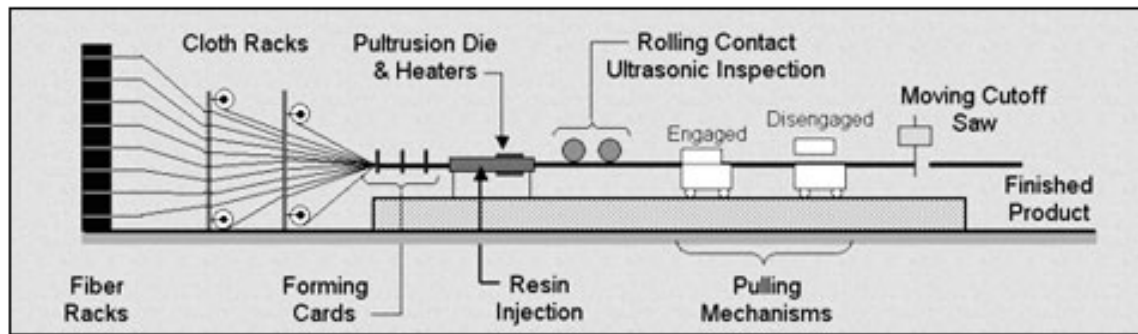


Figure 2.1 Schematic diagram of the pultrusion process.

*Source: http://www.industrialextrusionmachinery.com/plastic_extrusion_pultrusion.html

There are several advantages manufacturing FRP with the pultrusion process. High quality of composite profiles, consistent quality, high production, increase the strength due to fibre processed under tension, and low production cost because of automated machine are some benefits to produce FRP with this process. In other hand, difficulty to make a profile with complex cross section and high start-up cost are disadvantages of this process.

2.2.2 Hand layup process

Hand layup method is typical manual old method of producing FRP member. Hand layup is a process to make laminates/ panels of FRP composites by laying up the series of fibre layer and fill them with liquid resin polymer. This process is manufactured in the construction site and manually by human. This condition makes it important to have a good skill and quality control. Hand layup process is usually used to manufacture and install dry fibre strengthening sheets and fabrics. In bridge deck, the top and bottom part of the deck are produced and connected together by bonding them with core material.

Hand layup method has a simple principles and widely used because it is probably the oldest method of producing FRP parts. However, high possibility of voids due to human error is one of the concerns in this method. Moreover, expensive requisite due to health and safety consideration has made a high worker cost.

2.3 FRP bridge decks

There are many different manufacturers producing FRP bridge decks and the main production process could be divided into:

- Pultruded decks.
- Sandwich decks, either produced by VARTM or hand lay-up technology.

The most common production technology used for FRP decks is pultrusion, which generate a constant height of the profiles. The pultruded profiles are then glued together to form the deck, shape and height of the profiles depend on the manufacturer. A disadvantage of the pultruded decks is that the deck is considered to

transfer load in one direction only, namely the direction of pultrusion. Due to demands on maximum deflection the span is limited to around 2,7m. These conditions are why pultruded decks in the majority of cases are oriented transverse to the traffic direction; see Figure 2.2.

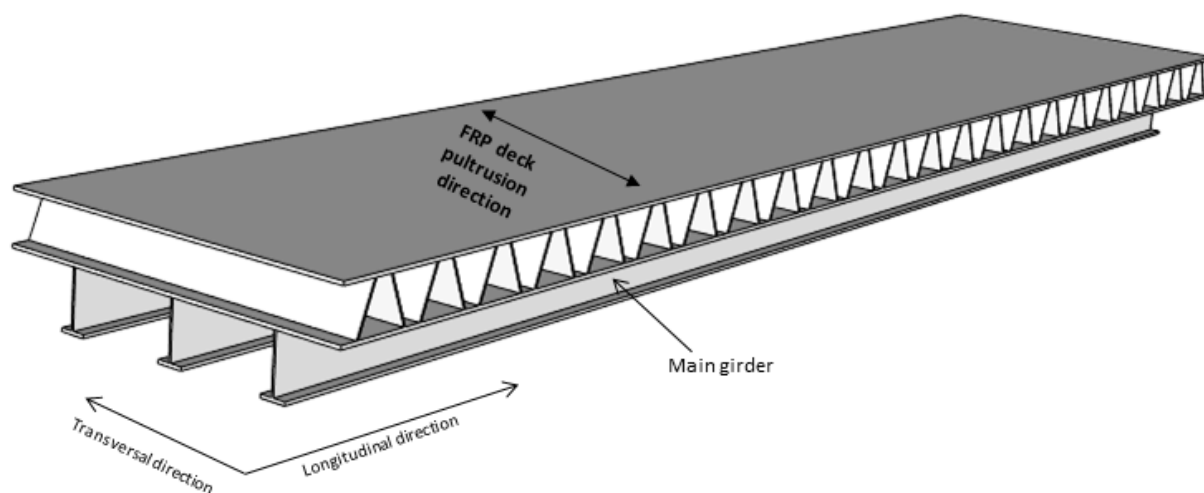

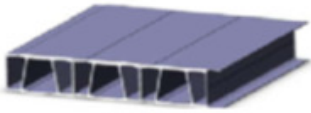




Figure 2.2 Deck pultrusion in transversal direction of main girders.

Sandwich decks are created using either VARTM or hand lay-up technique, this enables the possibility of having varying profile height and therefore custom decks could be produced. Sandwich decks are considered to be load bearing in both directions and are generally stiffer than pultruded decks hence larger spans are possible. Spans up to 10 m have been produced. Decks system from different manufacturers and their basic properties can be seen in Table 2.1.

Table 2.4 Basic data from different deck manufacturers. (Valbona Mara, 2011)

Deck System	Manufacturing Process	Deck Thickness (mm)	Deck Weight (kN/m ²)	Manufacturer	Illustration of The Deck
EZ-span deck	Pultruded	216	0.96	Creative Pultrusion Inc, USA	
Superdeck	Pultruded	203	1	Creative Pultrusion Inc, USA	
Strongwell	Pultruded	170	-	Strongwell, USA	
Duraspan deck	Pultruded	195	1.05	Martin Marietta Composites, USA	

ASSET deck	Pultruded	225	0.93	Fiberline A/S, Denmark	
Delta deck	Pultruded	200	-	Korea	
Hardcore deck	VARTM	variable	variable	Hardcore composites, USA	
Kansas deck	Hand lay-up	variable	variable	Kansas Structural Composites, USA	

In this master thesis, the ASSET deck was used in the Abaqus modelling due to availability of its properties. In addition, the height of the ASSET deck also corresponds to the height of existing member which is 225 mm. The assembled ASSET deck has a weight of 0.93kN/m^2 . See Figure 2.3 for illustration of the deck profile and Table 2.5 for profile properties of the ASSET bridge deck.

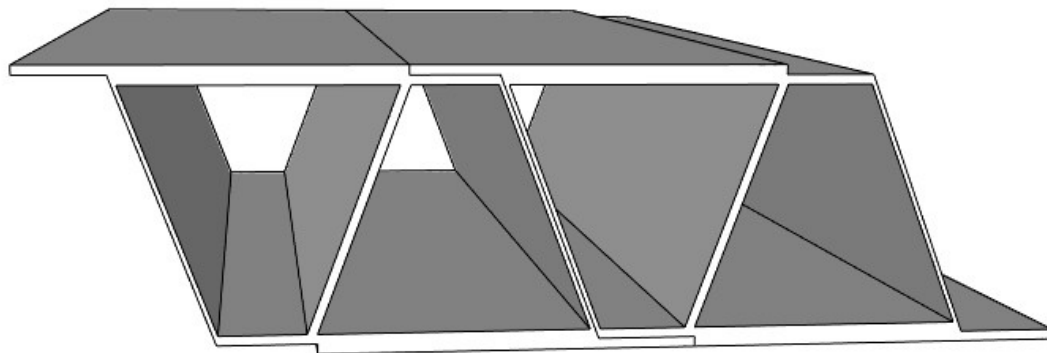


Figure 2.3 ASSET bridge deck profiles connected by adhesive bond.

Table 2.5 Material properties for the ASSET bridge deck (Valbona Mara, 2011)

Property	Flange plates	Outer web plates	Inner web plates
E_x [MPa]	23000	17300	16500
E_y [MPa]	18000	22700	25600
G_{xy} [MPa]	2600	3150	2000
G_{xz} [MPa]	600	600	600
G_{yz} [MPa]	600	600	600
f_{xu} [MPa]	300	180	255
f_{yu} [MPa]	220	213	225
ν_{xy}	0.3	0.3	0.3

*X: Pultrusion direction, Y: transverse direction, Z: vertical direction

2.4 Field applications

2.4.1 The Broadway bridge

This bridge is located in Portland, Oregon. With span around 42 m for each bascule leaves, this bridge is a vital connector to its surrounding areas. The bridge was built in 1912, and the FRP deck panels have been applied since 2004.

Due to its age and frequent use, the bridge had considerably problem with its surface grid decks. Low skid resistance of the decks grid had significant safety concern. Therefore the grid was chosen to be replaced. A replacement of the original grid decks with the new grid decks was an option; however, this option was not satisfying the construction time of during its process. Construction time had an important issue with this project because the bridge should be able to be opened every fourth-day for river commuters. With total the bridge's closure for vehicular traffic to 60 days period, the contractor had done the extensive structural rehabilitation such as; steel repair, paint abatement, and the grid deck replacement.

With those requirements, DuraSpan FRP bridge deck system had been chosen to replace the old-original steel grid on the bascule bridge. This FRP deck constituted of primarily glass fibers and polyester resin, with thickness 127 mm and weight 1.05 kg/cm².

The Installation process had been done with extra carefully. Two forklifts worked together to bring the FRP deck panel (weight 2720 kg) with maintaining tight clearances from each side of the bridge, see Figure 2.4. Total 32 deck panels were applied. The deck panels should be secured to the beams with temporary attachments before the bascule opening on the day fourth.



Figure 2.4: FRP deck panels were set in place with dual forklifts. (Matt Sams)

The connection between FRP deck panel and steel girder was using shear studs and grout filled, see Figure 2.5. With good track records of testing, this connection was applicable during that time. This typical of connection made FRP decks and steel beams to perform together in composite action. However, no consideration of composite action was applied when the beams carry the loads during the design processed.

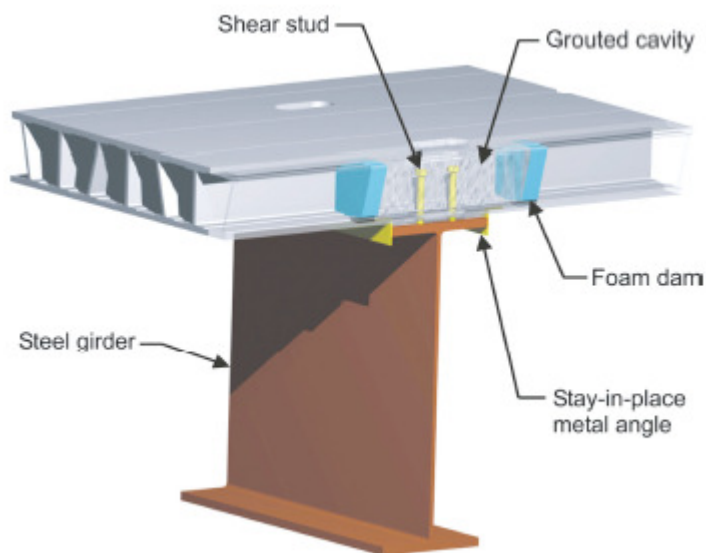


Figure 2.5: The FRP deck panel was attached above steel girder with shear stud. (Matt Sams)

2.4.2 The Grasshopper bridge

The Grasshopper Bridge is a small bascule bridge located in Zealand, Denmark. The Grasshopper was originally built in 1936, see Figure 2.6. The bridge has a counter weight of about 100 tons. In June 2011 the old bridge deck was replaced with FRP deck panels. The upgrade of the bridge resulted in Denmark's first road bridge with an FRP deck.

The old timber deck was in bad shape and severely rotten. This deck type was set to be replaced every five years which creates a lot of maintenance work and traffic disruption. The company in charge of the maintenance decided to use FRP deck for the upgrade due to its strength and durability but also because the panels are made of light weight material. The FRP materials today are more affordable and more widely used than for a decade ago. To upgrade old bridges with decks made of FRP is often a reasonable option today, especially for movable bridges.



Figure 2.6: Side view of “the Grasshopper”. (Fiberline)

The ASSET deck from Fiberline was chosen to replace the old rotten timber deck. One major advantage with the ASSET deck is that the panels are prefabricated and the installation can be done in a very rapidly, see Figure 2.7.



Figure 2.7: Preparation work for rapid assembly. (Fiberline)

The deck was lifted in place in small panels and thereafter installed. Because of the light weight nature and the strength of the panels the roadway could be widened by 30 cm and an additional footbridge could be attached. The installation was performed very quickly, in just one night the deck was installed with good results.

3 Fatigue

3.1 Introduction of fatigue

When structures experience its ultimate design load the structure fails in a plastic manner with large visual deformations. The ultimate load can just be reached once during the structure's lifetime. Unlike failure from ultimate load another failure could arise, namely fatigue failure. Fatigue is a process which is dependent on stress fluctuation and tends to localise where stress concentrations are present, such as welds and other connections. When one loading-unloading cycle occurs there will be micro cracks in the material provided that the stress variation is high enough. Each micro crack is a permanent damage in the structure in the material and therefore cannot be repaired. After repeated loading-unloading or so called load-cycles, the micro cracks propagate and grow together finally forming one larger crack. See Figure 3.1. When a larger crack reach a critical magnitude fatigue failure occur, often with a brittle nature without any large visual plastic deformation. Therefore it is very important to design members and connections in structures with fatigue in mind, many fatal accidents have taken place in the past due to lack in fatigue design.

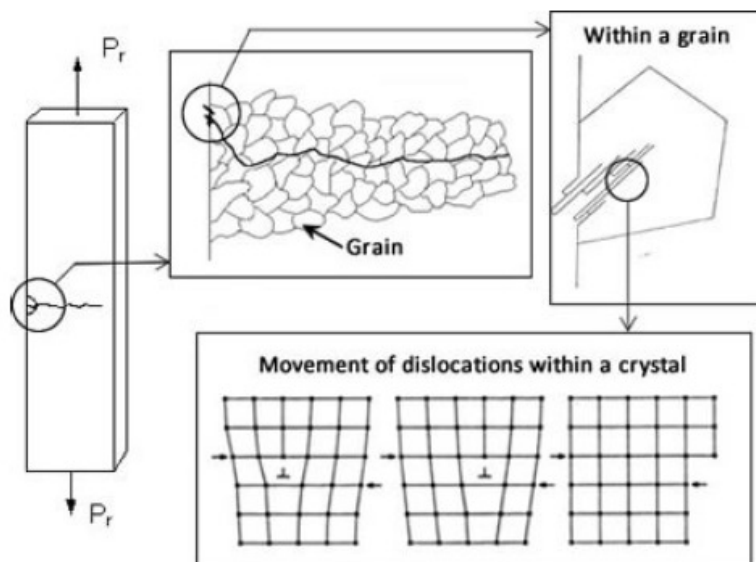


Figure 3.1 Propagation of fatigue cracks. (Heshmati 2012)

As mentioned before the fatigue is dependent on the stress variation, meaning the difference between the maximum and minimum stress for one load-cycle, see Figure 3.2 for illustration of definition of stress variation.

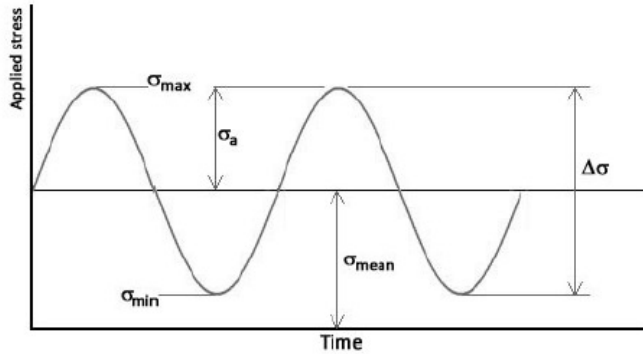


Figure 3.2 Definition of stress variation $\Delta\sigma$ (Heshmati 2012)

3.2 Fatigue assessment

In order to increase the live load capacity and at the same time lower the self-weight of the bridge a fatigue assessment has to be done. To determine the maximum and minimum stress range fatigue load model 3 was used in accordance with Eurocode. Eurocode states that fatigue load model 3 may be used for a simplified method for annual traffic when the fatigue assessment is performed. [EN1991-2 clause 4.6.1 (NOTE 2: d)]

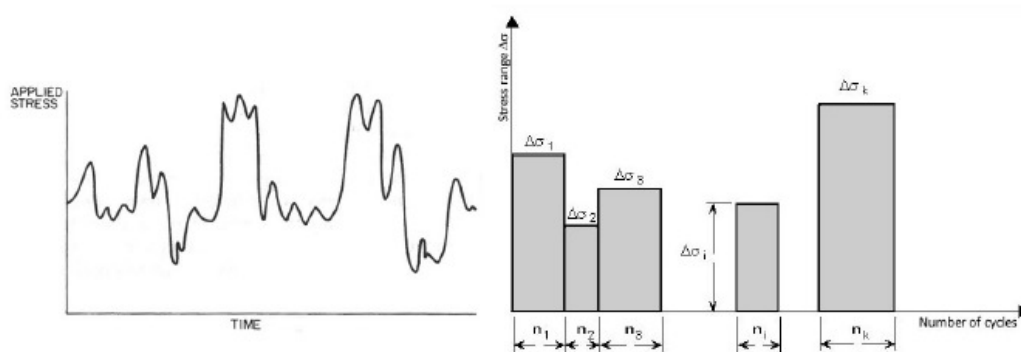
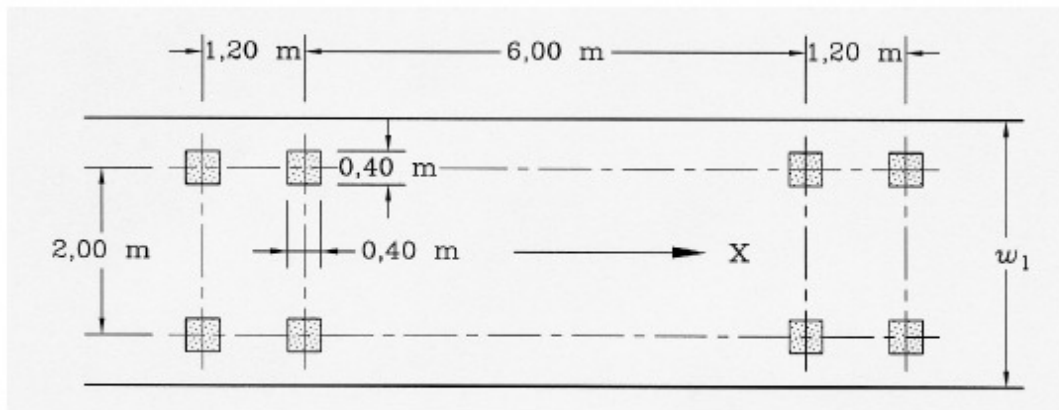


FIGURE 16: AN EXAMPLE OF VARIABLE AMPLITUDE LOADING AND STRESS HISTOGRAM AS A SIMPLIFICATION METHOD OF VARIABLE AMPLITUDE LOADED STRUCTURES

3.3 Fatigue load model 3 (FLM3)

The FLM3 simulates one single vehicle with four axle loads, each with a load of 120kN. Each axle spread the load on two squares with the sides of 0.4m, see Figure 3.3.



Key
 w_1 : Lane width
 X : Bridge longitudinal axis

Figure 3.3 Illustration of vehicle used in fatigue load model 3. (Eurocode 1991-2)

3.4 Nominal stress method

There are several different methods for assessing fatigue; in this thesis the nominal stress method was utilized. According to Eurocode the nominal stress method is sufficient to assess the fatigue life and the method is widely used. One major advantage with this method is the simplicity of how to determine the stresses for which the fatigue analysis was performed. The connections in the Koninginne Bridge are not that complex which also favours using the nominal stress method, because the accuracy of the method lowers with more complex connections.

The nominal stress method uses the nominal stress range, which corresponds directly to the applied load. Basically the method can be performed in two steps:

1. Calculation of stress in critical section
2. Determination of detail category from tables provided by codes and guidelines.

The detail category depends on which type of connection and what kind of load the member is experiencing, see Figure 3.4 for example of detail categories.

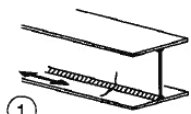

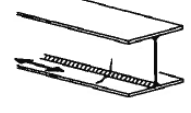
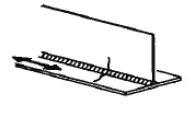
Detail category	Constructional detail	Description	Requirements
125	 	Continuous longitudinal welds: 1) Automatic butt welds carried out from both sides. 2) Automatic fillet welds. Cover plate ends to be checked using detail 6) or 7) in Table 8.5.	Details 1) and 2): No stop/start position is permitted except when the repair is performed by a specialist and inspection is carried out to verify the proper execution of the repair.
112	 	3) Automatic fillet or butt weld carried out from both sides but containing stop/start positions. 4) Automatic butt welds made from one side only, with a continuous backing bar, but without stop/start positions.	4) When this detail contains stop/start positions category 100 to be used.

Figure 3.4 Example of detail categories for some types of connections. (Eurocode 1993-1-9)

The value of the detail category corresponds to the value of stress variation that the connection can experience and fail due to fatigue after 2 million load cycles.

The detail categories are based on test results from a number of specimens with the identical connection type, which have been loaded until failure with varying stress variation. The resulting relation between stress variation (S) and number of cycles (N) before failure build the S-N curve, which can be seen in Figure 3.5. To the left in Figure 3.5 the specimen has been loaded with a high stress range, which results in a fewer number of loading cycles before failure.

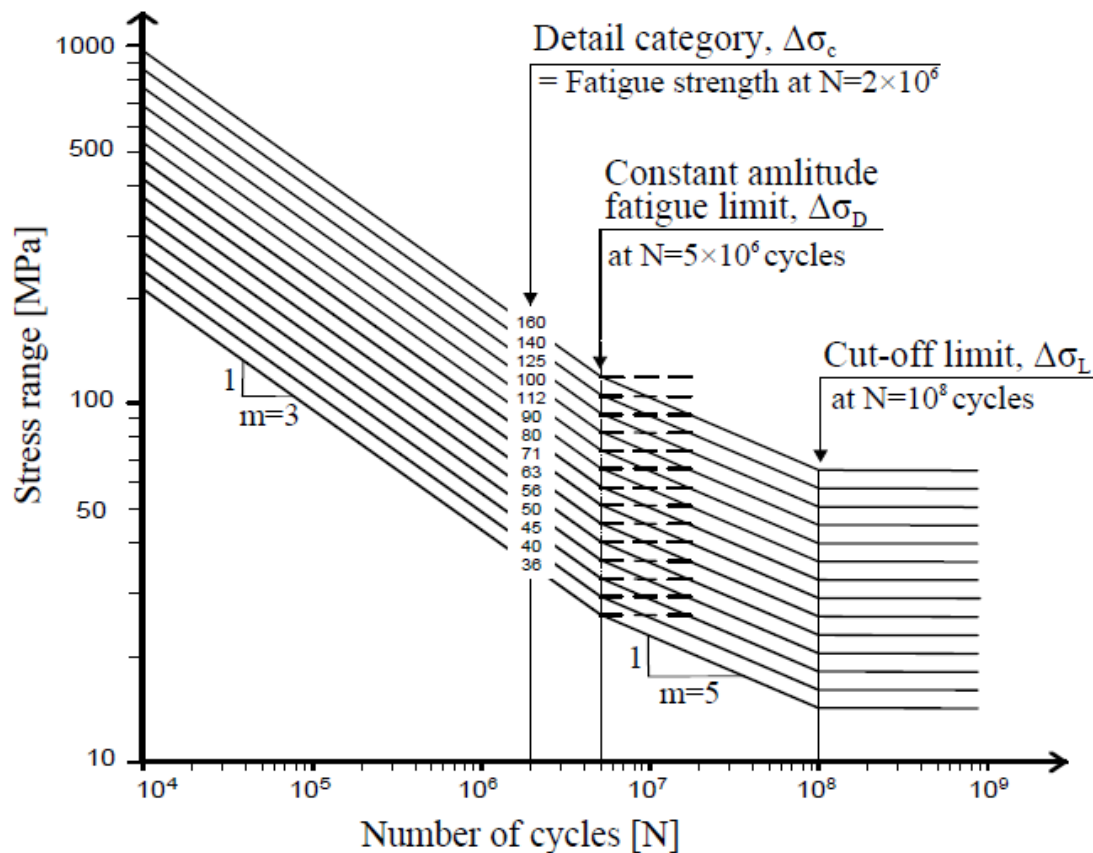


Figure 3.5 S-N curves of steel for normal stress range. (Eurocode 1993-1-9)

To the right in Figure 3.5 the stress range is so low that the members do not take any damage by the cyclic loading and therefore it is considered to be able to be loaded

infinitely number of times without failing to fatigue. The stress variation corresponding to this is called “Cut-off limit” and for steel the member that pass 10^8 cycles without failure is considered to be able to withstand an infinitely number of cycles at this stress range.

4 Concept of Force Transfer between Deck and Steel Girder

The stresses obtained in most part of the bridge members will decrease by replacing the bridge's existing steel deck with an FRP deck. Lower self-weight of the FRP deck in comparison to the steel deck will affect these stresses. Specifically in the stringers, this member will get even lower stresses due to two different aspects. These two aspects are explained in the two following subchapters.

4.1 Composite action - theory

The first aspect is caused by the effect of composite action between the stringers and the FRP deck. This interaction occurs because of the adhesive bond between the bottom plate of the FRP deck and the top flange of the stringer. The adhesive layer is usually 8-10 mm thick for a FRP-steel connection, see Figure 4.1.

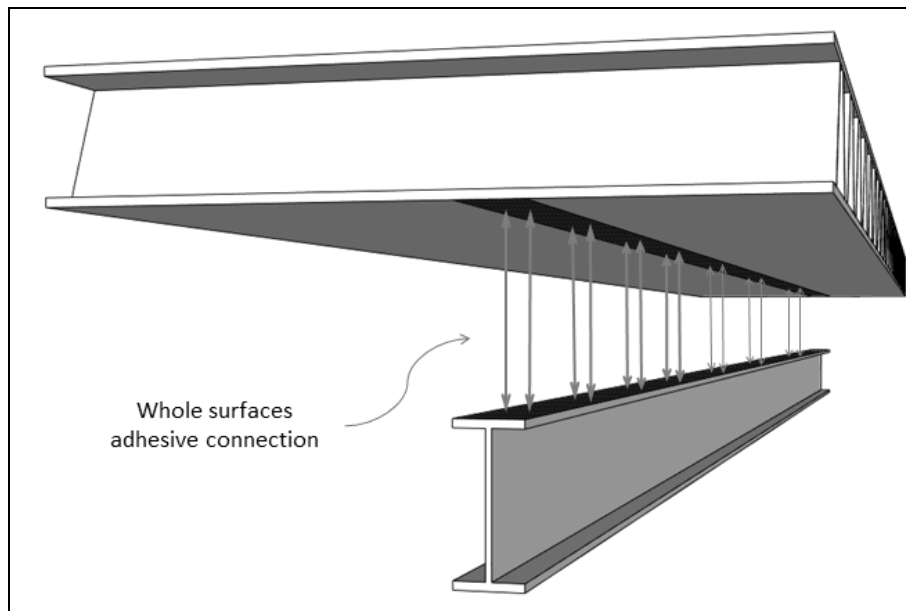


Figure 4.1 Illustration of adhesive connection between FRP deck and stringer.

In composite action, both members will work together as one new member and this condition will shift up the position of neutral axis of the new member (stringer with deck) in comparison to the existing condition (stringer with steel plate only). Figure 4.2 shows a steel stringer, IPN260, without any deck, this stringer will have its neutral axis exactly in the middle of its height. Strain and stress can be obtained easily from simple calculations. Figure 4.3 shows a steel stringer and a steel sandwich deck, the neutral axis in the stringer is shifted upwards because the total area of the combined member is greater. The shifting of the neutral axis can be achieved only if both materials in the connection are working very well together. The up shifting of the neutral axis automatically decrease the stress due to an increase in the section modulus for the new combined member.

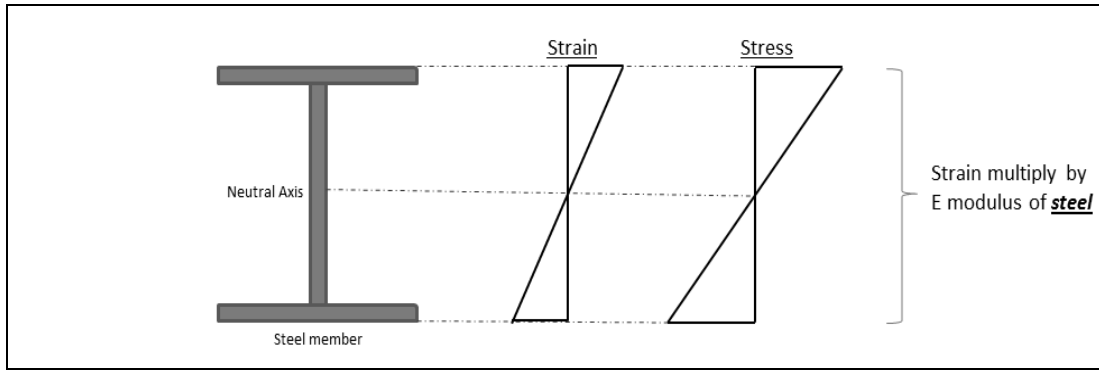


Figure 4.2 Stress-strain relation of a steel stringer.

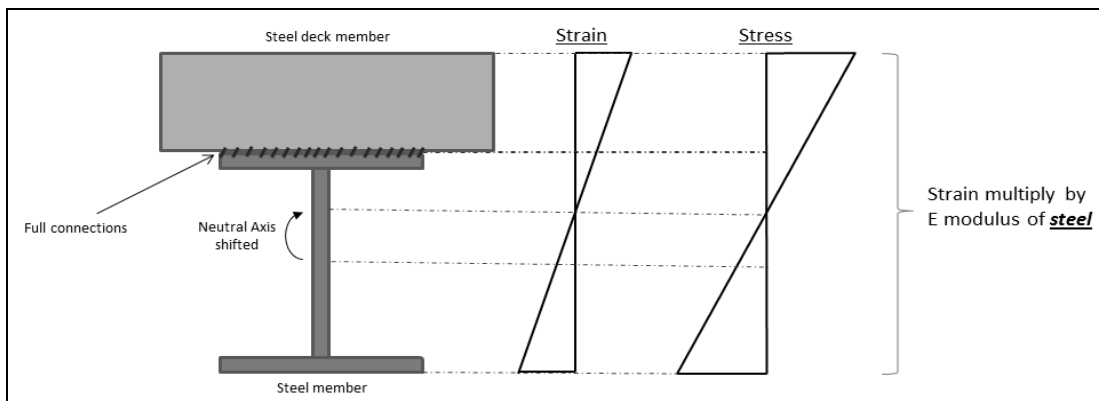


Figure 4.3 Stress-strain relation for composite action between a steel stringer and a steel sandwich deck.

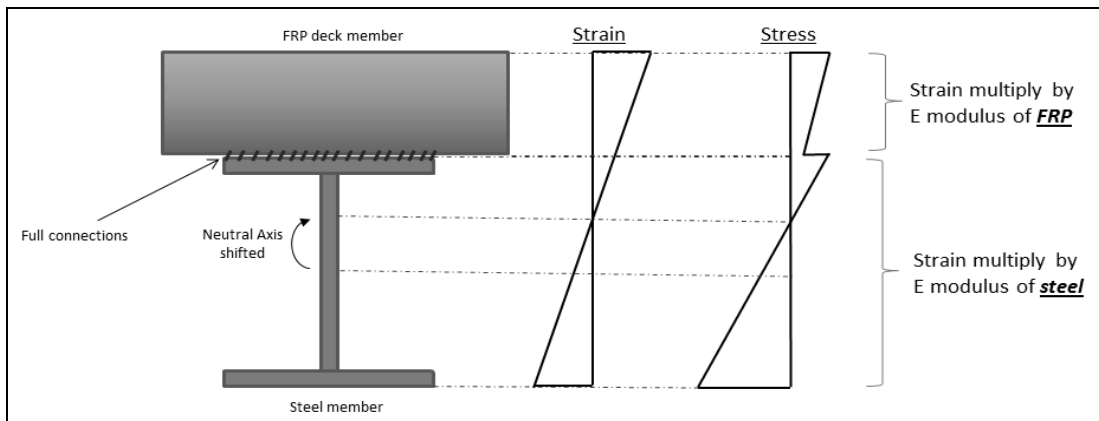


Figure 4.4 Stress-strain relation for composite action between steel stringer and an FRP deck.

From Figure 4.4, the neutral axis shifted due to additional FRP deck on the top of the steel stringer which made a difference in the moment of inertia and section modulus of a whole member. The shifted position of neutral axis will also make the stress in the top flange of the stringer decrease. In the following chapter, this mechanism will affect the service life of the stringer with respect to fatigue.

4.2 Lateral distribution of load – theory

Lower stresses in the structure can also be achieved by aligning the pultrusion direction of the FRP deck perpendicular to the traffic direction. This arrangement results in a load distribution which spread effectively to adjacent stringers. In addition, when the main stringer (where the load is applied) is deflected, the neighbouring stringers will work together to withstand the deflection due to transversal stiffness of the deck in the pultrusion direction. See Figure 4.5.

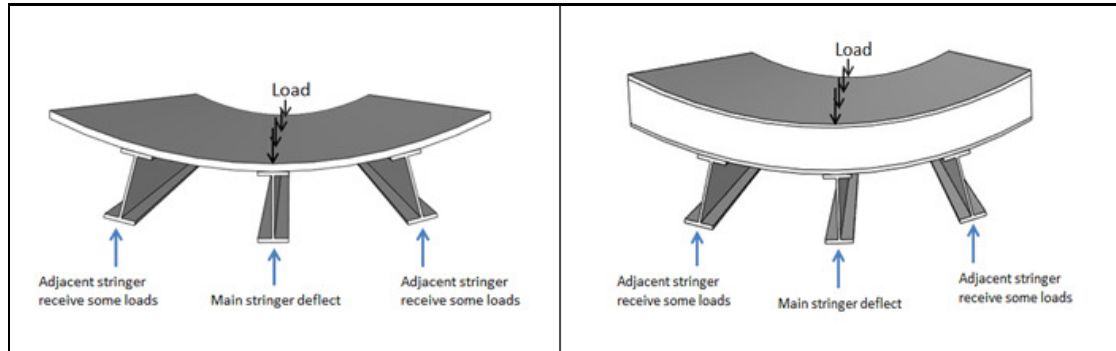


Figure 4.5 *The applied load will be spread to adjacent stringers due to transversal stiffness.*

5 Description and modelling of the bridge

5.1 Background of the bridge

The Koninginne Bridge is located in the city centre of Rotterdam, Netherlands. The bridge spans over the river *Nieuwe Maas* at the port of *Koningshaven* and provide an important connection for the urban traffic.

Initially the first Koninginne Bridge was constructed in 1870 and was then of a swing bridge type, rotating around the middle of the span enabling boats and ships to pass the crossing. Later, as the ships became bigger, the demand for a wider passage was created. Among other things this demand resulted in a reconstruction of the current bridge, which started 1928. This time the Koninginne Bridge was constructed as a double bascule bridge and in 1929 the bridge was completed.

Since then many modifications have been done, the bridge has for instance been widened enabling the addition of sidewalks on each side of the bridge and the original wooden deck has been replaced by an aluminium and steel plate deck. These changes have contributed to an increase in self-weight, which has to be tilted each time the bridge opens. The increased self-weight has resulted in very high counter weights. At the moment each end of the bridge has a counter weight of about 750-800 tons. The machinery that handles the opening mechanism is in frequent need of repairs due to the increased work load. The bridge is a very important traffic connection between the north and south side of the city centre; hence interruption of the traffic is not economical.

5.2 Bridge data

The Koninginne Bridge has 5 vehicular lanes, with approximately 3.5 meter width for each lane. The sidewalks were added in 1982 and have been widened since then. The bridge's longitudinal span for each cantilever is 25.75 meter. Each cantilever has two main truss girders connected to seven transversal beams with moment resisting connections, see Figure 5.1 and Figure 5.2.

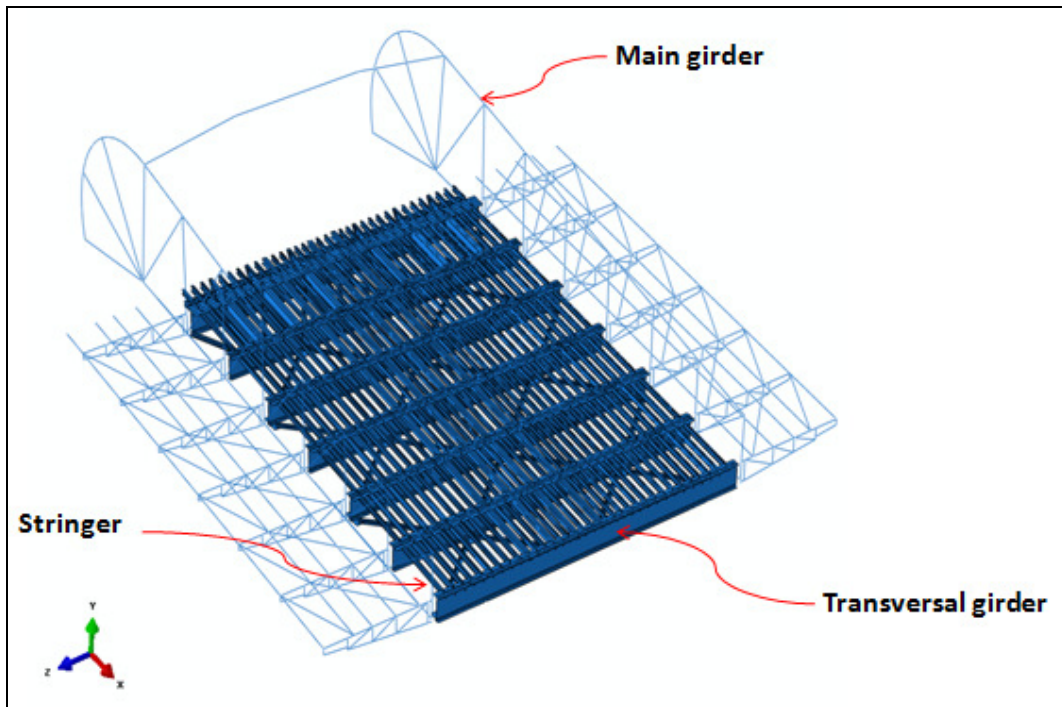


Figure 5.1 The two main girders were modelled with beam elements.

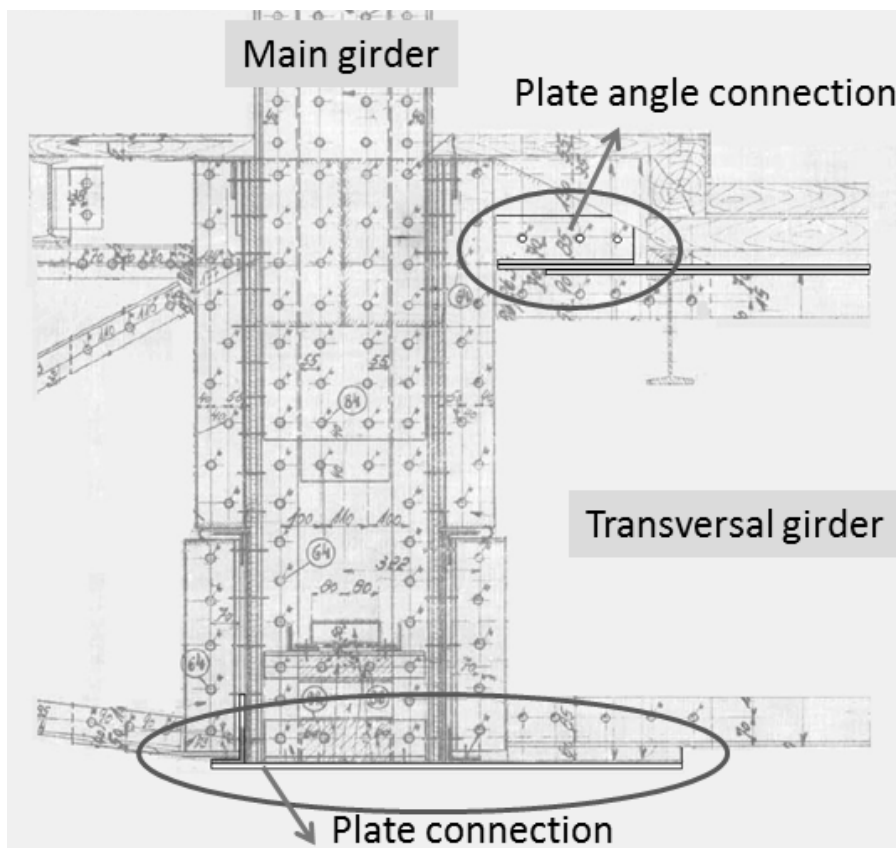


Figure 5.2 Detail of moment resisting connection between main girder and transversal girder.

A number of 4 meter long stringers connect the transversal beams. The connection between stringers and transversal beams is done by rivet connections in top flanges and in the web but not in the bottom flange of the stringers. The connections are considered as almost fixed. See Figure 5.3 for how the connection was modelled and Figure 5.4 for how the connection looks in reality.

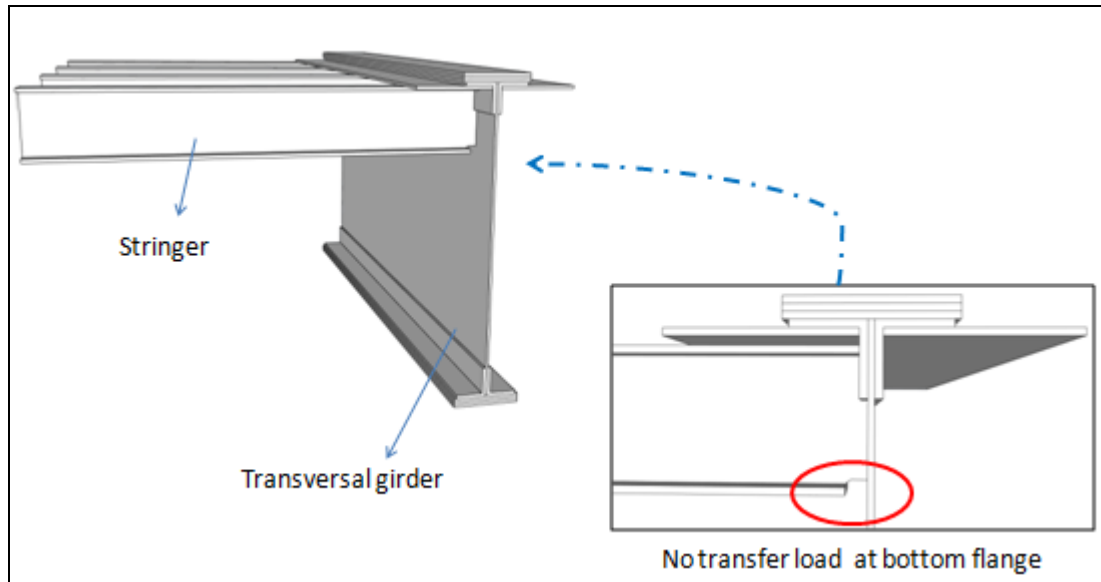


Figure 5.3 Illustration of how the connection between stringers and transversal girder was modelled in Abaqus.

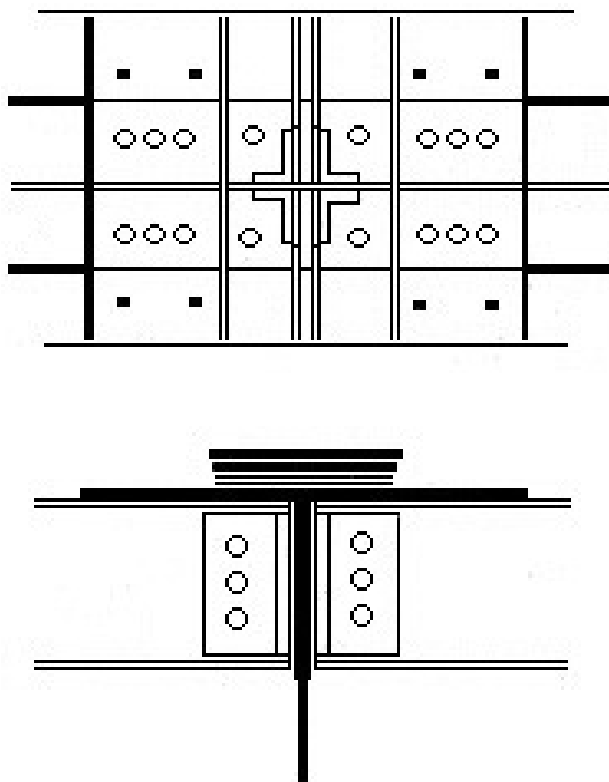


Figure 5.4 Detailed connection between transversal girder and stringers from refined original drawings.

The bridge deck plate is consisting of steel and aluminium, which is connected to pieces of timber beams running along on top of the stringers, see Figure 5.5. The pieces of timber are functioning as spacers to enable the deck to spread the load directly to the stringers without transferring the load directly onto the transversal beams. In Figure 5.3 it can be seen that several steel plates have been attached on top of the top flange of the transversal girder, this was done in order to increase the bending capacity of the transversal girder itself. These plates are connected by rivet connectors which has around 2 cm high rivet heads sticking up along the surface of the top flange of the transversal girder. Because of this situation, it is difficult to connect a member above the transversal girder. Another reason to use 190 mm timber is to keep the same elevation of the bridge deck since the original timber deck was changed.

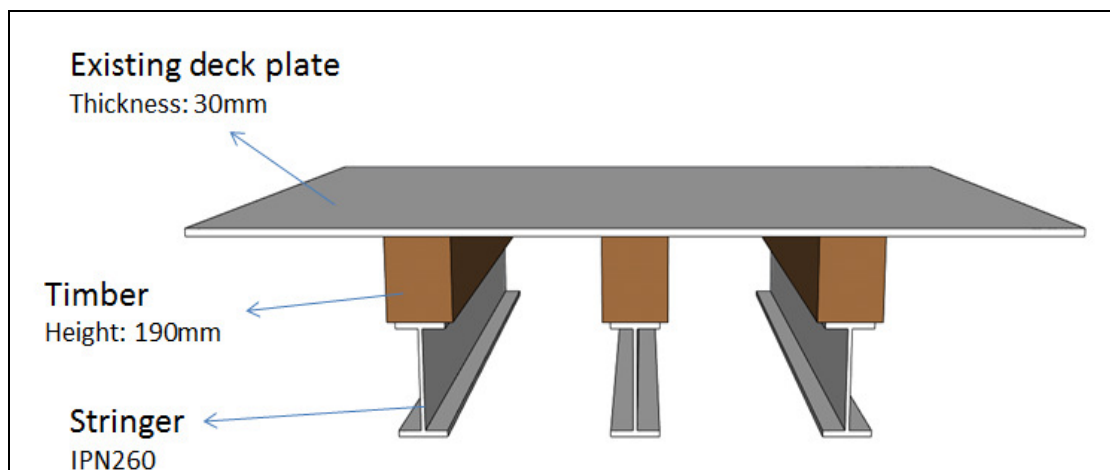


Figure 5.5 The existing steel plate is attached on top of pieces of timber, which are running on top of the stringers.

The main truss girders are supported in the centre of the radiant and also in the counter-weight position, see Figure 5.6. The total self-weight of the existing steel plate deck is around 120 tons for one side of the bridge, the corresponding value for the FRP ASSET deck is 52 tons. When the existing steel deck is replaced by a FRP deck, the difference of the loads between those decks will be 68 tons. This amount of load will decrease the counter weight by 123 tons to be able to achieve equilibrium. Hence each pair of hinges for a cantilever will experience a reduction in force resultant of 191 tons. Therefore each hinge will experience 80.5 tons less weight for the unloaded bridge. This is one out of several reasons why FRP deck has been chosen as a promising solution for the strengthening existing bridge.

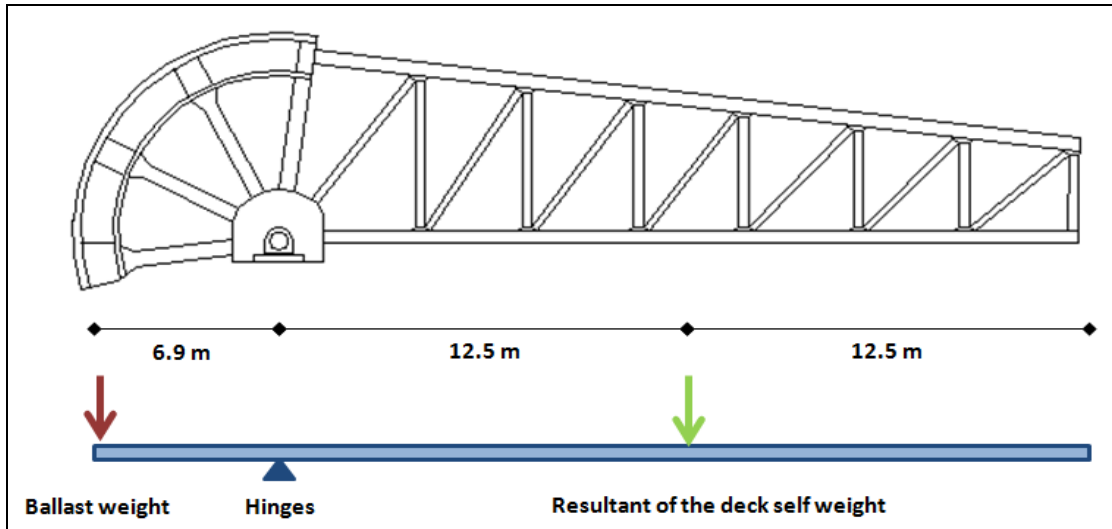


Figure 5.6 Schematic illustration of a main girder and acting forces.

In Figure 5.7 the bridge deck can be seen from below. The circles in the figure show two connections between the both cantilevers which functions as a shear lock in the middle of the bridge. The shear lock connections make it possible to balance the deflection of the two cantilevers with another. Different deflections between the two bridge sides will result in an uncomfortable bump in the intersection of the two bridge halves. In the Abaqus modelling both cantilevers were modelled and connected by tie constraints to represent the reality to a higher extent.

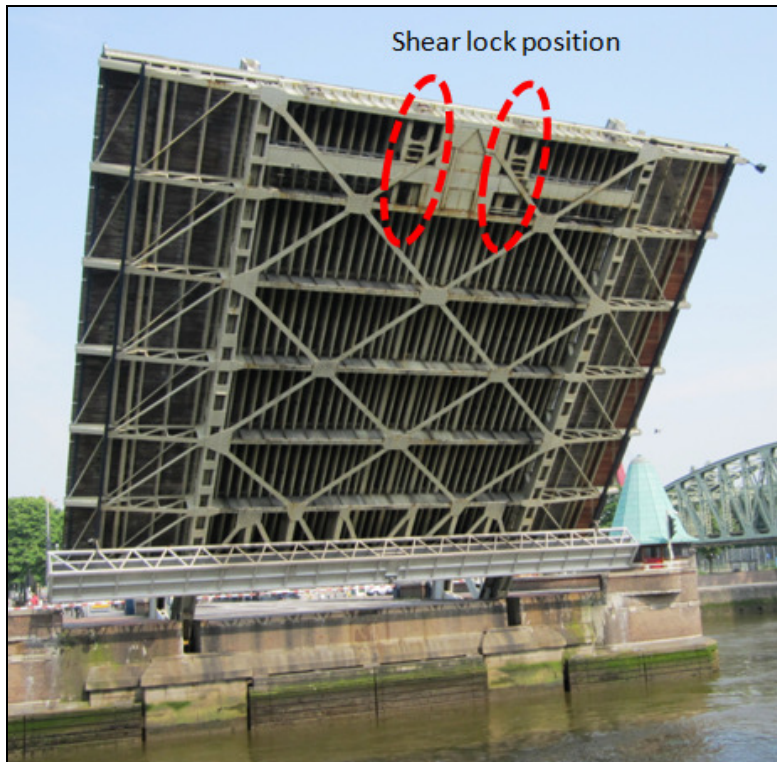


Figure 5.7 Picture of Koninginne Bridge from below. The shear lock connections between the two bridge halves are circled.

5.3 Bridge modelling

During the work with this thesis the bridge was modelled with a finite element (FE) model in Abaqus version 6-11.

For the steel members a Young's modulus of 210 GPa and a Poisson's ratio of 0.3 was utilized. The density of the steel was 7850 kg per m³. Based on the report *Koninginnebrug, V. De stalenbovenbouw* which was written in 1928, the bridge is built entirely in steel quality ST. 48 (both construction steel and rivets) with yield strength of 285 MPa, ultimate stress of 470-560 MPa and elongation of 18 %.

The main girders were modelled as simply supported in the hinges and in the ballast weight position, see Figure 5.6. 3D shell deformable elements were used throughout the model except for the main truss girders, the portal frame and the sidewalk parts where beam 3-D deformable elements were used. In general, mesh size is 80 mm and in places of interest mesh size of 25mm was utilized. The connections between beam element and shell element were modelled using multi point constraints (MPCs), which transfer forces in all 6 degree of freedom (DOF), see Figure 5.8. This type of constrained connection was applied considering the existing condition where moments and forces are transferred between these members.

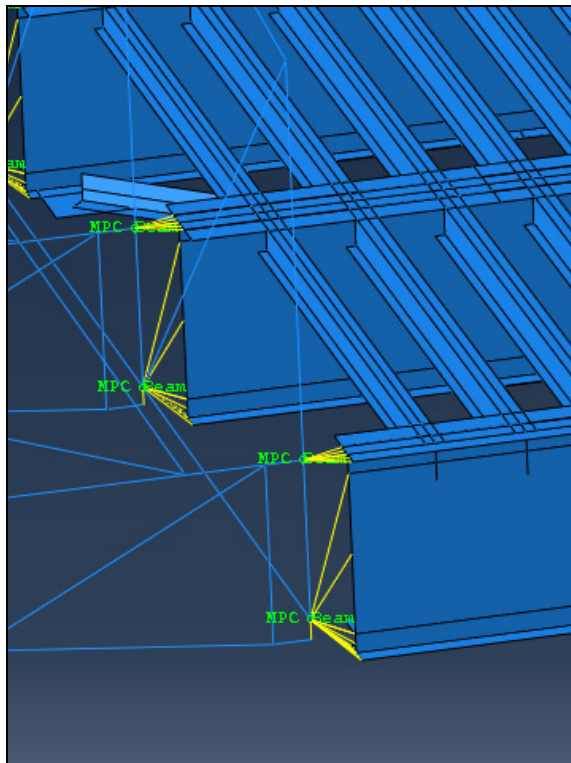


Figure 5.8 The figure shows Multi Point Constraints (MPCs) connections between the main girder and the transversal girders.

The connection between the two cantilever bridge halves was made by tie-tie 3 DOF shear connection between their girders. Meaning no moments are transferred, just shear force. Other connections between beam-beam elements and also between shell-shell elements were made by the merge function in Abaqus. Using the merge function means that shear and moment transfers between those members. The riveted connections in the real structure can transfer moment to a high degree, which means

that the merged connection used represents the real connection. See the connection between the stringer and the transversal girder in Figure 5.3.

The connection between steel plate/FRP and stringers used interaction type *surface-to-surface contact*. *Cohesive behaviour* was chosen under contact property option. Under eligible slave nodes *any slave nodes experiencing contact* was used. This means the cohesive behaviour not only for all nodes of the slave surface that are in contact with the master surface at the start of a step, but also for slave nodes that are not initially in contact but may come in contact during the course of a step was used in contact property of the interaction (ABAQUS User's manual).

Interaction contact property with *rough tangential* and *hard contact normal behaviour* can also be used with apparently the same result.

5.4 Simplifications

In the model the steel and aluminium deck plates were assumed to be a continuous steel plate with a thickness of 30 mm across the traffic area. In reality the deck consists of partly steel and aluminium. This simplification was done due to lack of information regarding the thickness and location of the aluminium deck plate.

There is also a piece of timber on top of stringers to adjust the elevation of the steel plate. In the model timber pieces are neglected because the properties of the timber are unknown and also because of the complex modelling. See Figure 5.9.

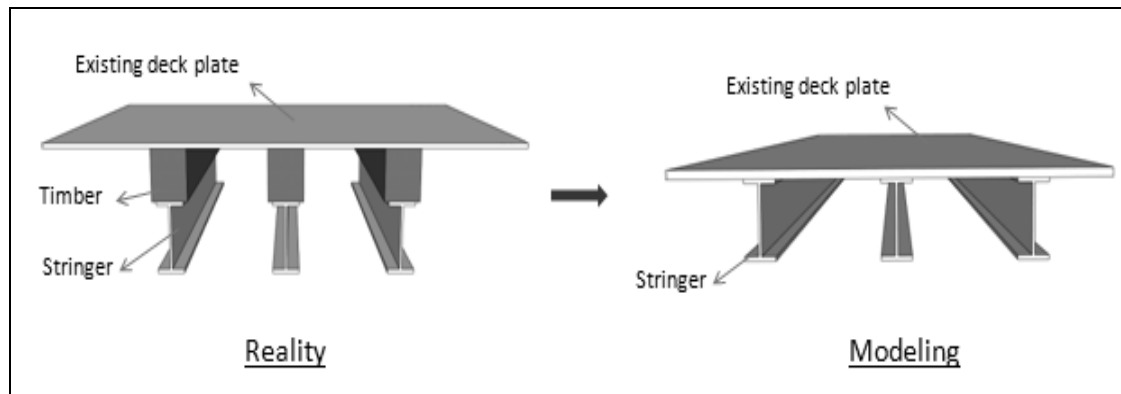


Figure 5.9 Model simplification without pieces of timber and with a solid steel plate.

Full connection between the steel deck and the stringers will result in composite action. It is not only composite action that is achieved, but also a higher side distribution between deck and stringers. It means that the loaded stringer (main stringer) in Figure 5.10 will be working together with adjacent stringers. Therefore part of the capacity depends on composite action and another part depends on the lateral load distribution. The steel deck has a lateral stiffness in the transversal direction which will transfer load to the adjacent stringers when the main stringer deflects, see Figure 6.6 and Figure 6.7 in chapter 6.1.2. The effect of the different concepts can be seen in Figure 5.10.

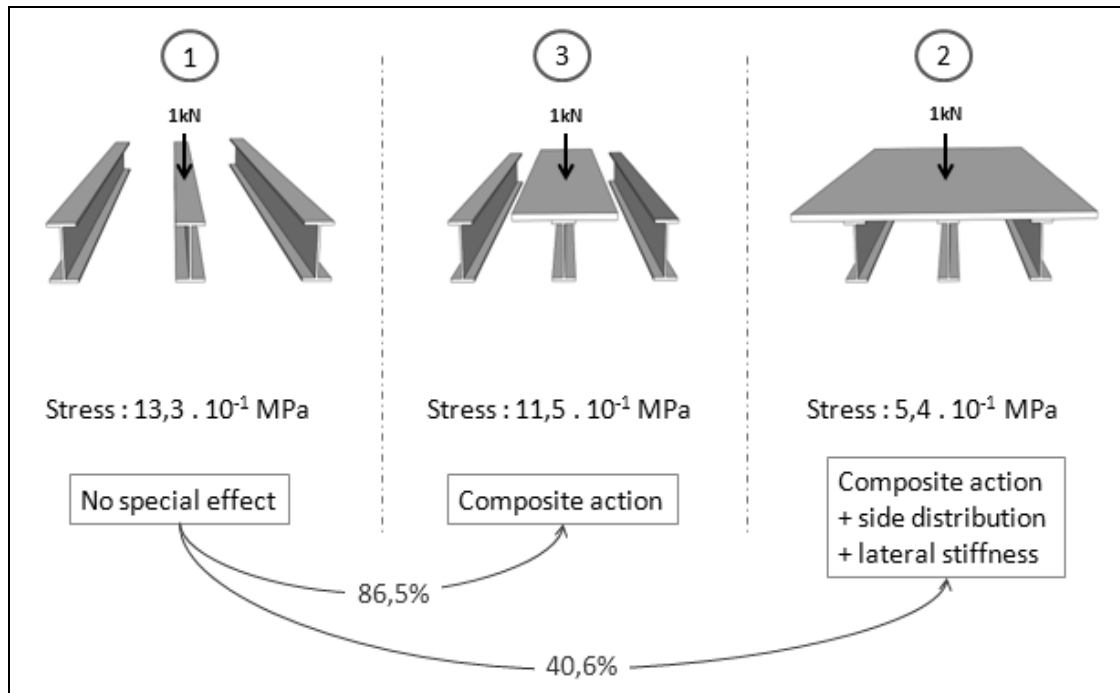


Figure 5.10 Contributing actions to lowering the stresses in stringers.

Another aspect which needs to be noted is the timber member in between the steel deck plate and each stringer. In reality when the softer timber is deforming, the plate and the stringer will not work as a member in full composite action. It means that the interaction between the both members is not completely working together and therefore full composite action is not achieved.

The lateral stiffness for the steel deck will be lower in reality than in the model. This is because the timber is much weaker and deforms easily compared to the steel. The composite action between the materials is a function of the spacing of the fasteners through the steel deck plate and the timber. When a load is applied on the steel deck as in Figure 5.11 the middle stringer will deflect causing the timber to skew. There will not be full interaction in reality because the steel will be able to slide compared to the timber due to the weak nature of the material and the large spacing of bolts through the members. The bolts have a spacing of about 450mm in a single but staggered row; this is too large spacing to achieve full composite action because slip between materials can be happened. Since it would be far too time-consuming to model the connection with the pieces of timber for the whole bridge and no data was known about the timber material a simplification was made to neglect the timber in the model. Some values for at what extent the composite action and the lateral stiffness contributed to the overall stiffness were achieved from smaller models, these number or percentages are used later in sub-chapter 6.3.3.

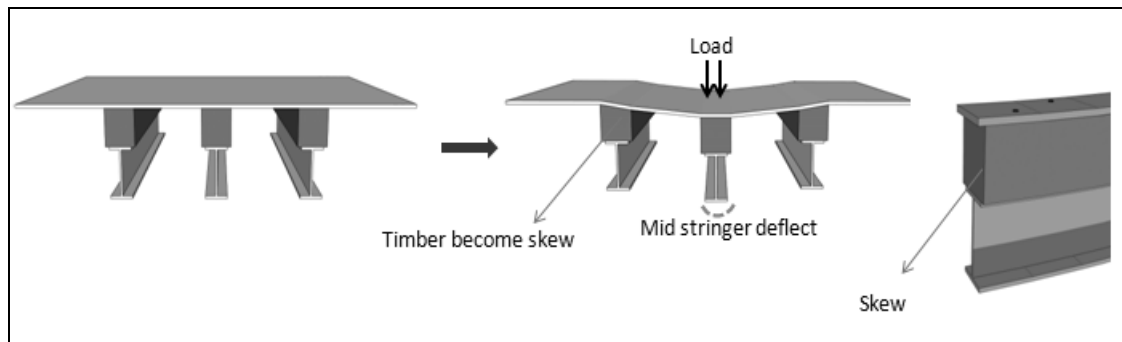


Figure 5.11 Influence of timber becoming skew when steel deck is loaded.

5.5 FRP deck shape suggestion

Due to a number of rivets heads sticking up above the transversal girder flange there is a problem with installing an FRP deck directly on top of the transversal girder. One of the solutions could be by using a modified FRP deck like in Figure 5.12. With the FRP deck with the pultrusion arrangement in the transversal direction, the majority of the load will be moving in transversal direction. This condition can create new problem when traffic load is located exactly above the transversal girder. To be able to transfer load in longitudinal direction the FRP part above the transversal girder has some additional options such as using:

- Additional filler (light concrete).
- FRP honeycomb sandwich deck.
- FRP textile shape.

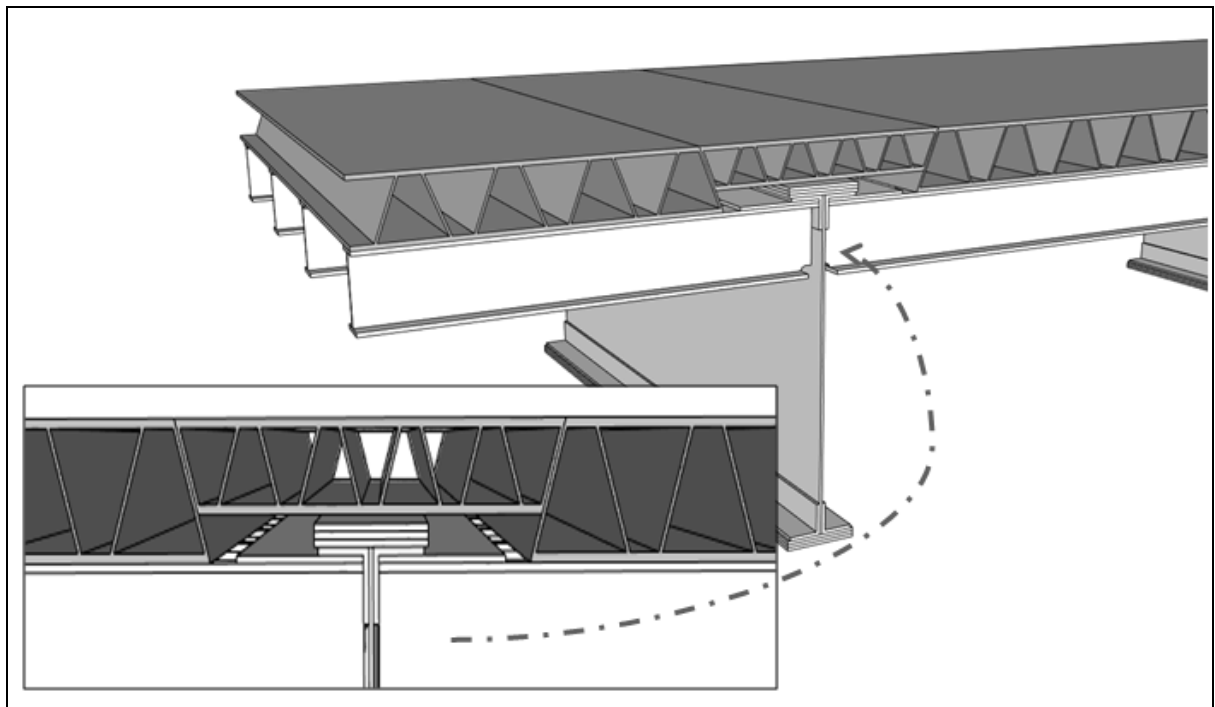


Figure 5.12 Suggestive illustration of how a special piece of FRP deck could be fitted over the transversal girder.

6 Results

6.1 Concept of force transfer - results

Three simple FE models were studied in order to learn the effect and behaviour of composite action and lateral load distribution for the different deck configurations. The results of these models are presented in the two following subchapters.

6.1.1 Composite action - result

A stringer and the FRP deck in the bridge was studied locally to see how composite action between the members worked. With traffic load according to Eurocode load model 1, the strain along the height of the member was plotted, see Figure 6.1. Complete adhesive connection between top flange of the stringer and bottom plate of the FRP deck made a smooth intersection of the strain between stringer and FRP deck. When the strains of each member were obtained, the stresses could be acquired by multiplying the corresponding strains with respective elastic modulus of the different materials. Because of the different material properties the stress in the bottom deck of FRP deck is lower compare to the stress in the top flange of steel stringer.

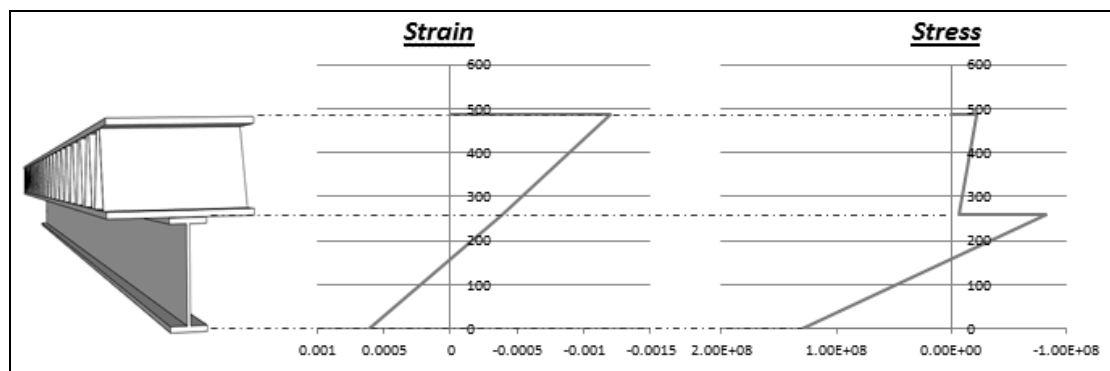


Figure 6.1 Measured stress-strain relation for steel stringer and the FRP deck, composite action was achieved.

Figure 6.2 explains how the stress distribution varies along the stringer. A path was made in the bottom flange of a stringer to record the stresses and 1 kN was applied in middle of the span. Two models were compared, one with FRP deck (red colour) and the other with the existing steel deck (blue colour). The purpose of this graph is to show how composite action affects the stresses for the whole span of the stringer.

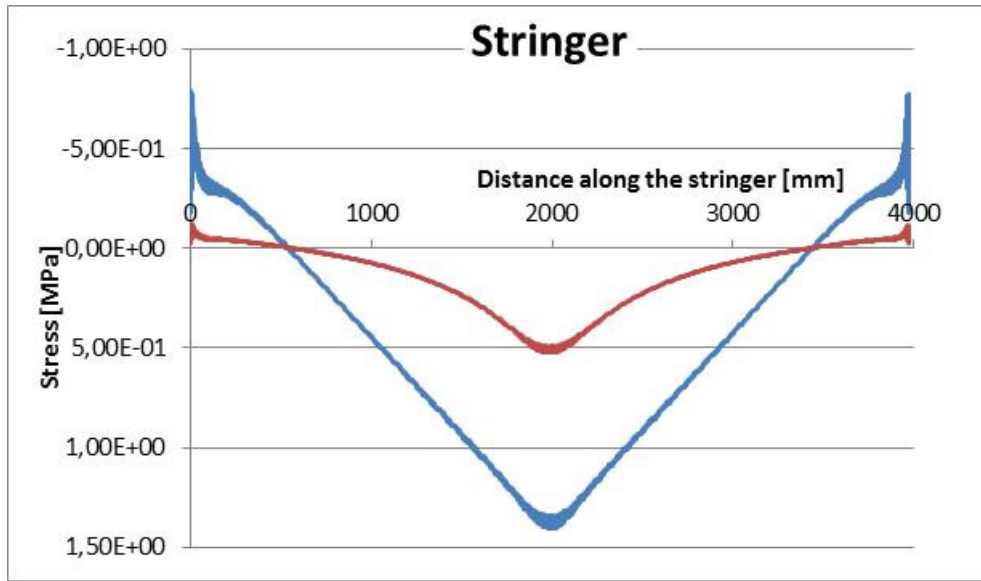


Figure 6.2 Stress distribution along the span of the stringer, blue colour for the existing steel deck and red colour for the FRP deck.

6.1.2 Lateral distribution of load – result

In Eurocode the presence of a set of bogie axles as live load has a decisive factor in the capacity of the bridge's member for the static and the fatigue analysis. Live load on the bridge is represented by a number of wheels for when the truck moves over the bridge. In theory, if the wheel is located exactly above one of the bridge's stringers then the whole load will be carried by that main stringer and the distribution factor of the load will be 100% in that main stringer. But in reality when the steel plate or the FRP deck is applied, the adjacent stringers will work together with the stringer underneath the wheel due to the transversal stiffness of the deck. Because of this effect, the load will not only be carried by one stringer (main stringer) but also by other stringers close to the one directly underneath the applied wheel load.

To study the behaviour of the lateral load distribution, due to the lateral stiffness, a small model of stringers with applied deck was modelled. See Figure 6.3 to Figure 6.5 for illustration of load spreading due to different lateral stiffness in the variety of applied decks. The boundary condition of the stringer was assigned in the bottom end of each stringer. The restraining degree was chosen to be pinned in one side and as a rolled connection in the other side of each stringer. The length of a stringer is 4000 mm in longitudinal direction and with a spacing of 450 mm. Three Abaqus models were made; stringers with FRP deck, stringers with steel deck (30 mm thickness) and finally stringers without any deck, see Figure 6.3 to Figure 6.5. The material properties of stringers and the steel deck were as for common steel. Material properties for the FRP deck are based on FRP ASSET-deck properties. A 1kN vertical point load was applied in the middle of each model. The reaction force at the connections of the stringers was recorded to see how the load distributed between stringers. Moreover stresses in the bottom flange at mid-span of the stringer were recorded as well to see how stresses were distributed, see Figure 6.6 and Figure 6.7.

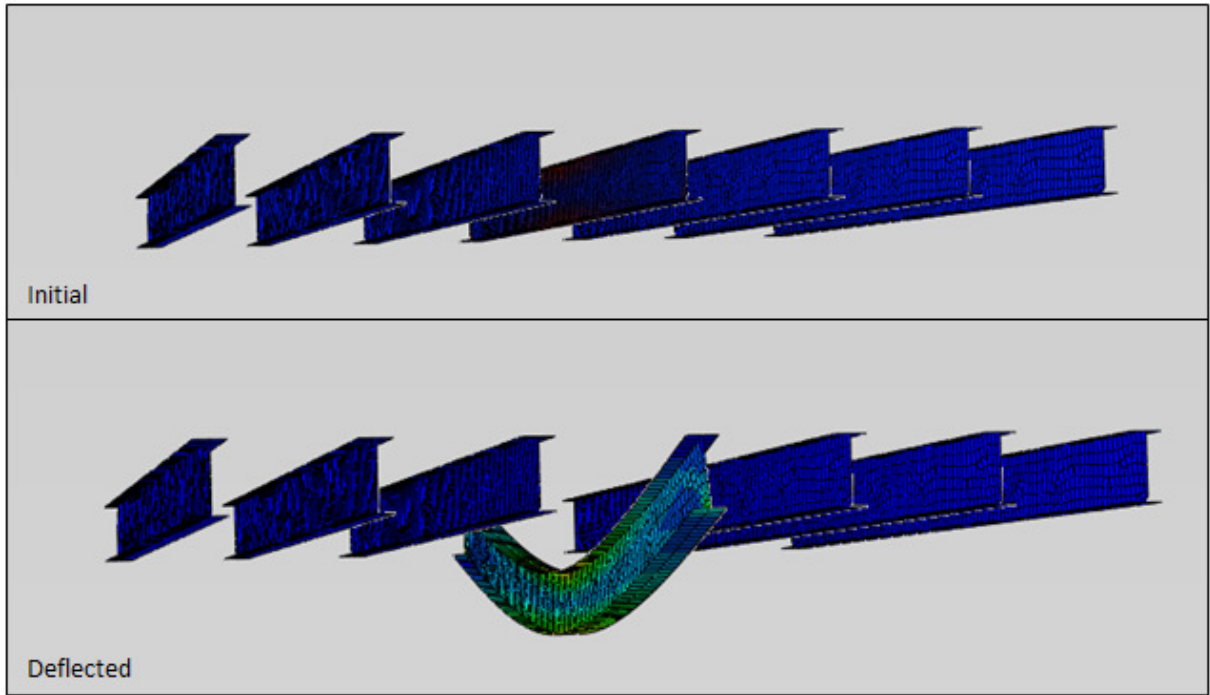


Figure 6.3 Stringers without deck, 1 kN applied directly on top of the mid-stringer.

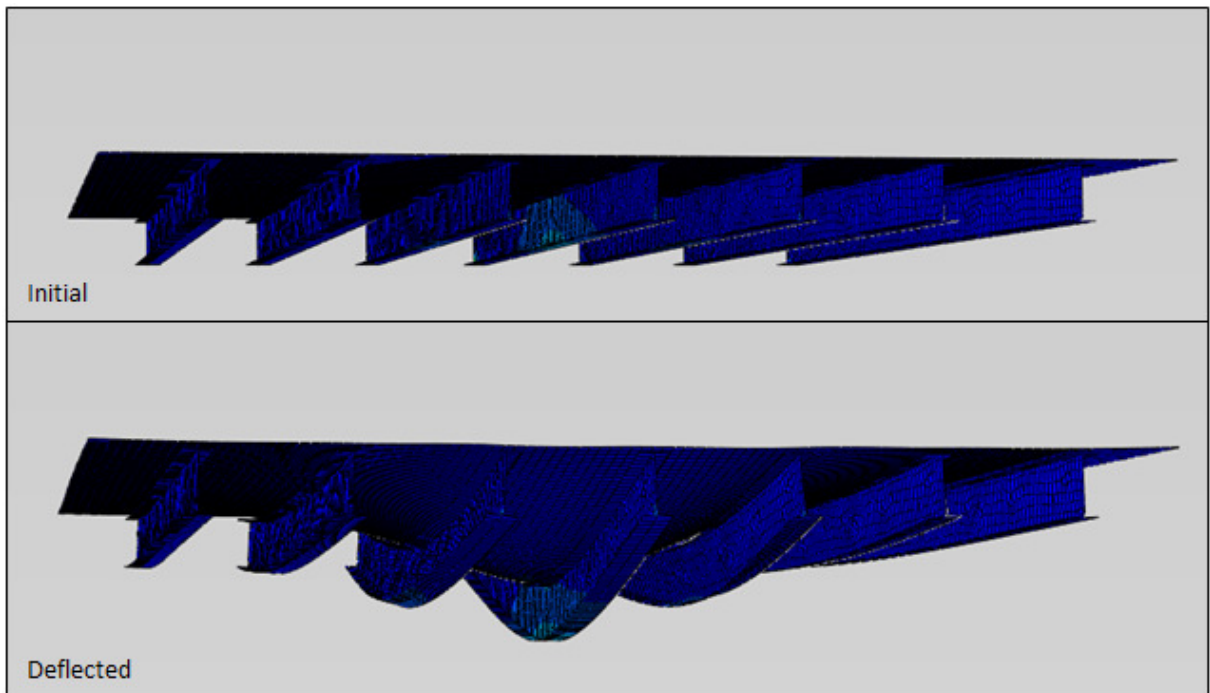


Figure 6.4 Stringers with applied steel plate deck, adjacent stringers help carry the load.

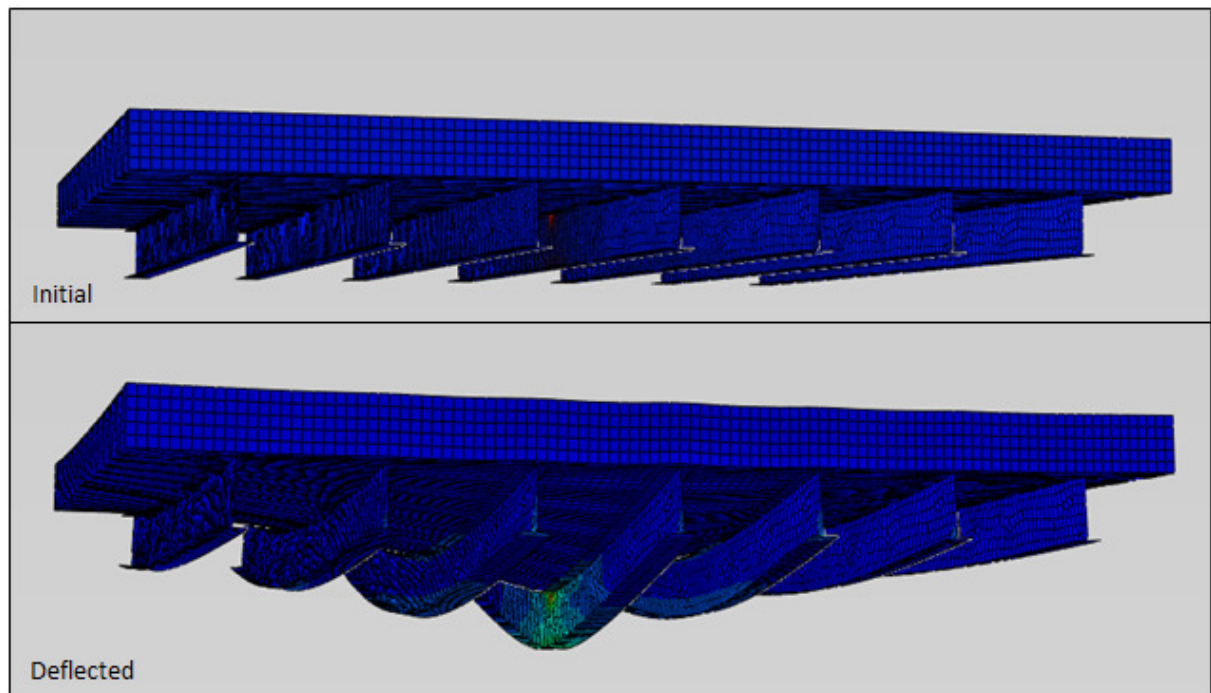


Figure 6.5 Stringers with applied FRP deck, the adjacent stringers help carry the load.

Figure 6.5 shows a magnification of the deflection when the FRP deck and the stringers work together. Main stringer (where the point load is applied) is located in middle of the deck. From the picture it can be seen that the deflection of this stringer is higher compared to the other stringers. In Figure 6.6, the stresses which were measured in the bottom flange at mid-span of the stringers were recorded. It is obvious that the stress in the main stringer is higher compared to other stringers. This can easily be reviewed from high strain due to high deflection in this area.

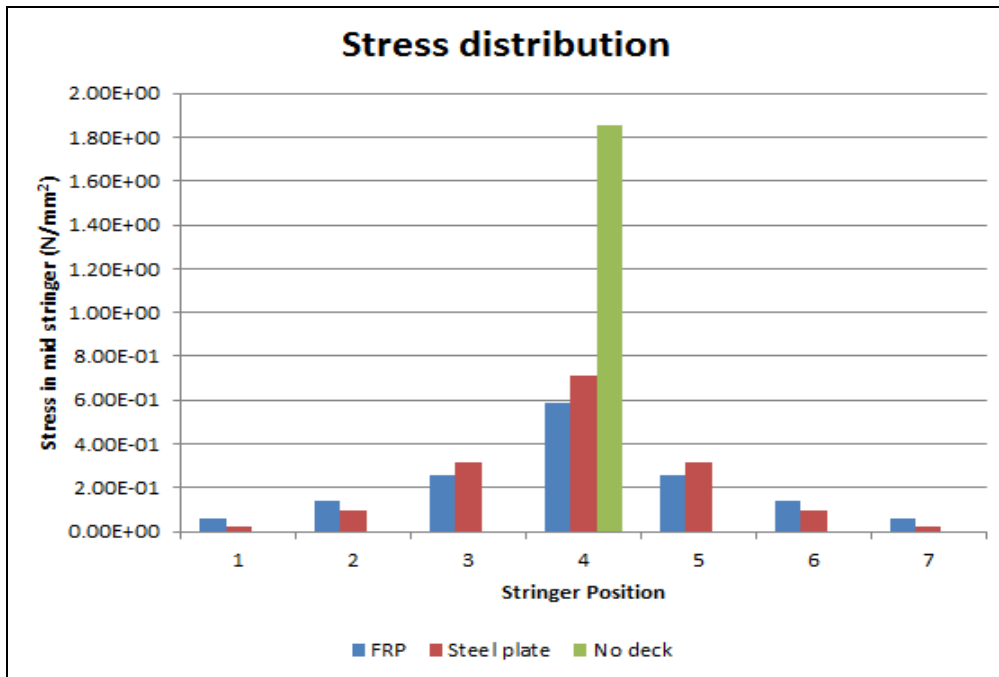


Figure 6.6 Stresses in bottom flange for each stringer at mid-span for the three different models. Stringer position 4 corresponds to where the load was applied.

Figure 6.7 explains how the load distribution varies because of the transversal stiffness. In the case without deck (green colour), the whole load is carried in the main stringer alone. For the model with the existing steel deck (red colour) shows that the load spreads to the other stringer but the main stringer still received a higher percentage of the load. In the case for which the FRP deck is applied (blue colour), the distribution of load is almost similar in the three stringers closest to where the load is applied. The load distribution percentage of adjacent stringers is slightly higher than in the stringer where the load was located. The explanation to this could be because of the longitudinal span of the stringer is longer compare to spacing between stringers. Because of this the deflection is greater in the main stringer at mid-span and therefore the transversal stiffness of the FRP deck distributes the load to the adjacent stringers, see Figure 6.8.

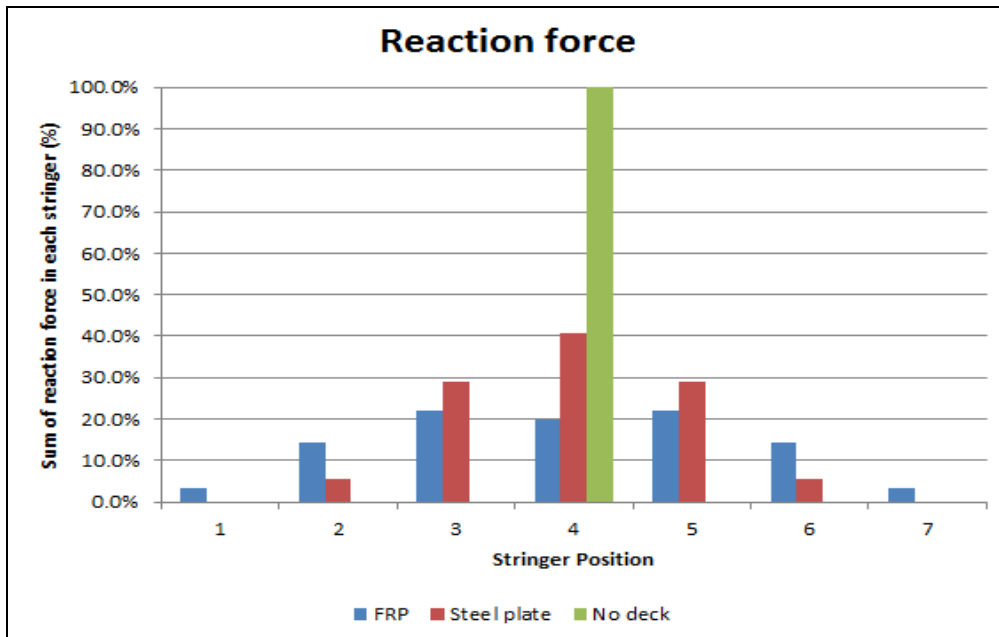


Figure 6.7 The diagram shows the proportion of the applied load that the stringers carry. Stringer position 4 corresponds to where the load was applied.

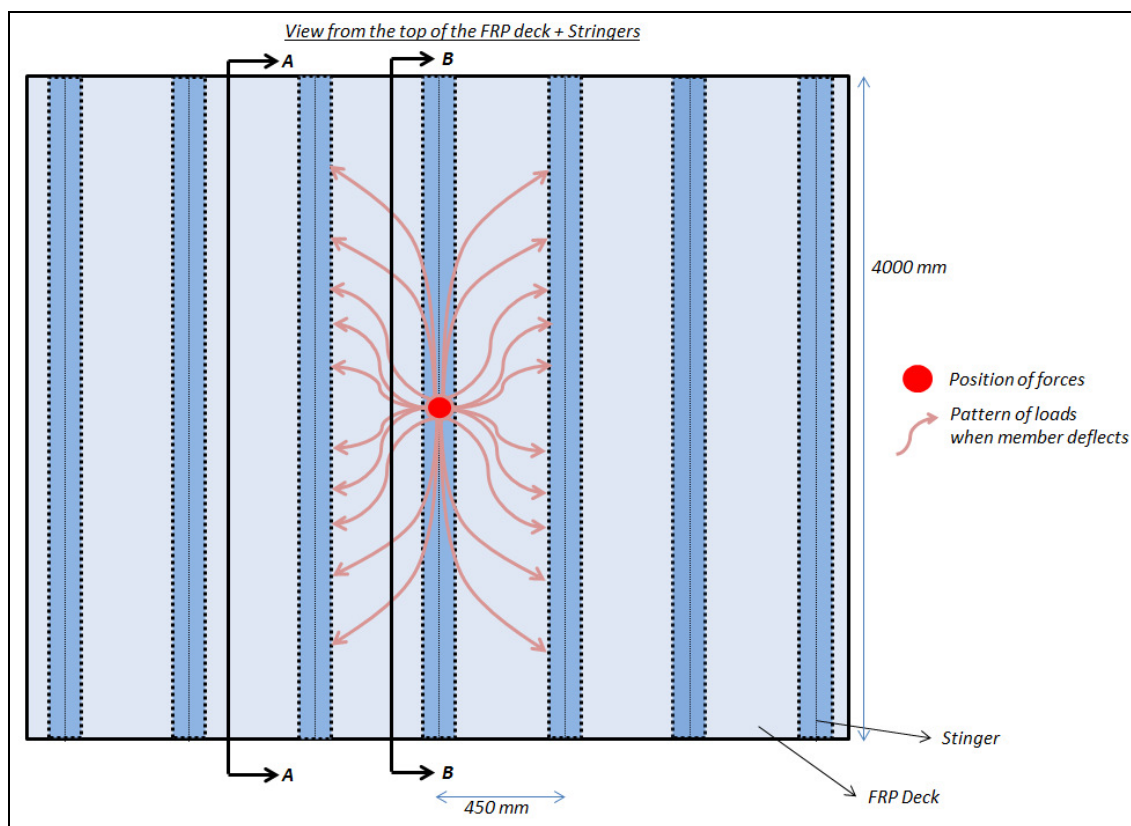


Figure 6.8 Schematics of how the load could be spreading from the point of application to the adjacent stringers.

Figure 6.9 shows detail section A-A and section B-B from previous Figure 6.8. It is obvious that the deflection of the main girder (section B-B) is shaped like of a triangle, which is typical for a point load. While the deflection of the adjacent girders (section A-A) represents a parabolic shape, which is typical for distributed loads. The distributed load is achieved because of the high stiffness of the FRP deck in its pultrusion direction. From Figure 6.10, diagrams of the shear stresses along the web of stringers can be seen. It is clear the shape of the diagram represents how load is applied (point load for the main stringer, while distributed load for the adjacent stringers).

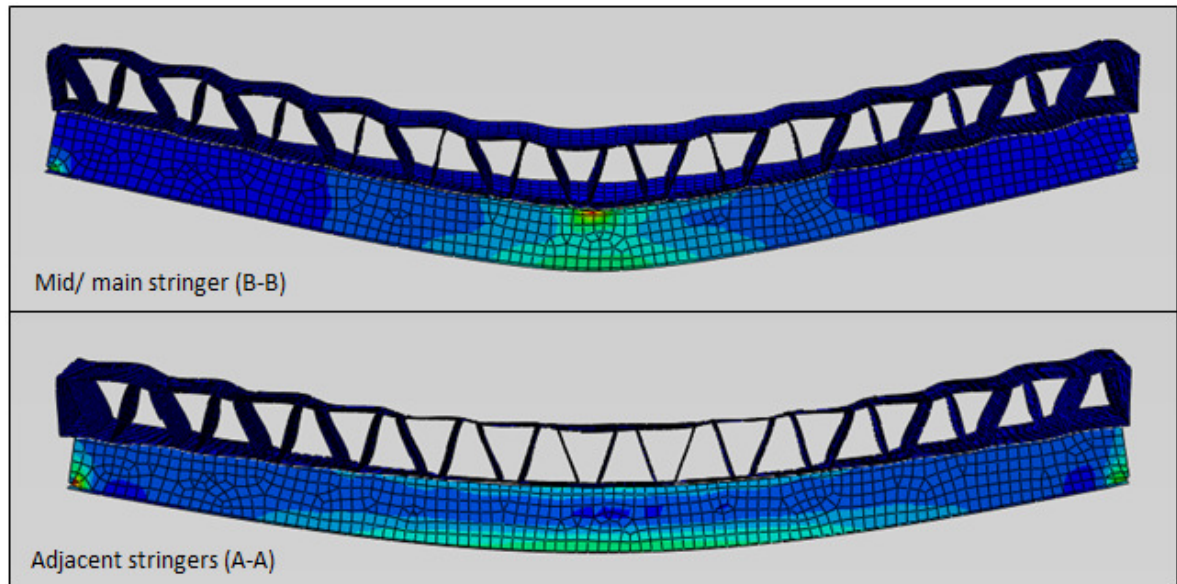


Figure 6.9 Illustration stress magnitude and deflection for two sections. In top: main stringer. In bottom: adjacent stringer.

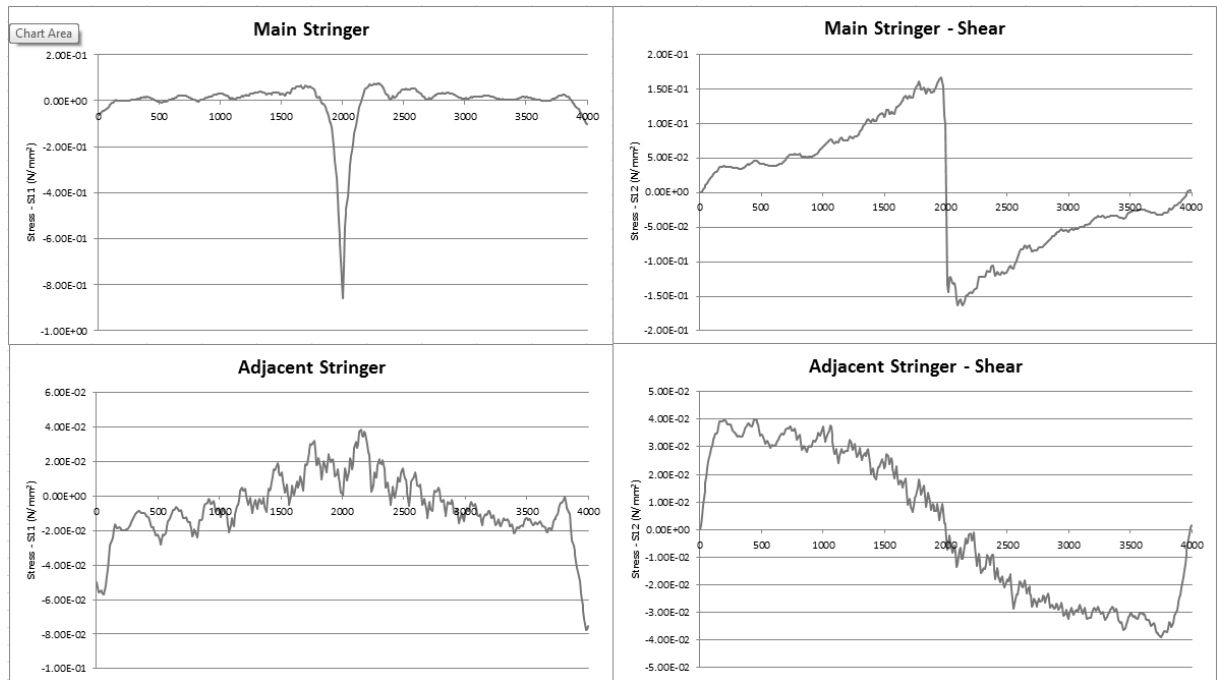


Figure 6.10 To the left: Plots of stress distribution along the stringers. To the right: Distribution of shear stress in the web along the stringer. In the top: Main stringer. In the bottom: Adjacent stringer.

6.2 Fatigue

6.2.1 Background information

One of the objectives of this thesis was to lower the self-weight of the bridge and see if the traffic load could be increased. Just by replacing the metal plate deck with an FRP deck a lot of weight is removed. To be able to carry an increase in traffic load the connection of the stringer and the transversal girders could be experiencing a higher stress. Therefore a fatigue assessment was performed to determine first of all if the traffic load could be increased and secondly if some stringers could be removed to strip the bridge of further excessive self-weight. By removing every other stringer a total weight reduction of around 15 tons could be accomplished, which was considered to be too low.

6.2.2 Method of analysis

Fatigue load model 3 was used for checking how the bridge was responding to fatigue loading. Two wheel loads were added in Abaqus with a unit load of 1kN each, this was done to simulate a unit axle load. The position of the axle load was then shifted from the start to the end of the bridge. Stresses were measured in different members for each new location of the axle load. The measured values were then imported in a Matlab program which created influence lines for the different members. In Figure 6.11 an influence line can be seen for a stringer in the middle of the bridge, the stars are values measured in Abaqus and the continuous line is the influence line connecting between the stars.

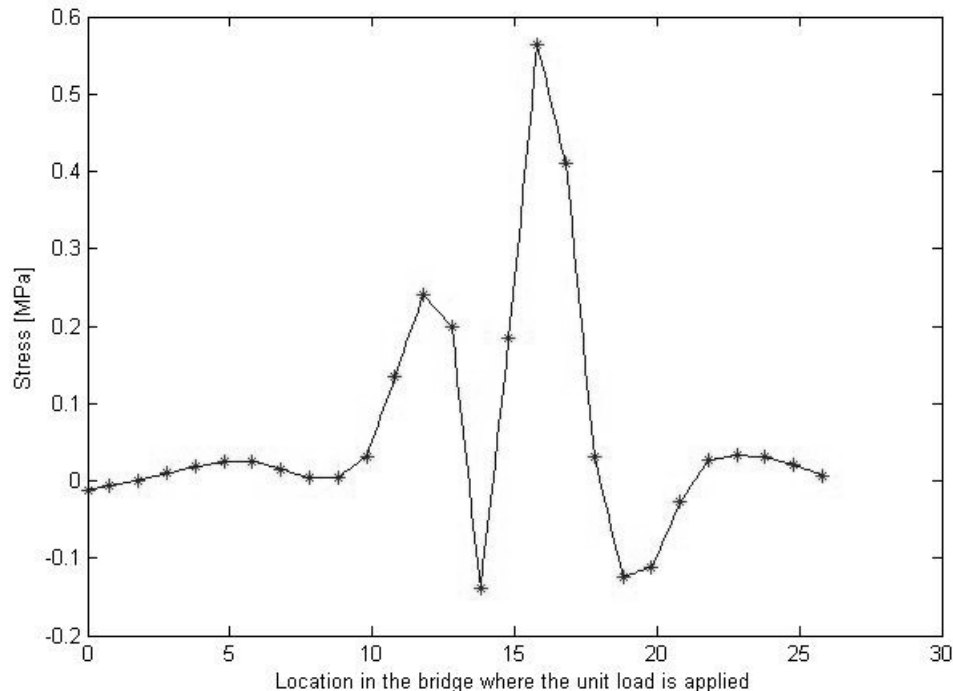
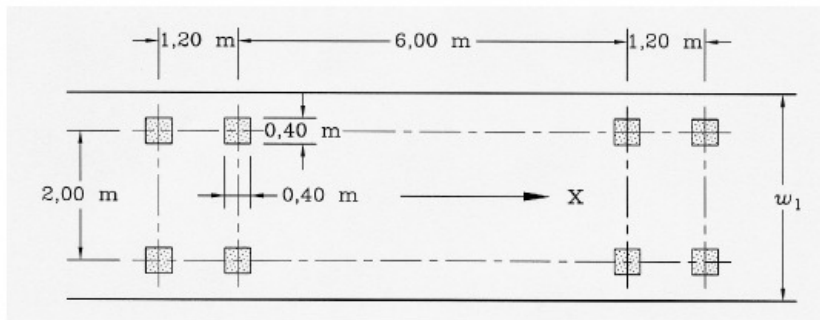


Figure 6.11 Influence line for a stringer connecting measured values from Abaqus.

The vehicle used in fatigue load model 3 is illustrated in Figure 6.12, each axle load has a load of 120kN. Because each wheel load was modelled as 1kN a factor 60 was used to determine the actual stresses generated by each axle.



Key
 w_1 : Lane width
 X : Bridge longitudinal axis

Figure 6.12 Vehicle used in fatigue load model 3.

From the influence line and the geometry of the vehicle used in fatigue load model 3 the stresses that the member experience from each vehicular passing can be determined. This was done by superposition of the stresses generated in the influence line from the location of the four different axle loads. The stress from fatigue load model 3 in a stringer in the middle of the bridge is illustrated in Figure 6.13.

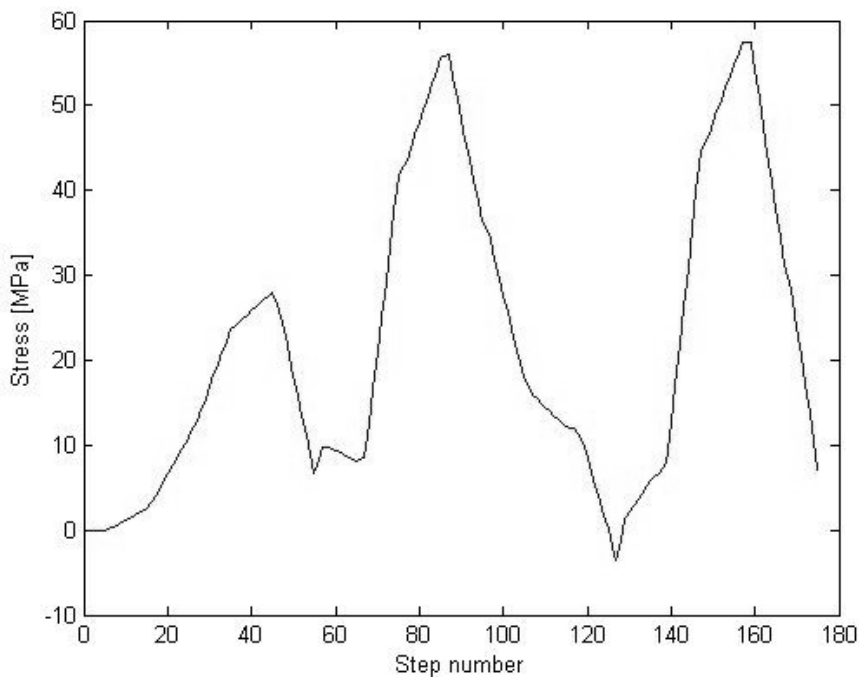


Figure 6.13 Total stress distribution for one vehicle passing across the bridge.

6.2.3 Results fatigue

In this section the results of the fatigue analysis is presented. For assessing the fatigue three critical members had their stress variation examined for fatigue load model 3. The same members were analysed with both the existing deck as well as for the FRP deck. The studied members were:

1. Stringer in the top flange and close to the connection to a transversal girder.
2. Transversal girder in the bottom flange at mid-span.
3. Main girder close to the base of the bridge in order to achieve maximum variation in axial stress.

When all members are presented for the both the steel deck and the FRP deck, a short summary of the stresses for each deck and member are shown in Table 6.1. When the stress variation is determined for each member and deck type, the respective detail category is inserted into the S-N curve. From there the number of cycles for the current stress variation can be seen and the number will tell if there will be problems with fatigue life.

6.2.3.1 Stringers

One stringer in the middle of the bridge is shown to study the stress variation due to fatigue loading corresponding to a vehicle passing the bridge. The lines in Figure 6.14 represent the movement of the wheel loads for one axle passing the bridge.

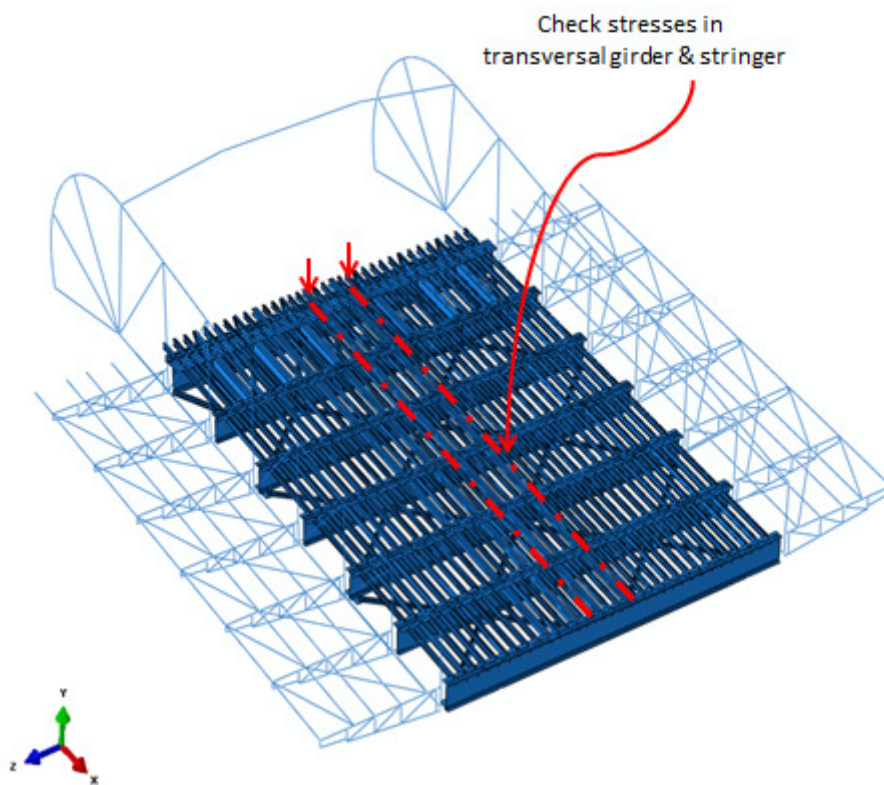


Figure 6.14 The lines represent the movement of the axle load, the picture also shows which stringer and transversal girder was checked with respect to fatigue.

The stringer and transversal girder that was checked with respect for fatigue loading can be seen in Figure 6.14 and the point where the stresses was checked can be seen in Figure 6.15.

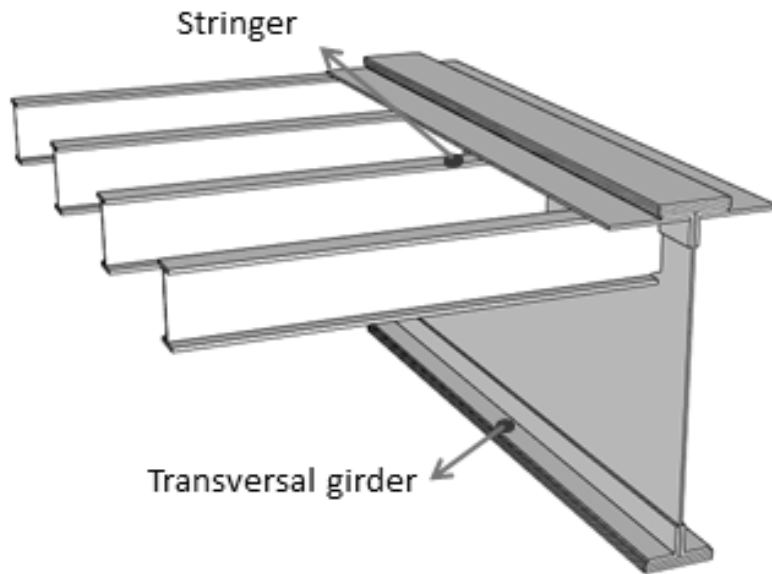


Figure 6.15 Picture showing where stresses were checked for fatigue assessment.

The axle load was applied so that the stringer experienced the worst case, meaning one of the wheels was placed directly on top of the stringer. The influence line can be seen in Figure 6.16.

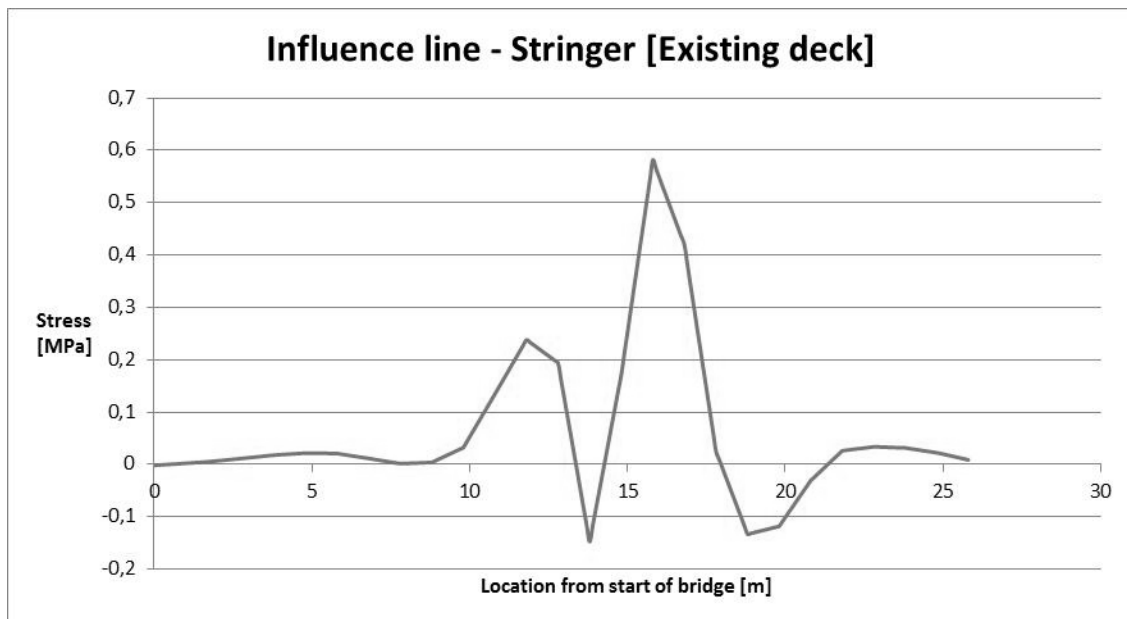


Figure 6.16 Influence line – Stringer [Existing deck]

The high peak value in Figure 6.16 corresponds to when the unit axle load is located in mid-span of the measured stringer.

The influence line in combination with the movement of the vehicle from fatigue load model 3 generates the stress variation in Figure 6.17.

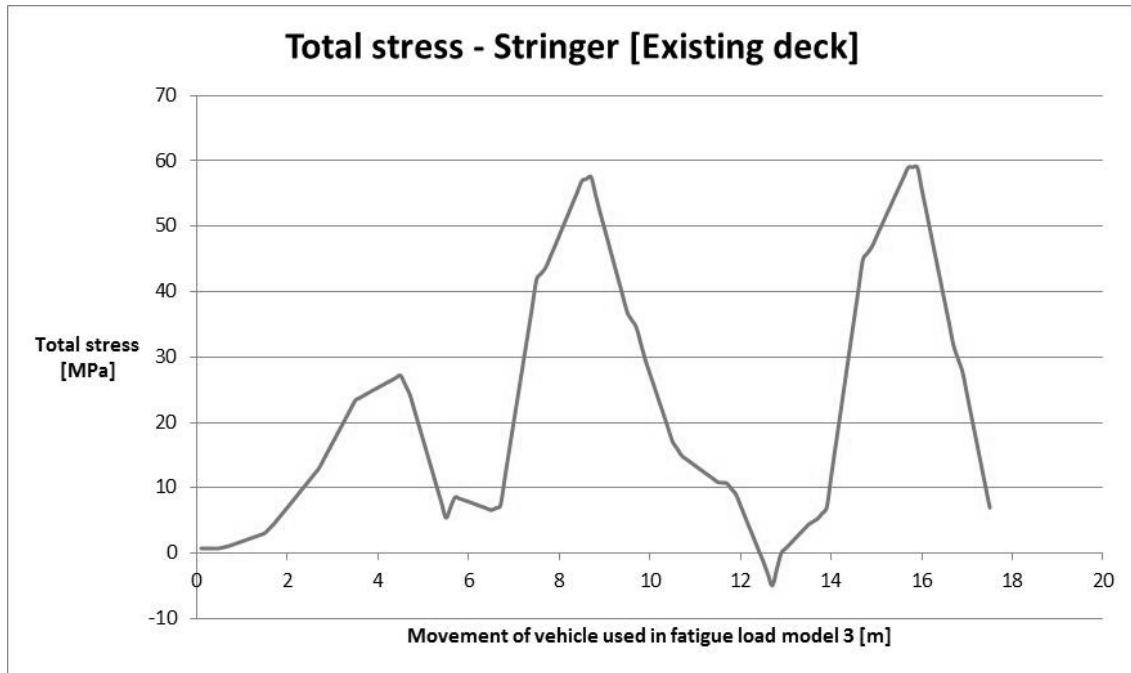


Figure 6.17 Total stress – Stringer [Existing deck]

The maximum stress obtained in the connection between stringer and girder was 59.06 MPa and the lowest stress was -4.92 MPa, thus the stress variation ($\Delta\sigma$) for one vehicle passing was 64.0 MPa.

Stringer FRP-deck

Similar to the model with the existing deck a unit axle load with the same magnitude and location was applied but this time on top of the FRP deck. The influence line created can be seen in Figure 6.18.

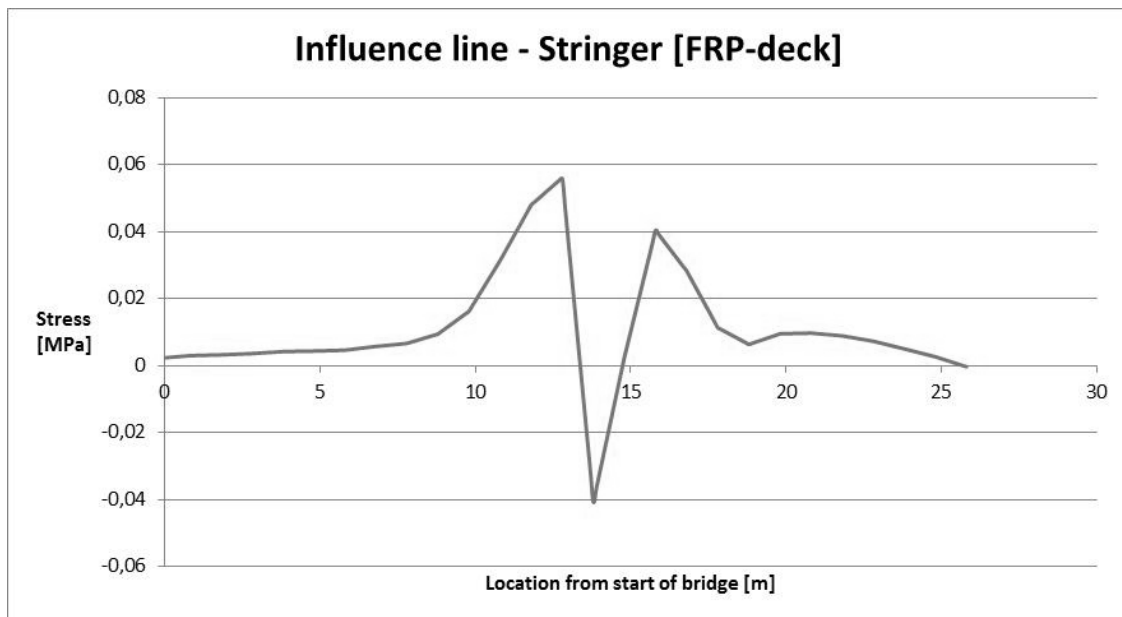


Figure 6.18 Influence line – Stringer [FRP-deck]

For the FRP deck the position of the unit axle load which create the peak value for the influence is shifted compared to for the existing deck. See Figure 6.18 for influence line for the FRP deck and compare to Figure 6.16 for existing deck. It can also be seen that the stress for the model with FRP deck is considerable lowered.

The influence line for the FRP deck model in combination with the movement of the vehicle from fatigue load model 3 generates the stress variation in Figure 6.19.

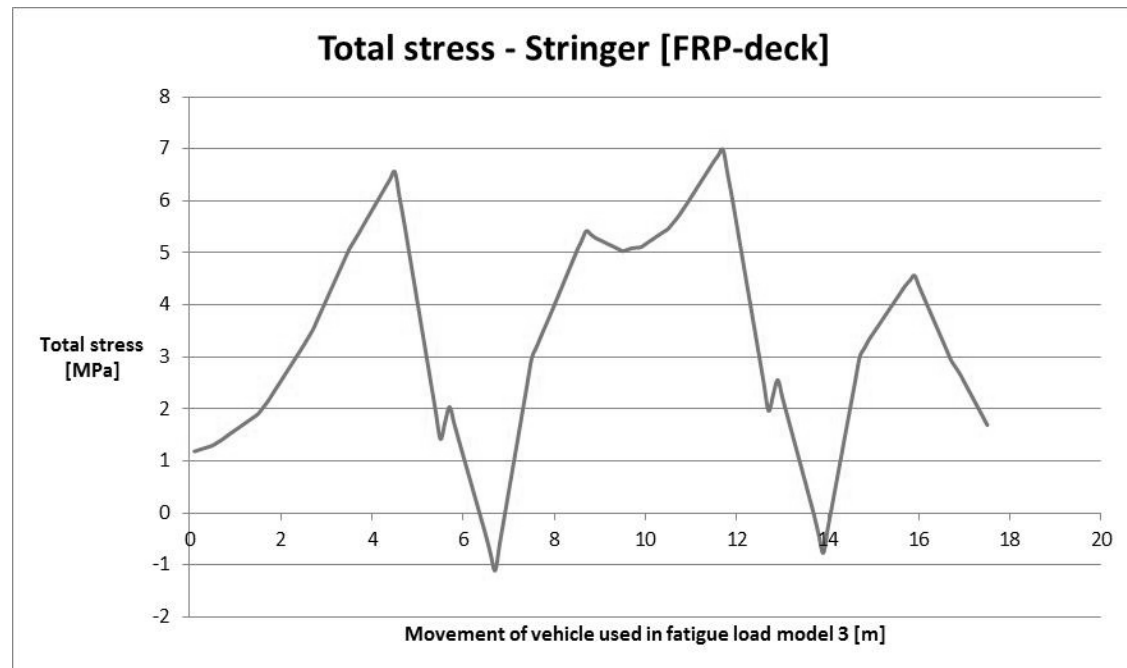


Figure 6.19 Total stress – Stringer [FRP-deck]

The maximum stress obtained in the connection between stringer and girder was 6.98 MPa and the lowest stress was -1.11 MPa, thus the stress variation ($\Delta\sigma$) for one vehicle passing was 8.1 MPa.

The possibility to a major decrease of nominal stress close to the connection between the stringer and the transversal girder has made fatigue failure in this area avoidable.

6.2.3.2 Transversal girder

One transverse girder in the middle of the bridge was chosen to assess the fatigue loading, see Figure 6.14 for location of the transversal girder under consideration. In order to measure the highest possible fatigue load stresses in the transversal girders the axle load was placed in the middle lane of the bridge and then moved along the length of the bridge.

The stresses measured in the bottom flange of the transversal girder for the different locations of the unit axle load can be seen in Figure 6.20.

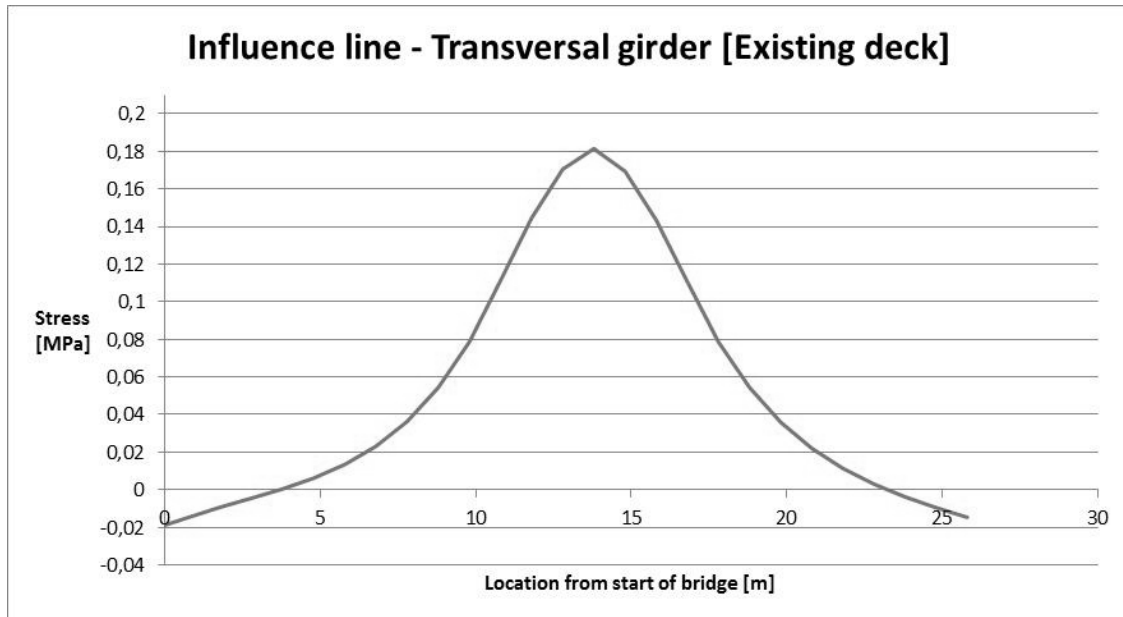


Figure 6.20 Influence line – Transversal girder [Existing deck]

The peak value in Figure 6.20 is the value for which the axle load is applied directly on top of the transversal girder for which the stresses were measured.

When the vehicle from fatigue load model 3 is applied to the influence line of the transversal girder the total stress variation is achieved and can be seen in Figure 6.21.

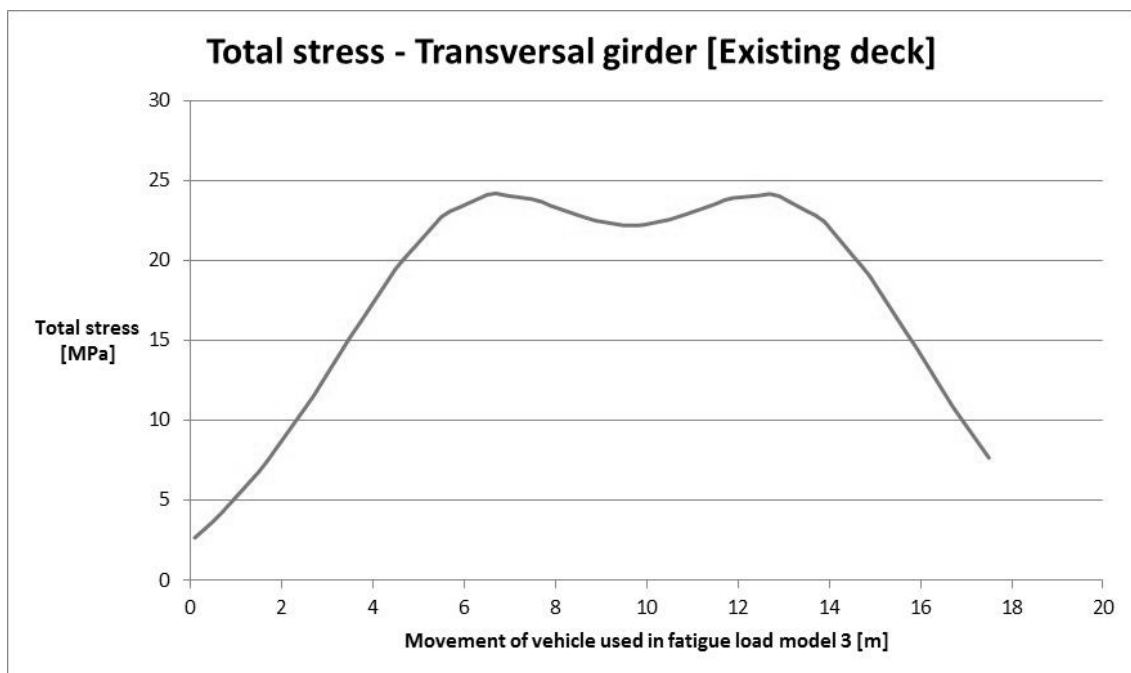


Figure 6.21 Total stress – Transversal girder [Existing deck]

The maximum stress obtained in the bottom flange in mid-span of the transversal girder was 24.20 MPa and the lowest stress was 2.68 MPa, hence the stress variation was 21.5 MPa.

Transversal girder FRP-deck

The same transversal girder was checked in the same position but with the FRP deck applied. The stresses measured for the model with the FRP deck the following influence line is illustrated in Figure 6.22.

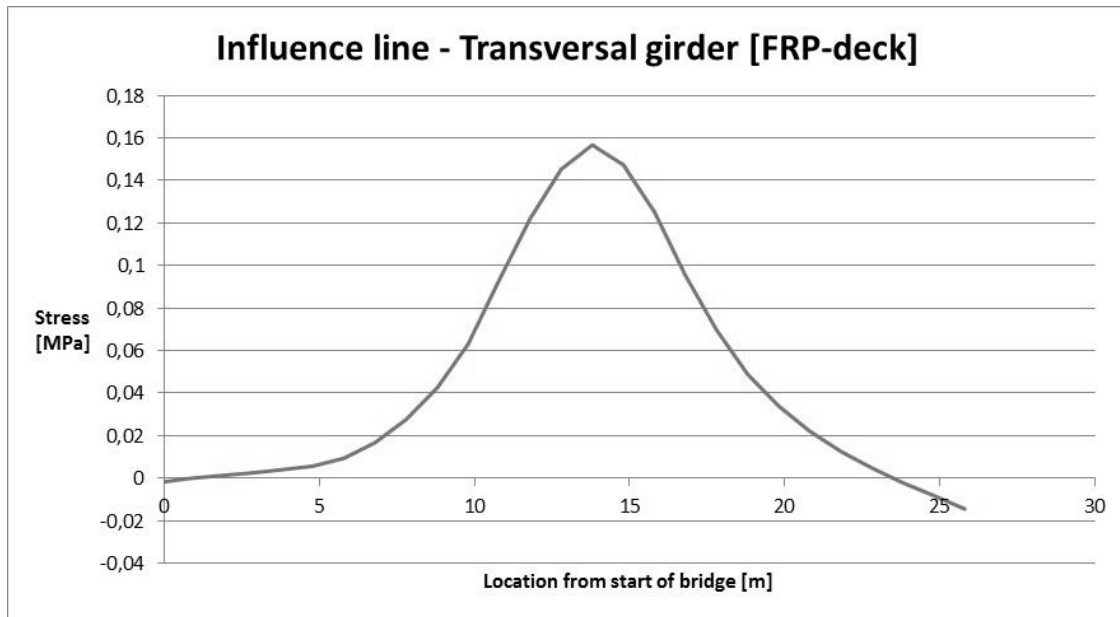


Figure 6.22 Influence line – Transversal girder [FRP-deck]

As can be seen, by comparing Figure 6.20 and Figure 6.22, the difference of the two decks is not as noticeable as for the stringers.

The total stress distribution when the vehicle from fatigue load model 3 passing the bridge can be seen in Figure 6.23.

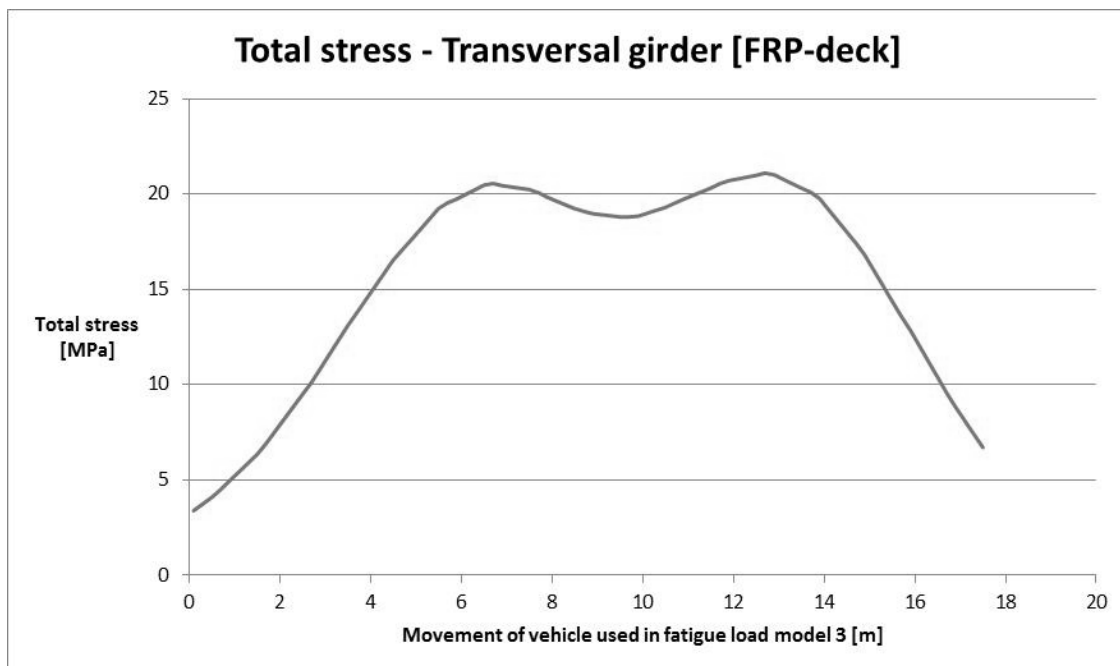


Figure 6.23 Total stress – Transversal girder [FRP-deck]

The maximum stress obtained in the bottom flange in mid-span of the transversal girder was 21.10 MPa and the lowest stress was 3.39 MPa, hence the stress variation was 17.7 MPa.

6.2.3.3 Main girder

The stress in the main girder was studied with respect to fatigue loading, see Figure 6.24 for illustration of the location in the main girder which was checked with respect to fatigue.

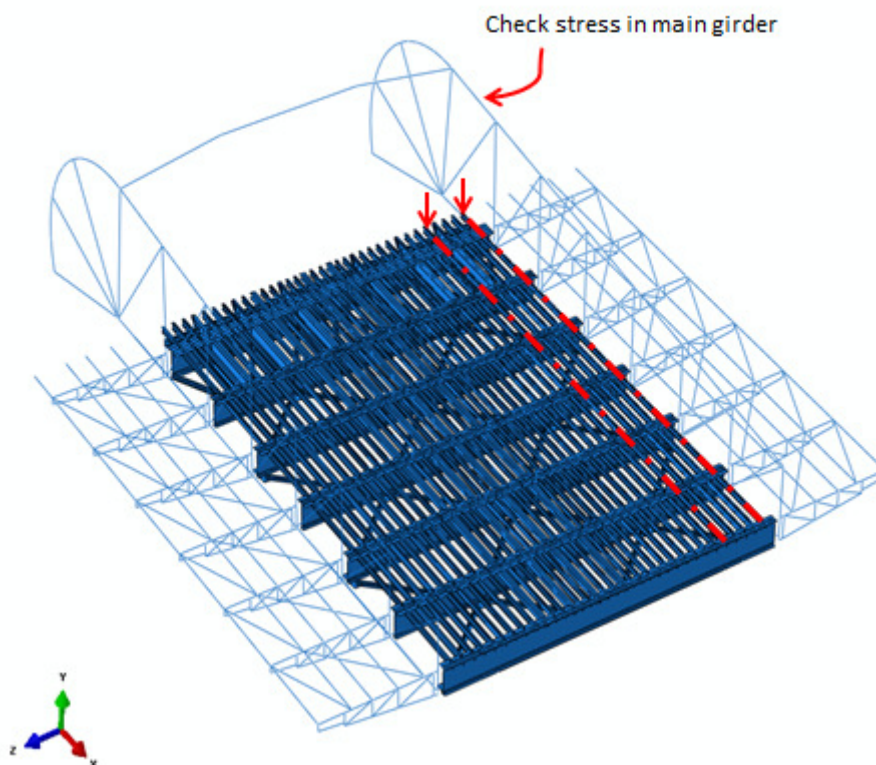


Figure 6.24 The lines represent the movement of the axle load, the picture also shows which part of the main girder that was checked with respect to fatigue.

The axle load used to establish the influence line for the member of interest was chosen to act in the lane closes to the girder in order to get the highest stress variation, see Figure 6.24 for illustration of the lane chosen.

The influence line created by the measured values in the beam element (main girder) for each location of the unit axle load across the length of the bridge can be seen in Figure 6.25.

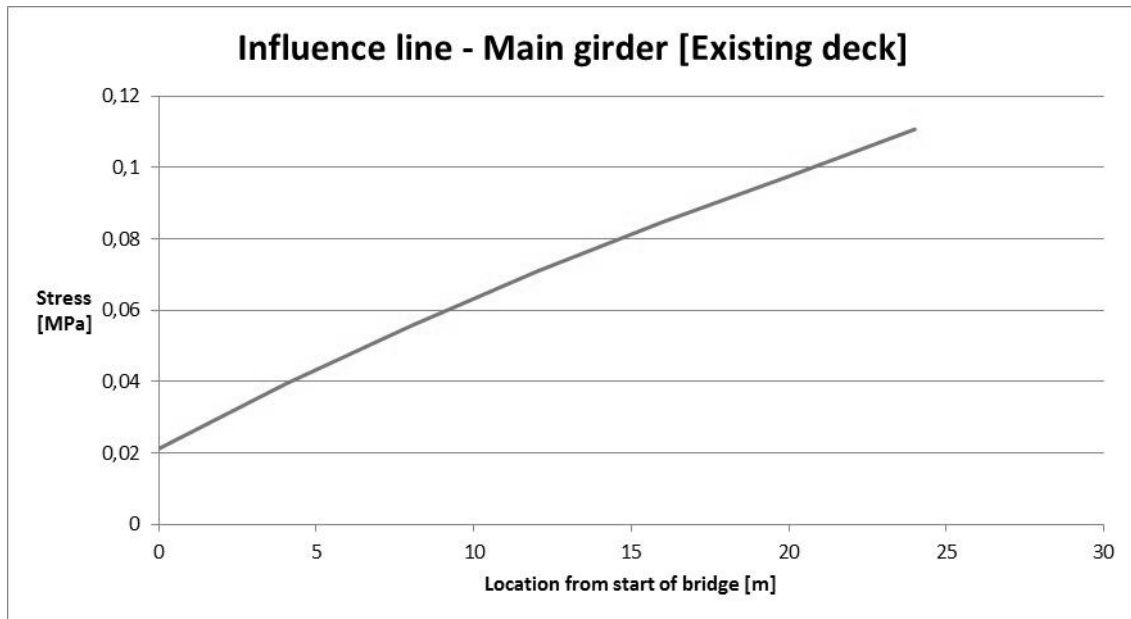


Figure 6.25 Influence line – Main girder [Existing deck]

The influence line reaches its maximum force when the axle load is located at the very end of the bridge, see Figure 6.25.

Application of the vehicle from fatigue load model generates the total stress variation that can be seen in Figure 6.26.

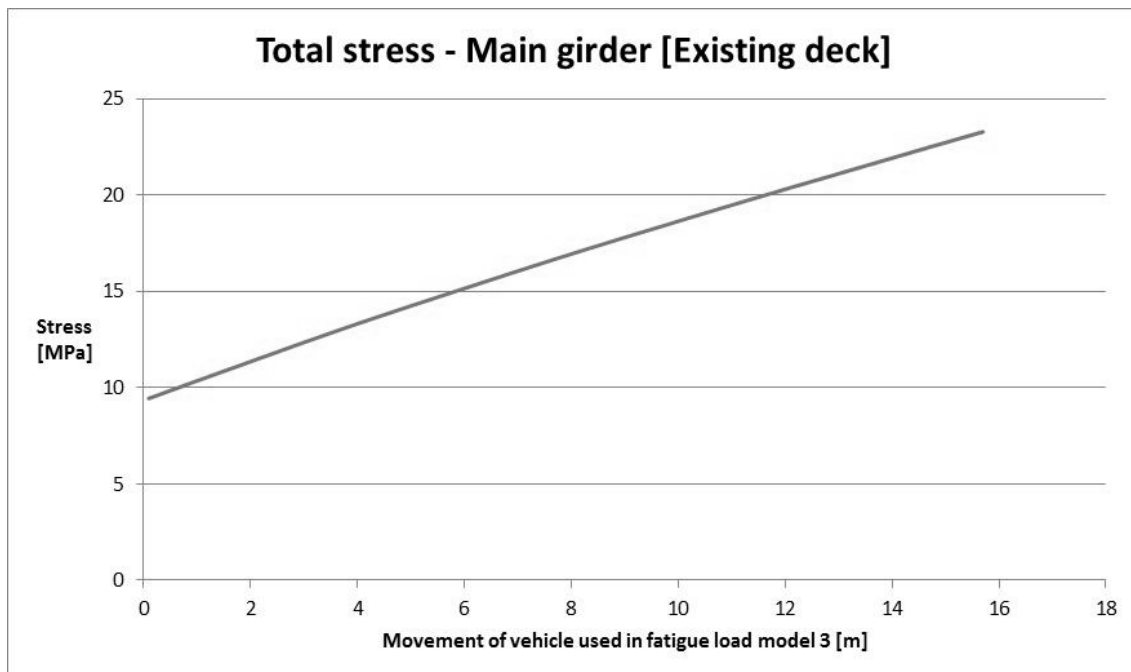


Figure 6.26 Total stress – Main girder [Existing deck]

The maximum stress generated by the vehicle in fatigue load model was 23.28 MPa and the lowest stress was 9.44 MPa, meaning that the stress variation was 13.8 MPa.

Main girder FRP-deck

For the model with FRP deck the same location of the main girder is checked for how the stress fluctuates when a unit axle load passes the bridge. The influence line for main girder in the FRP model can be seen in Figure 6.27.

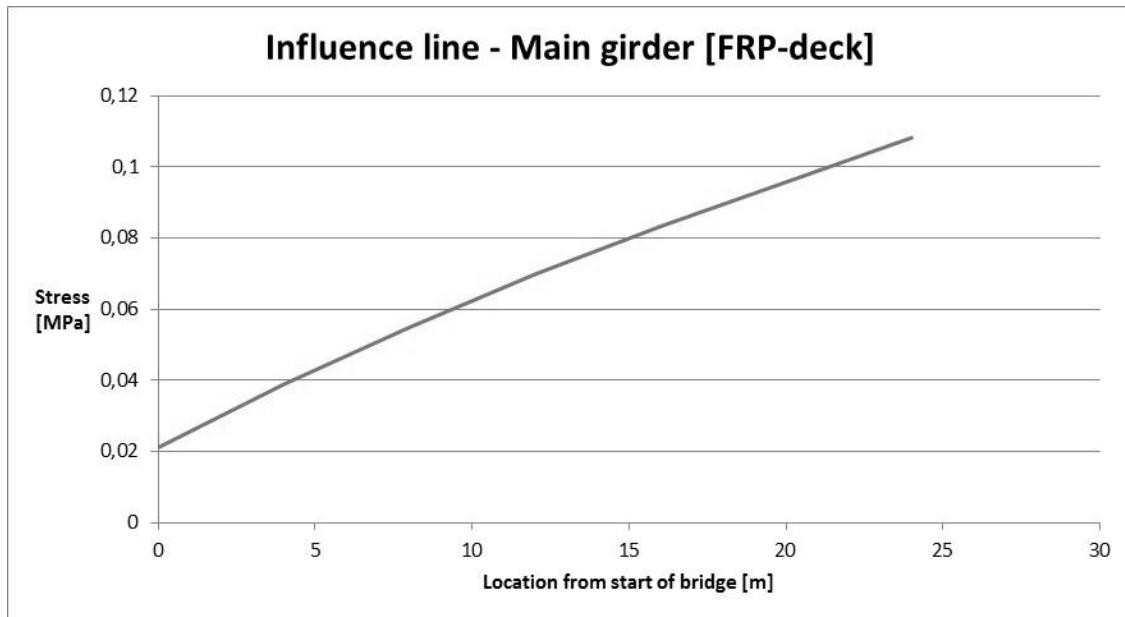


Figure 6.27 Influence line – Main girder [FRP-deck]

As in the case for the existing deck the peak value will be reached in the far end of the bridge. The differences between the influence lines are very small between the two models.

The total stress distribution for the unit axle load passing the bridge is illustrated in Figure 6.28.

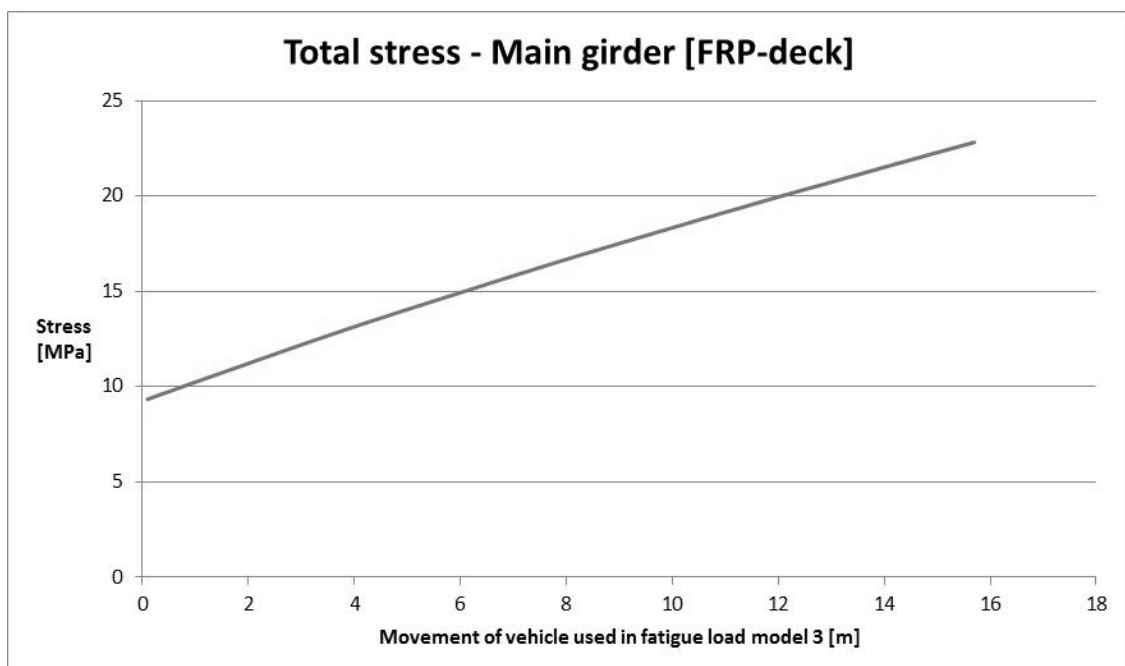


Figure 6.28 Total stress – Main girder [FRP-deck]

The maximum stress generated by the vehicle in fatigue load model was 22.82 MPa and the lowest stress was 9.34 MPa, meaning that the stress variation was 13.5 MPa.

6.2.3.4 Summary of fatigue results

A summary of the measured stresses for the different deck configurations can be seen in Table 6.1. The table shows the maximum, minimum and the stress variation for the both decks.

Table 6.1 Summary of stresses and stress variations for fatigue analysis.

Deck	Stringer		Transversal girder		Main girder	
	Existing	FRP	Existing	FRP	Existing	FRP
σ_{max} [MPa]	59.06	6.98	24.20	21.10	23.28	22.82
σ_{min} [MPa]	-4.92	-1.11	2.68	3.39	9.44	9.34
$\Delta\sigma$ [MPa]	63.98	8.09	21.52	17.71	13.85	13.48
Ratio [%]	12.65		82.30		97.36	

To assess the fatigue life of the critical connections the nominal stress method was utilized. The most critical connection was the stringer and this connection was determined to be classified as a *detail category 71* in the S-N curve in Figure 6.29.

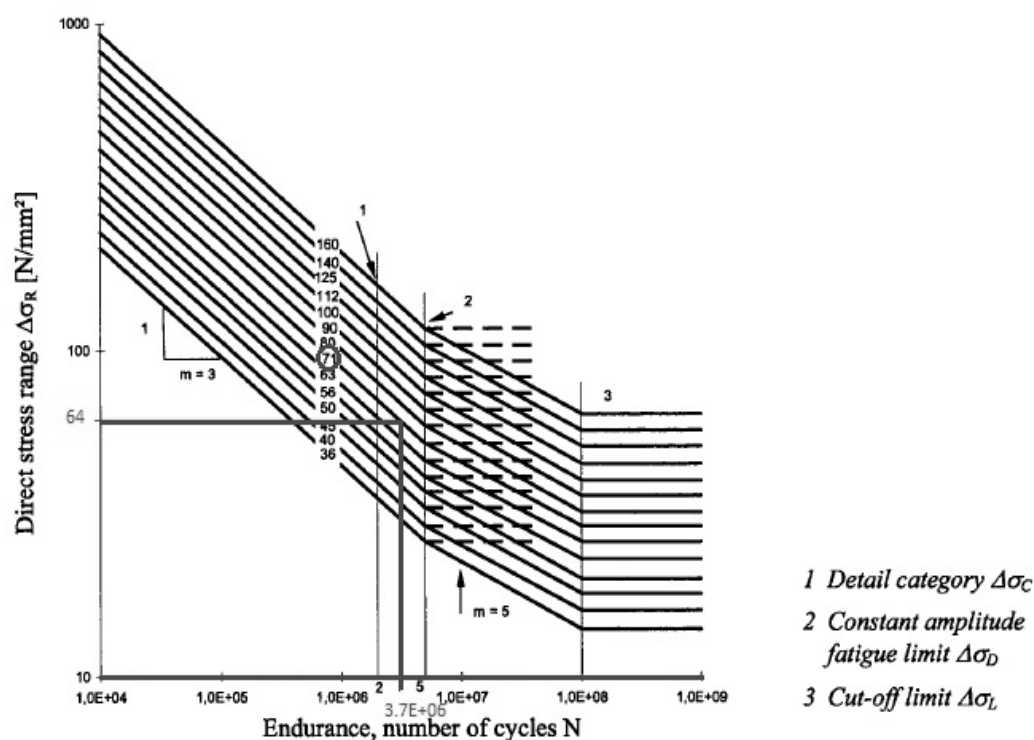


Figure 6.29 S-N curve for detail category 71 for fatigue stress range in stringer-transversal girder connection. 64 MPa stress range for the existing deck gives fatigue life of 3.7 million cycles, 8 MPa for the FRP deck results in infinitely many cycles.

The S-N curve in Figure 6.29 shows that for the stringer could be loaded around 3.7 million cycles before failing to fatigue for the existing deck. On the other hand the FRP deck offers a significant improvement in the fatigue performance and each load cycle does not contribute to any fatigue damage. Therefore the detail could be considered to have an infinite fatigue life at this stress variation.

6.3 Static

In this section the results from the static loading are presented. Vertical and horizontal loads applied were done according to Eurocode. The stresses were examined in the most critical locations. As in the part about the fatigue assessment this check considers the two different types of decks and the three different members:

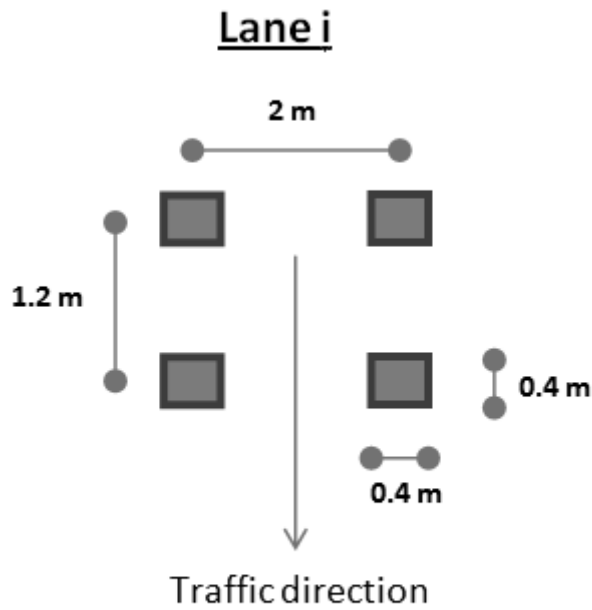
1. Stringer in the bottom flange in mid-span.
2. Transversal girder in the bottom flange at mid-span.
3. Main girder close to the base of the bridge in order to achieve maximum variation in axial stress.

When all members are presented for the both the steel deck and the FRP deck, a short summary of the stresses for each deck and member are shown in Table 6.2. Stresses in the adhesive zone between the stringers and the FRP deck were investigated to ensure that the shear could transfer without exceeding the capacity of the adhesive.

The maximum displacement for each member type was measured and compared to the maximum allowable deflection criteria according to Eurocode. A summary of the displacement check can be seen in Table 6.5.

6.3.1 Vertical load

For simulating the vertical traffic loads *load model 1* was utilized. This model consists of a double axle system with concentrated loads and a part of uniformly distributed load (UDL). The contact area of the each wheel is a square with the side 0.4m, the orientation of the wheels can be seen in Figure 6.30.



$$1 \text{ axle load} = Q_{ik}$$

Figure 6.30 Geometric disposition of the double axle load system used in load model 1.

Each wheel carries identical load corresponding to half the axle load. The values of axle loads and UDLs varies with number of lanes on the bridge, see Table 6.2 for values.

Table 6.2 Load model 1 axle loads and UDL for different lanes.

Location	Axle loads Q_{ik} [kN]	Uniform load q_{ik} [kN/m ²]
Lane 1	300	9.0
Lane 2	200	2.5
Lane 3	100	2.5
Other lanes	0	2.5

There are national adjustment factors, α , that possibly decrease some of the loads from Table 6.2, but these factors were chosen to be equal to unity to be on the safe side.

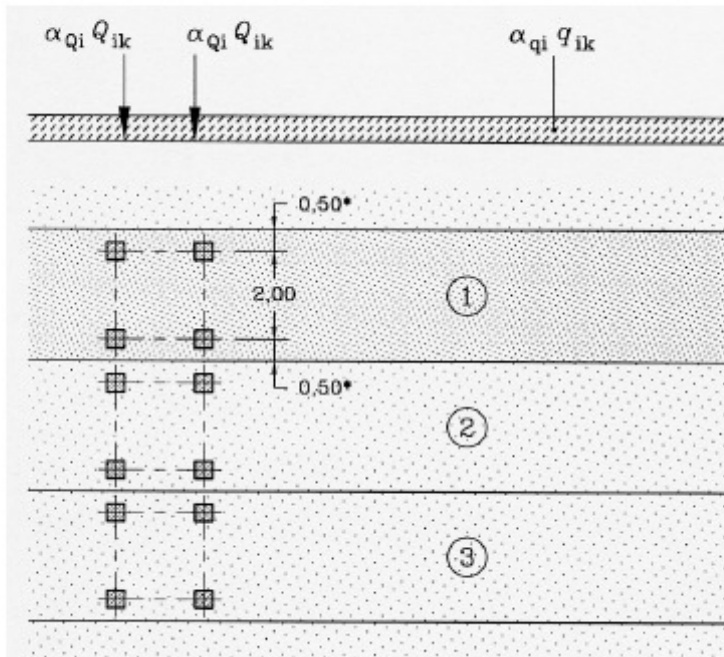


Figure 6.31 Illustration of notational lane numbering and load to be applied.

The lane number is chosen accordingly to achieve the worst case for the member of interest, meaning that the lane 1 – lane 3 not necessarily have to be in a sequence. Figure 6.31 shows an example of how the notational lanes could be oriented.

In order to find the worst loading case for the different members the influence lines were studied. From the influence lines it could clearly be seen in which areas to apply load in order to achieve the highest stress in the member under consideration. Figure 6.32 shows the influence line for a critical section in a stringer, the shaded area shows where to apply the load in order for it to contribute to maximal stress in the bottom flange in the stringer under consideration. The uniformly distributed load should be applied in the location of the bridge corresponding to the marked area in Figure 6.32.

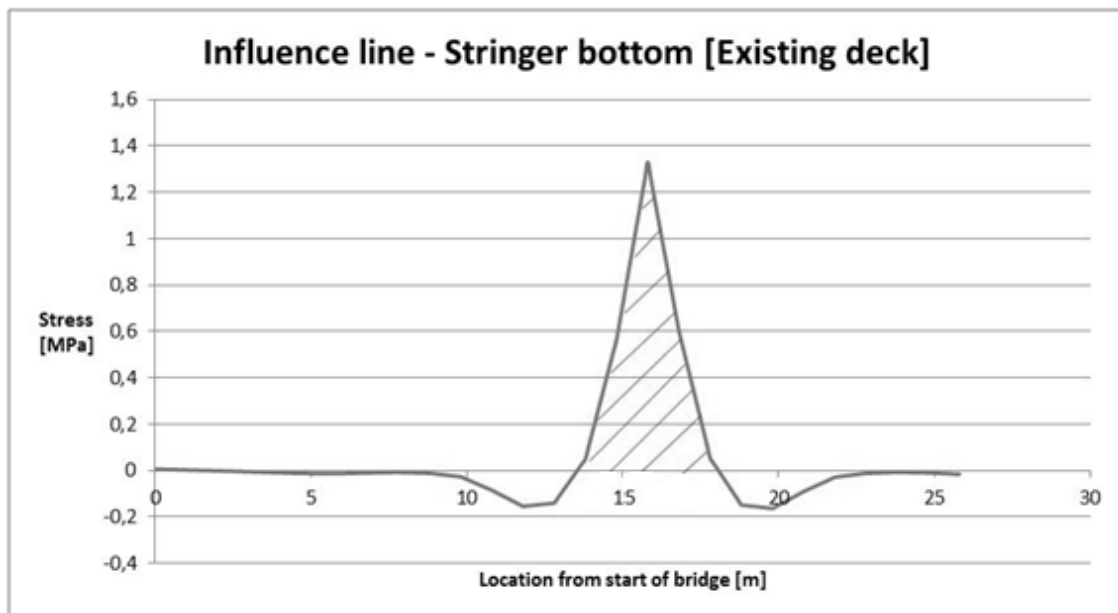


Figure 6.32 Influence line for critical section in a stringer, the shaded area shows where to apply load in order to achieve maximum stress in the stringer.

To find where the double axle system were to be applied the same methodology as in the fatigue part were utilized. Meaning superposition of the individual axles and from there find the location that yields the maximum stress for the member of interest. See Figure 6.33 for result of the double axle system for lane 1 passing the bridge.

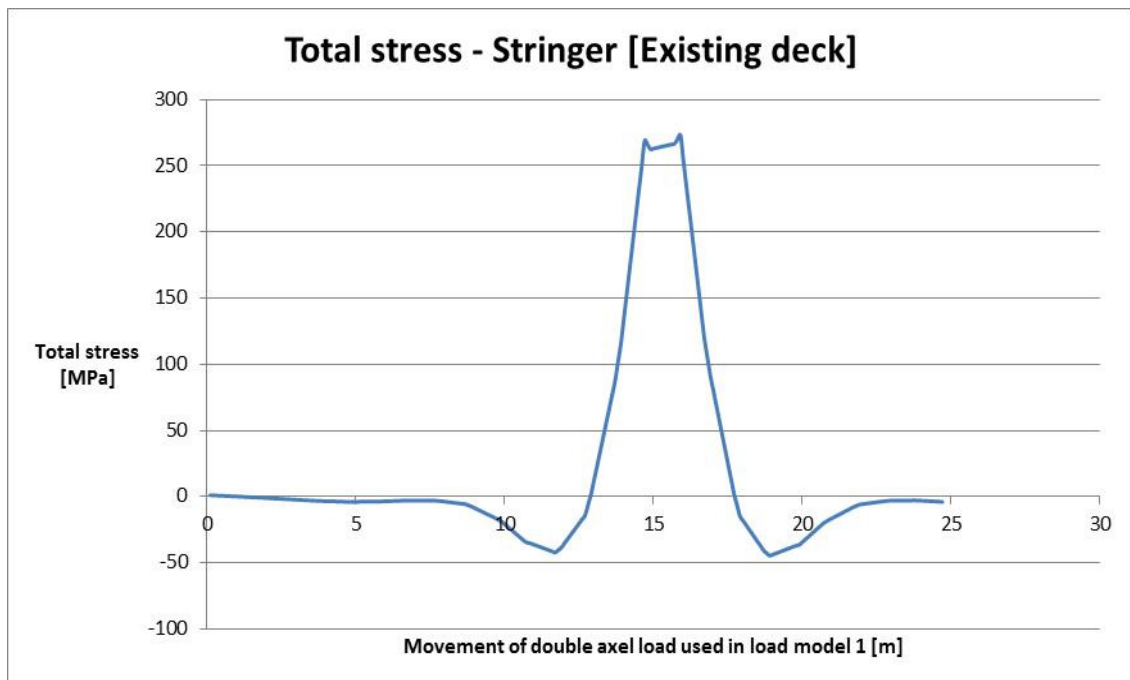


Figure 6.33 Total stress in the bottom flange in the stringer when a double axle load is applied.

The location of the axles were then determined for the moved distance corresponding to the maximum value in Figure 6.33. The wheels that transfer the axle loads to the bridge deck can be seen in Figure 6.34 together with the UDL's. For achieving the maximum stress in the bottom flange of the stringer under consideration the loaded strip was quite thin.

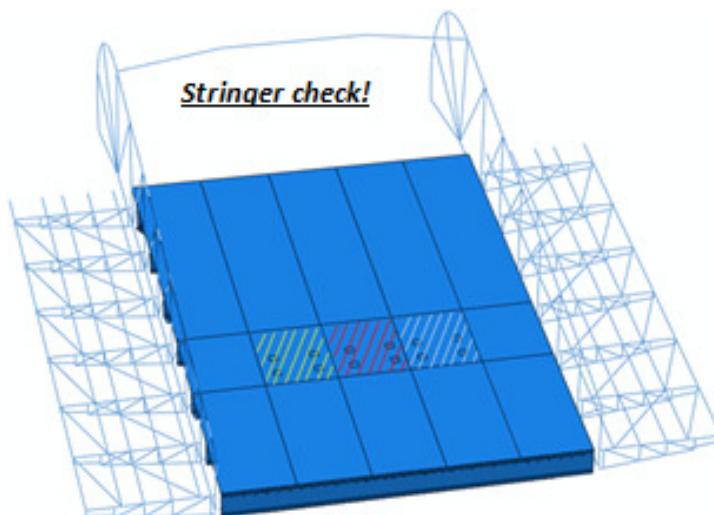


Figure 6.34 For checking the maximum stress in the stringer the load was applied in a small strip across the bridge. The notational lanes were as follows: red – lane 1, yellow – lane 2, white – lane 3 and the outermost lanes where loaded as other lanes.

For the rest of the members the maximum stress was determined analogous to the stringer. The loaded areas and placement of the axle loads can be seen in Figure 6.35 for the transversal girder and Figure 6.36 for the main girder.

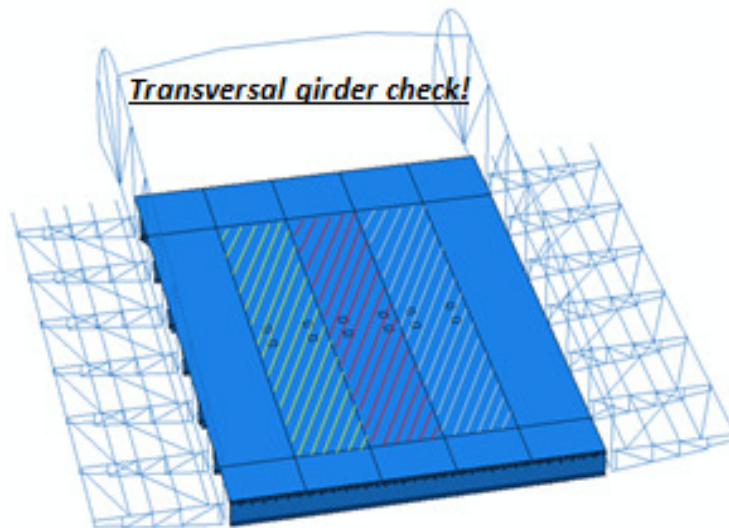


Figure 6.35 For checking the maximum stress in the transversal girder the load was applied in a large strip across the bridge. The notational lanes were as follows: red – lane 1, yellow – lane 2, white – lane 3 and the outermost lanes where loaded as other lanes.

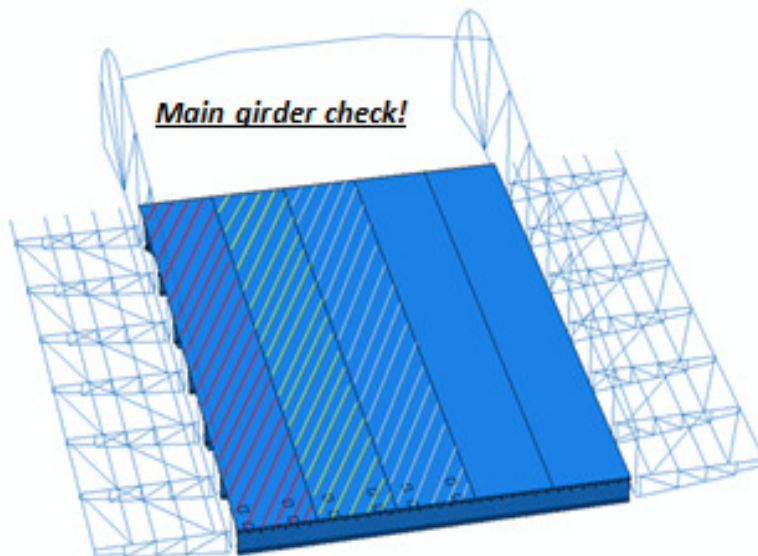


Figure 6.36 For checking the maximum stress in the main girder the load was applied all over the bridge. The notational lanes were as follows: red – lane 1, yellow – lane 2, white – lane 3 and the two lanes to the right where loaded as other lanes. The both sidewalks were loaded with crowd load according to Eurocode (4 kN/m^2).

6.3.2 Horizontal load

The horizontal force due to braking or acceleration is acting directly on top of the deck surface. The magnitude of the braking force should according to Eurocode be taken as a portion of the maximum vertical forces acting in lane 1 from load model 1.

$$Q_k = 0.6\alpha_{q1}(2Q_{1k}) + 0.1\alpha_{q1}q_{1k}w_1L$$

The acceleration force should be considered with the same magnitude as the braking force but in the opposite direction.

Eurocode also states that lateral forces with a magnitude of 25% of the braking or acceleration force should be accounted for due to skew braking or skidding. The lateral force and the braking/acceleration force act simultaneously at the top of the carriageway level.

Table 6.3 Horizontal traffic load.

Braking force [kN]	Acceleration force [kN]	Lateral force [kN]
429.7	429.7	107.4

6.3.3 Result summary of static load

For checking the stresses the loads were multiplied with factors for checking the structure in ultimate limit state (ULS), the self-weight was multiplied by 1.35 and all live load were multiplied by a factor 1.5. The stresses in the most critical members can be seen in Table 6.4. It can be seen that the stringer for the existing deck two different values. The lower value is measured directly from the model and the higher value corresponds to when the worst case is considered, meaning neither composite action nor lateral distribution is considered within the steel plate. See section 5.4. Both these values represent the lower and the higher ends of the spectrum for which the actual stress in the stringer. It is very hard to tell exactly how high stress there will be in reality.

Table 6.4 Summary of maximum stresses from ULS static loading.

Member		Existing deck [MPa]	FRP-deck [MPa]	Ratio [%]
Stringer	Composite action + LDF	185	143	77,30
	No special effect	455,6		31,39
Transversal girder		198	173	87,37
Main girder		230	214	93,04

Eurocode states that the relative deflection in the service limit state (SLS) for members has to fulfil a requirement depending on the span of the member under

consideration. The requirement used was $L/300$, where L is the span of the member checked. The applied loads were not multiplied by a factor in SLS as was done for the ULS loads. See Table 6.5 for summary of the largest deflections for the members and for respective deck type.

Table 6.5 SLS deflection table with maximum allowable deflection limit.

Member	Existing deck [mm]	Limit - $L/300$ [mm]	Ratio [%]	FRP-deck [mm]	Limit - $L/300$ [mm]	Ratio [%]
Stringer	4.36	13.33	32.71	3.15	13.33	23.63
Transversal girder	22.73	59.10	38.46	24.88	59.10	42.09
Main girder	109.10	192.16	56.77	102.08	192.16	53.12

6.4 Stresses in adhesives connection

In the Abaqus model, strains result in the connection between the top flange of the stringer and the bottom plate of FRP deck was used to predict the stresses in adhesives connection. By taking median strain values of the same node, the strain of adhesives can be determined, see Table 6.6.

Table 6.6 Tensile and compression properties of epoxy and polyurethane adhesives.

Member	Strain (‰)	E-mod (MPa)	Stress (MPa)
Stringer (steel)	-0.3927		
SikaForce 7851 Polyurethane	-0.39275	571	-0.224
Deck (FRP)	-0.3928		

Table 6.7 shows the capacity of two different adhesive types for FRP connection. From that table, *SikaForce 7851 polyurethane* was chosen because of inexpensive and un-conservatives in compared to *SikaDur 330 epoxy*.

Table 6.7 Tensile and compression properties of epoxy and polyurethane adhesives (Keller, T. and T. Vallée, 2005)

Adhesive	Loading	Nominal Stress (MPa)	Strain (%)	E-modulus (MPa)
SikaDur 330 epoxy	Tension (ISO 527) (5 specimens)	38.1 ± 2.1 (failure)	1.0 ± 0.1 (failure)	4550 ± 140
	Compression ASTM 694 (5 sp.)	-80.7 ± 2.6 (maximum)	-3.7 ± 0.1 (maximum)	3050 ± 33
SikaForce 7851 Polyurethane	Tension (ISO 527) (5 specimens)	18.4 ± 1.0 (failure)	37.1 ± 1.5 (failure)	571 ± 56
	Compression ASTM 694 (5 sp.)	-85.6 ± 2.5 (at -60% strain)	-60 (experiments stopped)	371 ± 37

From the Abaqus model, strain result due to brake load in adhesives connection was only -0.0148 ‰. And this value is smaller in compare of the strain due to static load model 1 Eurocode. That is why result from static load model 1 was used to calculate stress in adhesive in this report.

The nominal stress failure capacity of the *SikaForce 7851 Polyurethane* adhesive is 18.4 MPa (Tension). By comparing this stress capacity and stress achieved in the model, it can be seen the ratio is obviously in the safe side.

7 Conclusion

The work carried out in this thesis has resulted in the following conclusions:

- The Counter weight on each side of the bridge can be lowered by around 123 tons by removing the steel deck plate and replace it with an ASSET FRP deck.
- The vertical force resultant in each hinge is lowered by 80.5 tons for the unloaded bridge.
- The FE-model shows that by substituting the existing steel deck plate with an ASSET FRP deck the load will spread in a more effective manner, thus lowering stresses in the most critical members.
- Furthermore the fatigue assessment showed that the stringer- transversal girder connection is significantly improved for the case when the ASSET FRP deck is applied to the structure. The improvement is so great that the detail can be considered to have no problems with fatigue what so ever. For the rest of the members no significant problem with regard to fatigue was noted.
- The static loading was applied according to Eurocode and it was showed that the bridge with applied FRP deck was able to carry standard Eurocode traffic load, both with regard to stresses and the displacement criteria. For the bridge in its existing condition however no exact answer could be found, only a range for the actual stress could be achieved. To get exact values measurements in the field has to be done. (Strain gauges)
- The FRP deck and the stringers are connected by adhesive bonding, which was modelled to achieve full interaction. The highest stress noted in the adhesive zone was well below the critical stress. Therefore all shear stresses could be transferred between the both members, meaning full composite action.

8 Discussion

The substitution of the bridge deck will lower the overall self-weight of the bridge up to 68 tons, which will enable to lighten the counter weight by 123 tons. Therefore the total weight loss acting on the hinges will be 191 tons per bridge half, or 89.5 tons per hinge. However this is for the bridge with self-weight only, no traffic load is applied. For a high increase in traffic load the stresses in the hinges are most likely to be even higher than before, for short periods of times. Meaning that for the most cases the bridge will be with no or low traffic load and the hinges will experience lower stresses in most cases while in ULS the stresses will be higher than the existing bridge with the current load limitation.

In the modelling full composite action was assumed, in reality perhaps 100% composite action could not be achieved. However a high level of composite action should be possible due to large contact areas compared to the spacing of stringers, about 20 % of the deck area will be attached with adhesive to the stringers. The large bonding area also provides low stresses in the adhesive zone, which will not compromise the composite action.

In this thesis work the construction drawings from 1928 and 1982 were used for creating the models. However some corrosion exists, which would decrease the thickness of certain members and thereby lowering their capacity. An assessment of the corrosion in the bridge was made in 2011 and presented in the report, *Bijzondere inspecties Rotterdam – reference: U2011/21399*, however some inconsistencies of member profiles were found. Therefore the effect of the corrosion was left outside of the thesis work, this because of the uncertainties of the existing profiles in certain locations. As this thesis work is being finished the work of making a new assessment of the current state of the bridge is in process. In this thesis work the stringer profile used in modelling was IPN260 which is smaller than IPN300 from the conflicting information in the report from 2011, meaning that the stresses will not be higher in the un-corroded members.

9 References

Bank, Lawrence Colin (2006). Composites for construction: structural design with FRP materials. John Wiley & Sons, Inc., Hoboken, New Jersey.

Eurocode 1, EN-1991-2. Eurocode 1: Actions on Structures – Part 2: Traffic loads on bridges, (2003).

Eurocode 3, EN-1993-1-9. Eurocode 3: Design of Steel Structures – Part 1-9: Fatigue, (2005).

Gürtler, Herbert W. (2004). Composite action of FRP bridge decks adhesively bonded to steel main girders. EPFL, Lausanne, Switzerland.

Heshmati, Mohsen (2012). Fatigue life assessment of bridge details using finite element method. Chalmers, Göteborg, Sweden.

Keller, Thomas (2001). Recent all-composite and hybrid fibre-reinforced polymer bridges and buildings. EPFL, Lausanne, Switzerland.

Keller, T. and T. Vallée (2005). Adhesively bonded lap joints from pultruded GFRP profiles. Part II: joint strength prediction. Composites Part B: Engineering, 2005. Page 34-3.

Keller, T. and H. Gürtler (2005). Composite Action and Adhesive Bond Between Fiber-Reinforced Polymer Bridge Decks and Main Girders.

Mara, Valbona (2011). Fibre reinforced polymer bridge decks: A feasibility study on upgrading existing concrete-steel bridges. Chalmers, Goteborg, Sweden.

Mara, Valbona (2011). Fibre reinforced polymer composite bridge decks: State of the art report. Chalmers, Goteborg, Sweden.

Sams, Matt (2005). Broadway Bridge Case Study: Bridge Deck Application of Fiber-Reinforced Polymer. Transportation Research Board. Washington DC, USA.

<http://da.wikipedia.org/wiki/Gr%C3%A6shoppebroen>
[2012-08-01]

<http://www.fiberline.com/structures/profiles-and-decks-bridges/profiles-road-bridges/case-stories-road-bridges/grasshopper-gl/grasshopper-glass-fibre>
[2012-08-01]

http://www.industrialextrusionmachinery.com/plastic_extrusion_pultrusion.html
[2012 - 06 - 01]

<http://www.pultrusions.org/articles/advantages.html>
[2012 - 06 - 01]

APPENDICES

Appendix A: Fatigue Main Girder

```
%%%%%%%%%%%%%%%%%%%%%%%%%%%%%%%%%%%%%%%%%%%%%%%%%%%%%%%%%%%%%%%%%%%%%%%%
%   - INFLUENCE LINES - Main Girder
%
%   This file generates the influence line for the main girder and
%   apply the fatigue load model 3 to find the maximum stress
%   variation.
%
%   By: Karl Engdahl and Kresnadya Desha Rousstia
%   2012-04
%%%%%%%%%%%%%%%%%%%%%%%%%%%%%%%%%%%%%%%%%%%%%%%%%%%%%%%%%%%%%%%%%%%%%%%%

clc
clear all
close all

%% Generating influence line

% Measured values from Abaqus at different distances are imported
from
% Excel and stored in variables point and x
sheet1 = 'BeamElement';
sheet2 = 'BeamElement - FRP';
sheetNR = sheet2;

ExcelImport = xlsread('lanel.xlsx',sheetNR);

% Area of cross-section for main truss beam mm^2
Area = 46975;

point = ExcelImport(1:7,2)./Area;
x = ExcelImport(1:7,3);

for i = 1:length(point)-1

    % Slope between points
    k(i) = (point(i)-point(i+1))/(x(i)-x(i+1));

end

% Generating influence lines between the measured points.
line_dist = x(1):0.1:x(end);
line_value = zeros(1,length(line_dist));

for i = 1:length(k)

    for j = 1:length(line_dist)

        if line_dist(j) >= x(i)
            line_value(j) = k(i)*(line_dist(j)-x(i))+point(i);
        end

    end

end

end
```

```

plot(x,point,'r*',line_dist,line_value)
xlabel('Location in the bridge where the unit load is applied')
ylabel('Stress [MPa]')

%% Applying axle loads (Fatigue Load Model 3)

% Axle spacing
axle = [0 1.2 7.2 8.4]';

% Step for axle loads each 0.1m
value_location = 10*axle + ones(size(axle));

% Loop for finding the values for each stepping of the axle loads
through
% out the length of the bridge
delta_tot = zeros(size(value_location));

for k = 1:length(line_value)-value_location(end)+1

    delta = zeros(4,1);

    for wheel = 1:length(axle)

        % Value from each axle load (Each wheel has a load of 60kN)
        delta(wheel) = 60*line_value(value_location(wheel));

        % Total value from all axle loads combined at the given step
        delta_tot(k) = sum(delta);
    end

    % Move axle loads one step
    value_location = value_location + ones(size(axle));

end

figure (2)
x_loc = [1:k]';
plot(x_loc,delta_tot)

sigma_max = max(delta_tot);
sigma_min = min(delta_tot);
delta_sigma = sigma_max - sigma_min;
xlabel('Step number')
ylabel('Stress [MPa]')

disp('Delta sigma = [MPa]')
disp(delta_sigma)

Stresses = [sigma_max; sigma_min; delta_sigma];

ExcelExport1 = [line_dist',line_value'];
ExcelExport2 = [delta_tot,0.1.*x_loc];

xlswrite('lanel.xlsx',ExcelExport1, sheetNR, 'F4:G244');

```

```
xlswrite('lane1.xlsx',ExcelExport2,sheetNR,'H4:I160');  
xlswrite('lane1.xlsx',Stresses,sheetNR,'L4:L6');
```

Appendix B: Fatigue Transversal Girder & Stringer

```
%%%%%%%%%%%%%%%%%%%%%%%%%%%%%%%%%%%%%%%%%%%%%%%%%%%%%%%%%%
%   - INFLUENCE LINES - Transversal Girder & Stringer
%
%   This file generates the influence line for the transversal girder
%   and the stringer. The file also applies the fatigue load model 3
%   to find the maximum stress variation.
%
%   By: Karl Engdahl and Kresnadya Desha Rousstia
%   2012-04
%%%%%%%%%%%%%%%%%%%%%%%%%%%%%%%%%%%%%%%%%%%%%%%%%%%%%%%%%%
clc
clear all
close all

%% Generating influence line

% Measured values from Abaqus at different distances are imported
from
% Excel and stored in variables point and x
sheet1 = 'stringer';
sheet2 = 'stringer - FRP';
sheet3 = 'stringer bottom';
sheet4 = 'stringer bottom - FRP';
sheet5 = 'Transversal';
sheet6 = 'Transversal - FRP';
sheet7 = 'Add.check - stringer';
sheet8 = 'Add.check - stringer - FRP';

sheetNR = sheet8;

ExcelImport=xlsread('lane3.xlsx',sheetNR);

point = ExcelImport(1:27,2);
x = ExcelImport(1:27,3);

for i = 1:length(point)-1

    % Slope between points
    k(i) = (point(i)-point(i+1))/(x(i)-x(i+1));

end

% Generating influence lines between the measured points.
line_dist = x(1):0.1:x(end);
line_value = zeros(1,length(line_dist));

for i = 1:length(k)

    for j = 1:length(line_dist)

        if line_dist(j)>= x(i)
            line_value(j) = k(i)*(line_dist(j)-x(i))+point(i);
        end

    end

end
```

```

end

plot(x,point,'r*',line_dist,line_value)
xlabel('Location in the bridge where the unit load is applied')
ylabel('Stress [MPa]')

%% Applying axle loads (Fatigue Load Model 3)

% Axle spacing
axle = [0 1.2 7.2 8.4]';

% Step for axle loads each 0.1m
value_location = 10*axle + ones(size(axle));

% Loop for finding the values for each stepping of the axle loads
through
% out the length of the bridge
delta_tot = zeros(size(value_location));

for k = 1:length(line_value)-value_location(end)+1

    delta = zeros(4,1);

    for wheel = 1:length(axle)

        % Value from each axle load (Each wheel has a load of 60kN)
        delta(wheel) = 60*line_value(value_location(wheel));

        % Total value from all axle loads combined at the given step
        delta_tot(k) = sum(delta);
    end

    % Move axle loads one step
    value_location = value_location + ones(size(axle));

end

end

figure (2)
x_loc = [1:k]';
plot(x_loc,delta_tot)

sigma_max = max(delta_tot);
sigma_min = min(delta_tot);
delta_sigma = sigma_max - sigma_min;
xlabel('Step number')
ylabel('Stress [MPa]')

disp('Delta sigma = MPa')
disp(delta_sigma)

stresses = [sigma_max; sigma_min; delta_sigma];

ExcelExport1 = [line_dist',line_value'];
ExcelExport2 = [delta_tot,0.1.*x_loc];

```

```
xlswrite('lane3.xlsx',ExcelExport1, sheetNR, 'F4:G262');  
xlswrite('lane3.xlsx',ExcelExport2, sheetNR, 'H4:I178');  
xlswrite('lane3.xlsx', stresses, sheetNR, 'L4:L6');
```


Appendix C: Static Main Girder

```
%%%%%%%%%%%%%%%%%%%%%%%%%%%%%%%%%%%%%%%%%%%%%%%%%%%%%%%%%%%%%%%%%%%%%%%%%
%   - STATIC LOAD MODEL 1 - Main Girder
%
%   This file generates the influence line for the main girder and
%   apply the load model 1 to find where to apply the axle loads in
%   order to obtain the maximum stresses in the member.
%
%   By: Karl Engdahl and Kresnadya Desha Rousstia
%   2012-04
%%%%%%%%%%%%%%%%%%%%%%%%%%%%%%%%%%%%%%%%%%%%%%%%%%%%%%%%%%%%%%%%%%%%%%%%%

clc
clear all
close all

%% Generating influence line

% Measured values from Abaqus at different distances are imported
from
% Excel and stored in variables point and x
sheet1 = 'BeamElement';
sheet2 = 'BeamElement - FRP';
sheetNR = sheet2;

ExcelImport = xlsread('static_lanel.xlsx',sheetNR);

% Area of cross-section for main truss beam mm^2
Area = 46975;

point = ExcelImport(1:7,2)./Area;
x = ExcelImport(1:7,3);

for i = 1:length(point)-1

    % Slope between points
    k(i) = (point(i)-point(i+1))/(x(i)-x(i+1));

end

% Generating influence lines between the measured points.
line_dist = x(1):0.1:x(end);
line_value = zeros(1,length(line_dist));

for i = 1:length(k)

    for j = 1:length(line_dist)

        if line_dist(j) >= x(i)
            line_value(j) = k(i)*(line_dist(j)-x(i))+point(i);
        end

    end

end

end
```

```

plot(x,point,'r*',line_dist,line_value)
xlabel('Location in the bridge where the unit load is applied')
ylabel('Stress [MPa]')

%% Applying axle loads (Fatigue Load Model 3)

% Axle spacing
axle = [0 1.2]';

% Step for axle loads each 0.1m
value_location = 10*axle + ones(size(axle));

% Loop for finding the values for each stepping of the axle loads
through
% out the length of the bridge
delta_tot = zeros(size(value_location));

for k = 1:length(line_value)-value_location(end)+1

    delta = zeros(2,1);

    for wheel = 1:length(axle)

        % Value from each axle load (Each wheel has a load of 1500kN)
        delta(wheel) = 150*line_value(value_location(wheel));

        % Total value from all axle loads combined at the given step
        delta_tot(k) = sum(delta);
    end

    % Move axle loads one step
    value_location = value_location + ones(size(axle));

end

figure (2)
x_loc = [1:k]';
plot(x_loc,delta_tot)

[sigma_max,loc1] = max(delta_tot);
[sigma_min,loc2] = min(delta_tot);
[sigma,which] = max([abs(sigma_max) abs(sigma_min)]);

if which == 1
    loc = loc1;
else loc = loc2;
end

xlabel('Step number')
ylabel('Stress [MPa]')

disp('Maximum sigma = MPa')
disp(sigma_max)

location = loc*0.1;
output = [sigma_max; sigma_min; location];

```

```
ExcelExport1 = [line_dist',line_value'];  
ExcelExport2 = [delta_tot,0.1.*x_loc];  
  
xlswrite('static_lanel.xlsx',ExcelExport1,sheetNR,'F4:G244');  
xlswrite('static_lanel.xlsx',ExcelExport2,sheetNR,'H4:I232');  
xlswrite('static_lanel.xlsx',output,sheetNR,'L4:L6');
```

Appendix D: Static Transversal Girder & Stringer

```
%%%%%%%%%%%%%%%%%%%%%%%%%%%%%%%%%%%%%%%%%%%%%%%%%%%%%%%%%%%%%%%%%%%%%%%%
%   - STATIC LOAD MODEL 1 - Transversal Girder & Stringer
%
%   This file generates the influence line for the Transversal Girder
%   and the Stringer and apply the load model 1 to find where to
%   apply the axle loads in order to obtain the maximum stresses in
%   the member.
%
%   By: Karl Engdahl and Kresnadya Desha Rousstia
%   2012-04
%%%%%%%%%%%%%%%%%%%%%%%%%%%%%%%%%%%%%%%%%%%%%%%%%%%%%%%%%%%%%%%%%%%%%%%%

clc
clear all
close all

%% Generating influence line

% Measured values from Abaqus at different distances are imported
from
% Excel and stored in variables point and x
sheet1 = 'stringer';
sheet2 = 'stringer - FRP';
sheet3 = 'stringer bottom';
sheet4 = 'stringer bottom - FRP';
sheet5 = 'Transversal';
sheet6 = 'Transversal - FRP';

sheetNR = sheet6;

ExcelImport=xlsread('static_lane3.xlsx',sheetNR);

point = ExcelImport(1:27,2);
x = ExcelImport(1:27,3);

for i = 1:length(point)-1

    % Slope between points
    k(i) = (point(i)-point(i+1))/(x(i)-x(i+1));

end

% Generating influence lines between the measured points.
line_dist = x(1):0.1:x(end);
line_value = zeros(1,length(line_dist));

for i = 1:length(k)

    for j = 1:length(line_dist)

        if line_dist(j)>= x(i)
            line_value(j) = k(i)*(line_dist(j)-x(i))+point(i);
        end
    end
end
```

```

        end

    end

end

plot(x,point,'r*',line_dist,line_value)
xlabel('Location in the bridge where the unit load is applied')
ylabel('Stress [MPa]')

%% Applying axle loads (Fatigue Load Model 3)

% Axle spacing
axle = [0 1.2]';

% Step for axle loads each 0.1m
value_location = 10*axle + ones(size(axle));

% Loop for finding the values for each stepping of the axle loads
through
% out the length of the bridge
delta_tot = zeros(size(value_location));

for k = 1:length(line_value)-value_location(end)+1

    delta = zeros(2,1);

    for wheel = 1:length(axle)

        % Value from each axle load (Each wheel has a load of 150kN)
        delta(wheel) = 150*line_value(value_location(wheel));

        % Total value from all axle loads combined at the given step
        delta_tot(k) = sum(delta);
    end

    % Move axle loads one step
    value_location = value_location + ones(size(axle));

end

end

figure (2)
x_loc = [1:k]';
plot(x_loc,delta_tot)

[sigma_max,loc1] = max(delta_tot);
[sigma_min,loc2] = min(delta_tot);
[sigma,which] = max([abs(sigma_max) abs(sigma_min)]);

if which == 1
    loc = loc1;
else loc = loc2;
end

xlabel('Step number')
ylabel('Stress [MPa]')

```

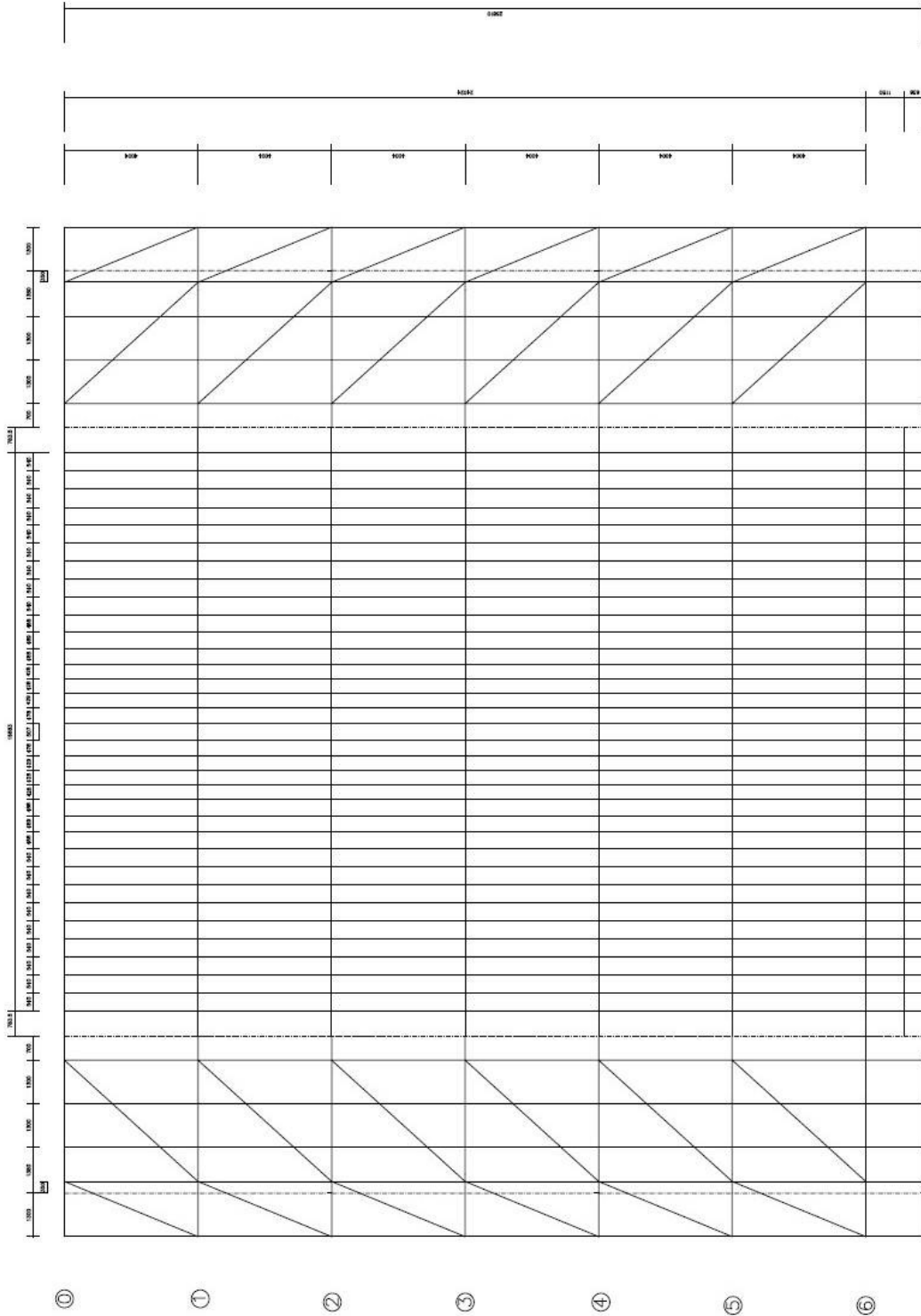
```
disp('Maximum sigma = MPa')
disp(sigma_max)

location = loc*0.1;
output = [sigma_max; sigma_min; location];

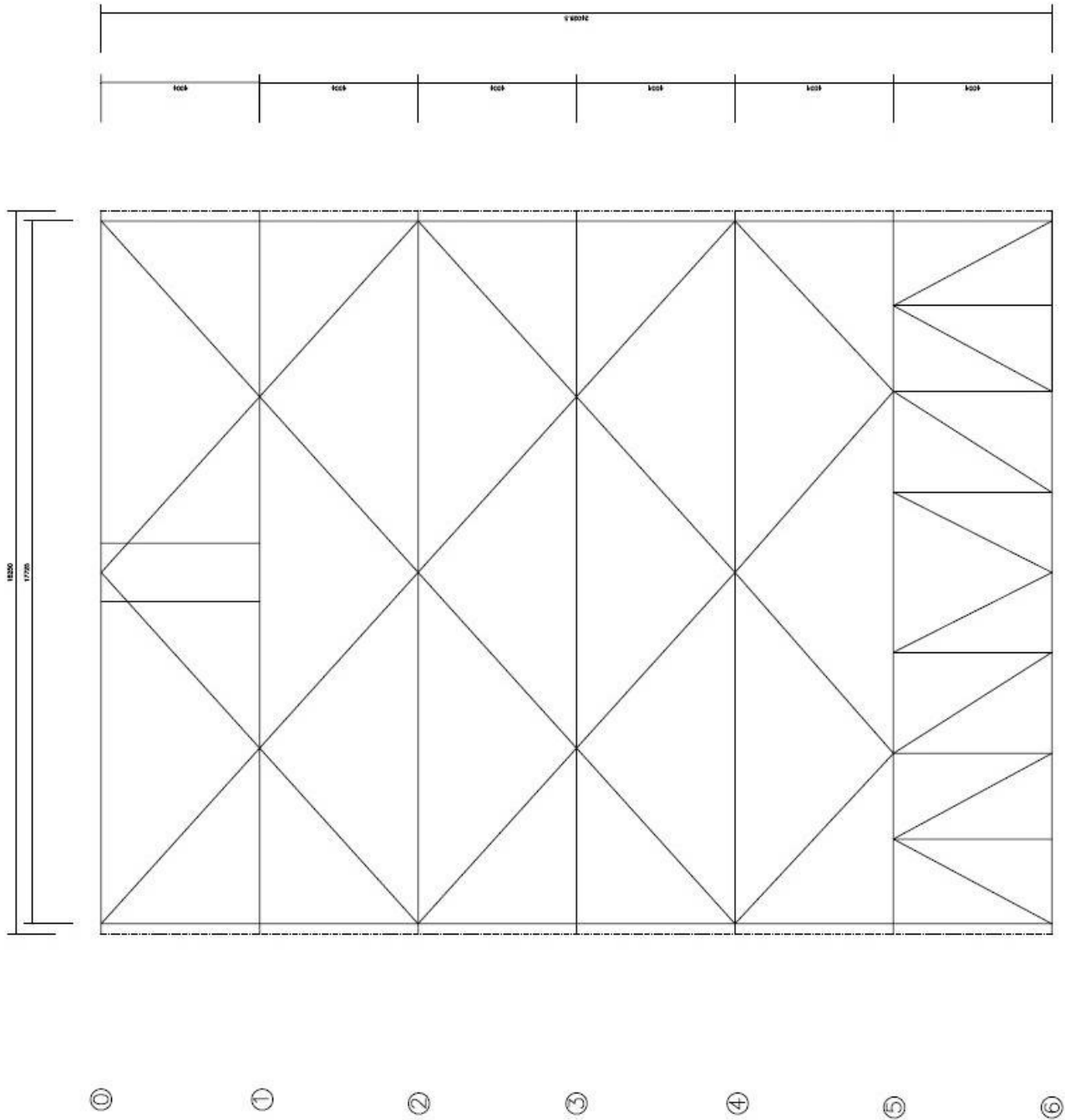
ExcelExport1 = [line_dist',line_value'];
ExcelExport2 = [delta_tot,0.1.*x_loc];

xlswrite('static_lane3.xlsx',ExcelExport1,sheetNR,'F4:G262');
xlswrite('static_lane3.xlsx',ExcelExport2,sheetNR,'H4:I250');
xlswrite('static_lane3.xlsx',output,sheetNR,'L4:L6');
```


Appendix F: Top view of the bridge [centre lines]



Appendix G: Top view of bottom wind bracing



Appendix H: Side view of a main girder

